Topological magnetic structures in MnGe and CeAlGe: Neutron diffraction and symmetry analysis

Vladimir Pomjakushin
Laboratory for Neutron Scattering and Imaging LNS, Paul Scherrer Institut PSI
Switzerland

Neutron wide-angle diffraction experiments:	HRPT, DMC /PSI
SANS (CeAlGe):	SANS-I/PSI, D33/LLB
Samples:	Solid State Chemistry group PSI and University of Tokyo (MnGe)
Hall effect:	University of Tokyo

MnGe: V. Pomjakushin, I. Plokhikh, J. S. White, Y. Fujishiro, N. Kanazawa, Y. Tokura, and E. Pomjakushina Phys. Rev. B **107**, 024410 (2023)

CeAlGe: P. Puphal, V. Pomjakushin, N. Kanazawa, V. Ukleev, D.J. Gawryluk, J. Ma, M. Naamneh, N.C. Plumb, L. Keller, R. Cubitt, E. Pomjakushina and J.S. White
Physical Review Letters, **124**, 017202 (2020)

Plan

- Intro to topological textures for multi-k structures
- For both MnGe and CeAlGe
- Samples. Neutron diffraction experiments
- Magnetic structures 1k, 2k and 3k in respective Magnetic Superspace Groups MSSG
- Note on continuous limit of topological structures
- Calculation of topological charges
- Summary

Famous metallic topological materials with long magnetic periodicity

MnSi	Weyl semi-metal CeAlGe	MnGe
	Magnetic modulation length	
200 Å	70 Å	30 Å
T_N=35K	4K	170K

Non coplanar magnetic textures☆ $\mathbf{n}(x, y, z)$ defined by multi-k magnetic structure, have non zero topological charge Q, responsible for THE etc.

for 2k-structure

$$Q = (1/4\pi) \int \vec{n}(\partial\vec{n}/\partial x \times \partial\vec{n}/\partial y)dxdy$$

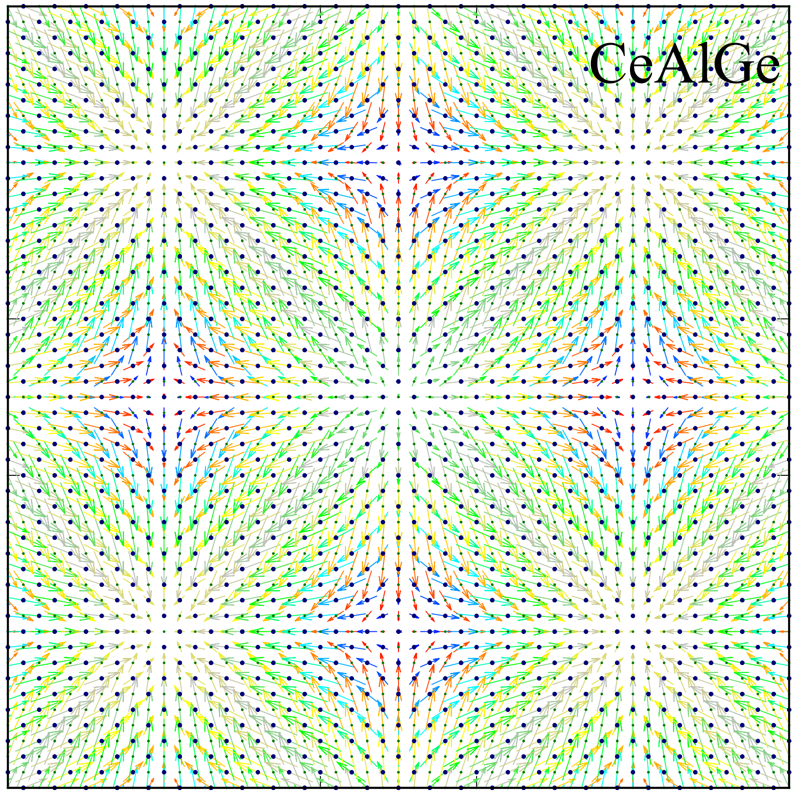

I4$_1$md1'(a00)000s(0a0)0s0s

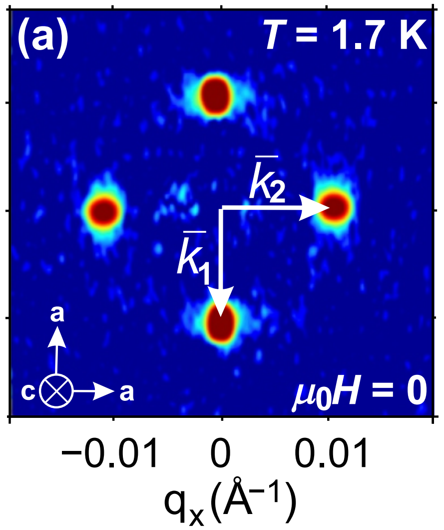

☆stabilised by Dzyaloshinsky-Moria interaction $\mathbf{D}_{ij} \cdot [\mathbf{S}_i \times \mathbf{S}_j]$, where $\mathbf{D}_{ij} \propto [\mathbf{r}_i \times \mathbf{r}_j]$

Magnetic symmetry for multi-k structure models

wavevector or propagation vector of modulated magnetic structure $\sim \cos(2\pi \mathbf{t}_n \mathbf{k} + \varphi)$

k1=[0,g,0], k2=[g,0,0]

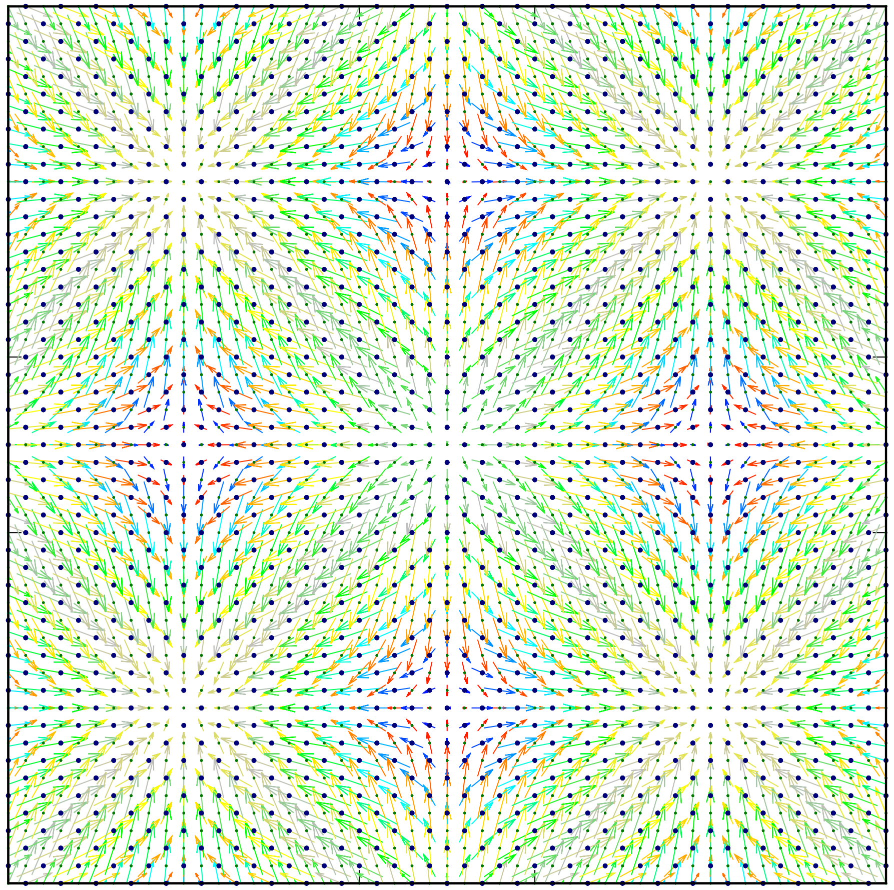

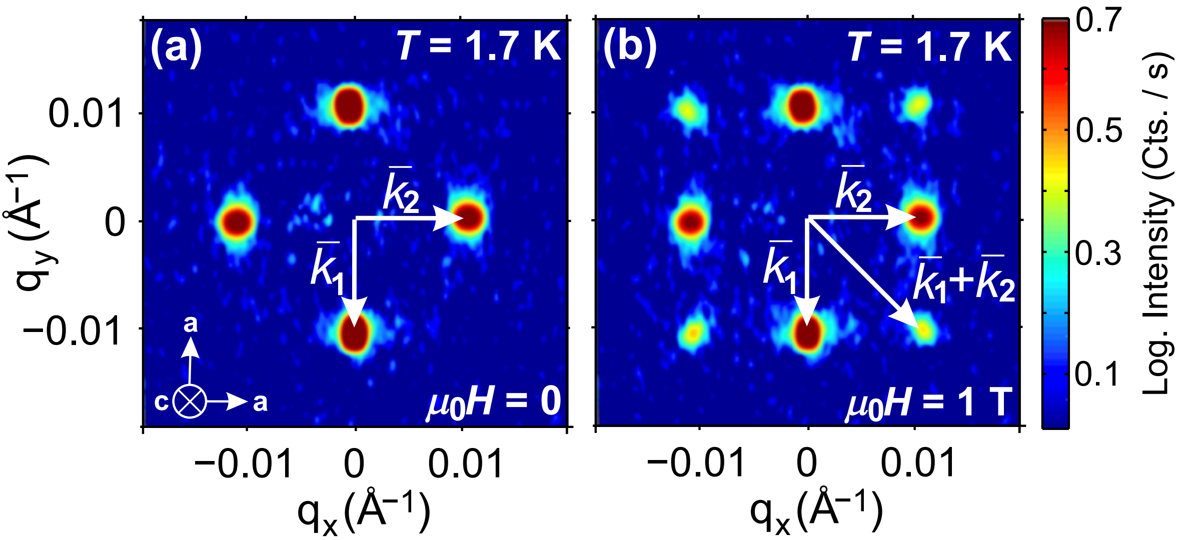

multi-arm vs. multi-k

1. Multi-k structure is not very special case by magnetic symmetry

2. Symmetry analysis is done in a similar way for both multi-arm case and the case of multidimensional irreps (irreducible representations)

3.Multi-k/arm structures are special because only they can have non-trivial topological properties.

Motivation to study MnGe

Apply a state-of-the-art analysis of all possible magnetic superspace structures allowed by the crystal symmetry in metallic MnGe (P213) that are consistent with neutron diffraction data.

MnGe has been long-studied for its remarkable phenomena related to the topological magnetic order, but surprisingly, the detailed magnetic structure underlying such phenomena was not addressed before this study.

MnGe samples

1. Single crystals are not possible to grow.
2. Powders are difficult - only high pressure (8 GPa) synthesis was known.

new chemical route to synthesize MnGe!

a combined mechanochemical and solid-state route at ambient pressures and moderate temperatures

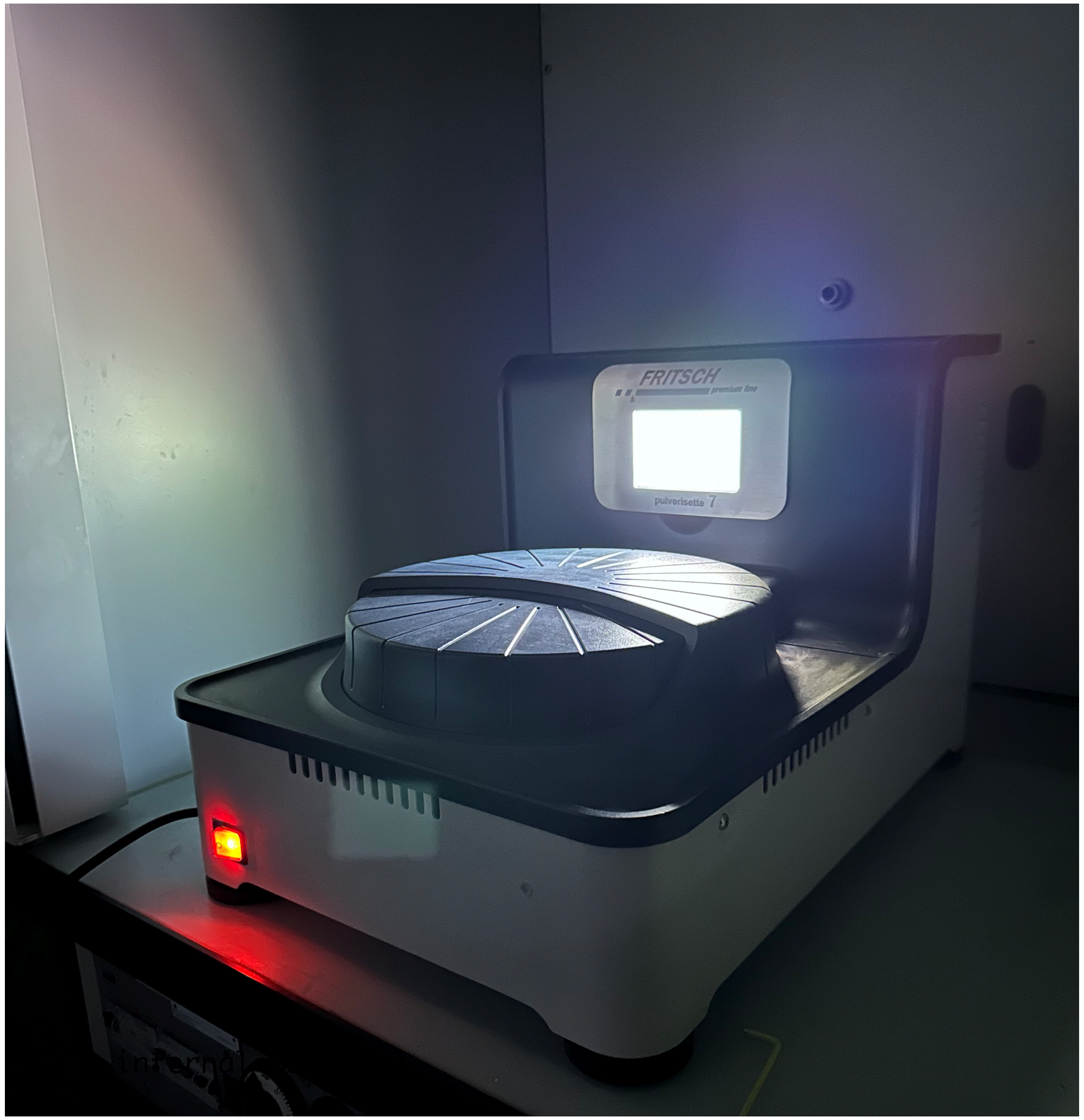

Crystal structure. Neutron diffraction patterns

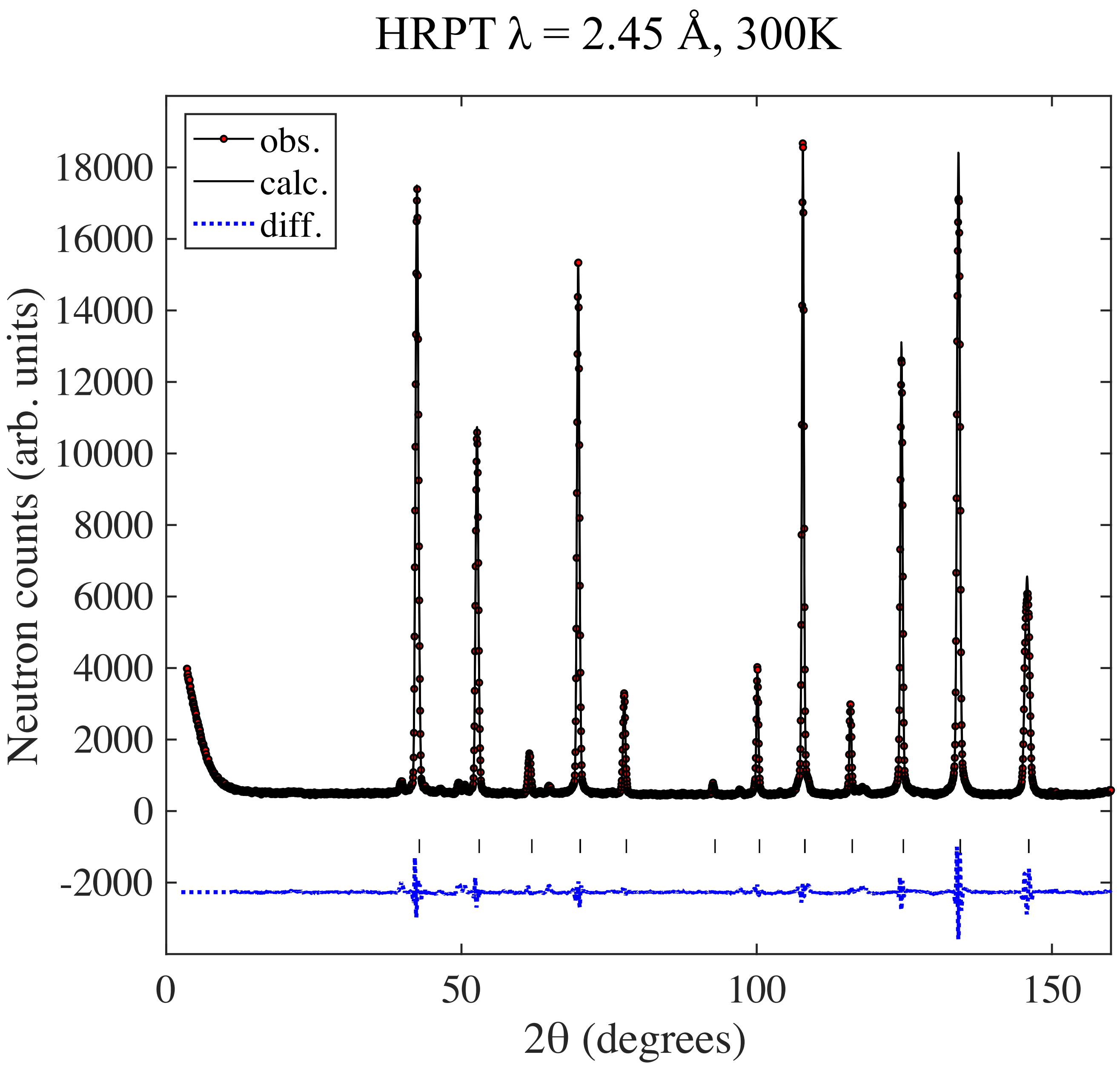

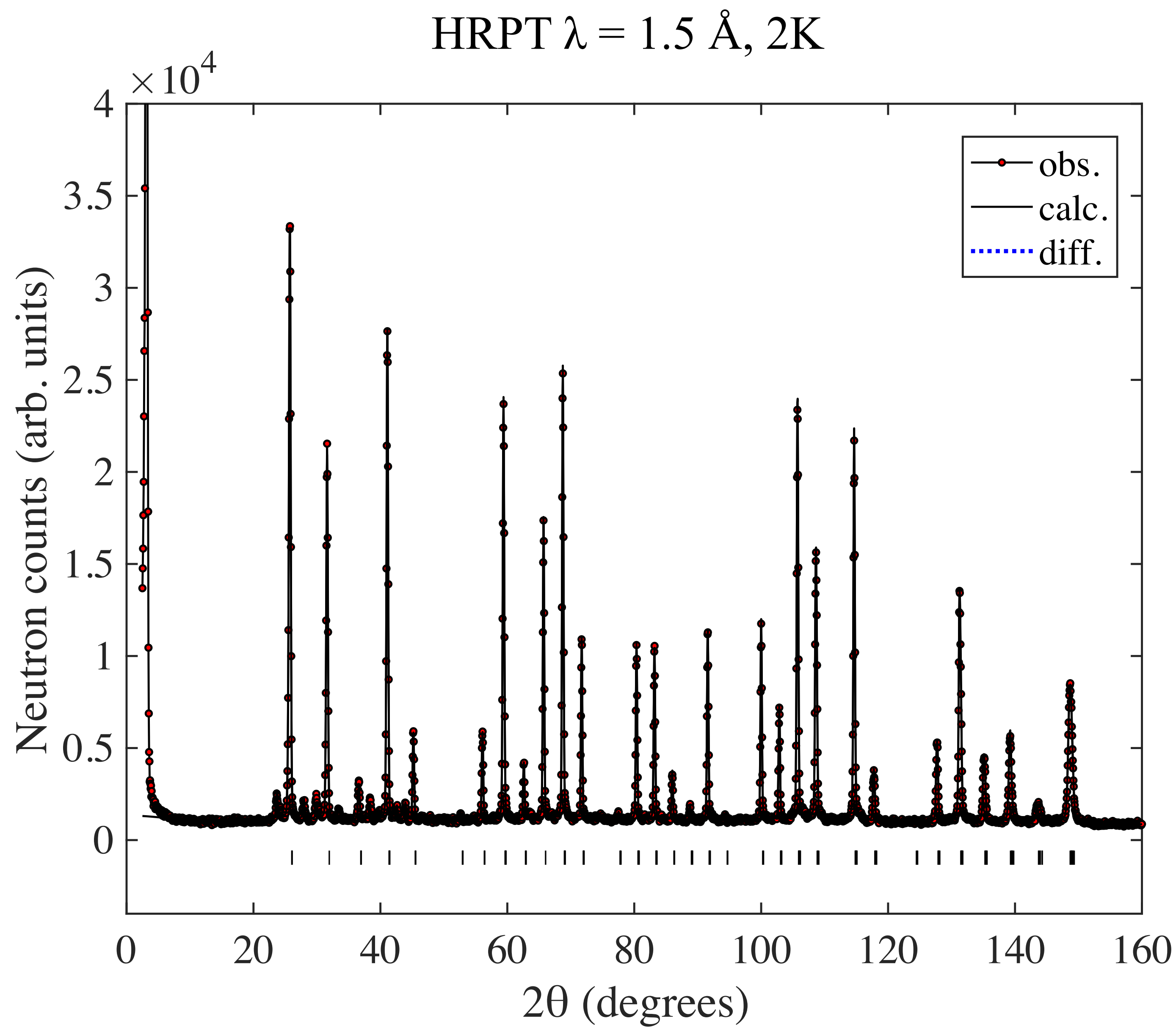

Crystal structure. P2_13 space group T=@300K

Mn (4a) (x,x,x) three 2-fold axes

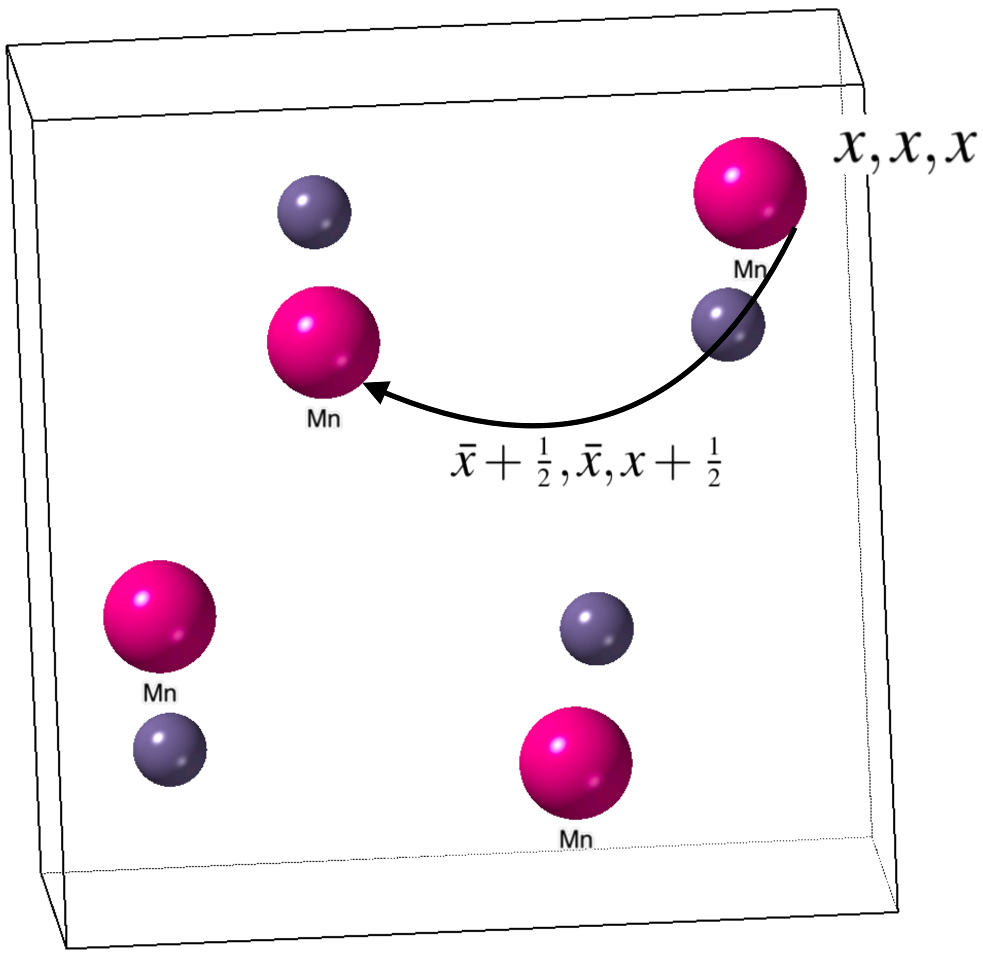

HRPT λ = 2.45 Å

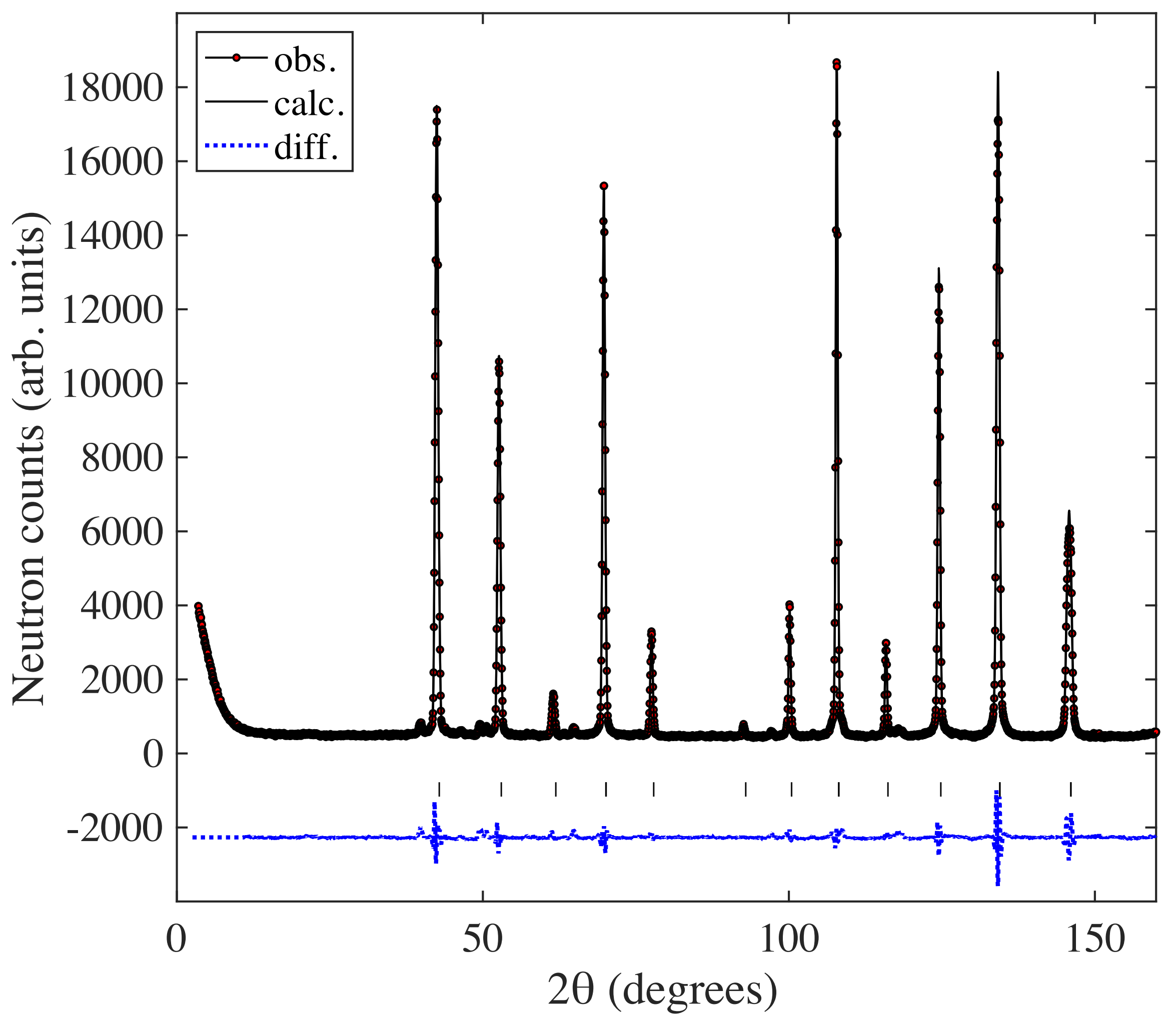

Pure magnetic neutron diffaction pattern “2K”-“300K”

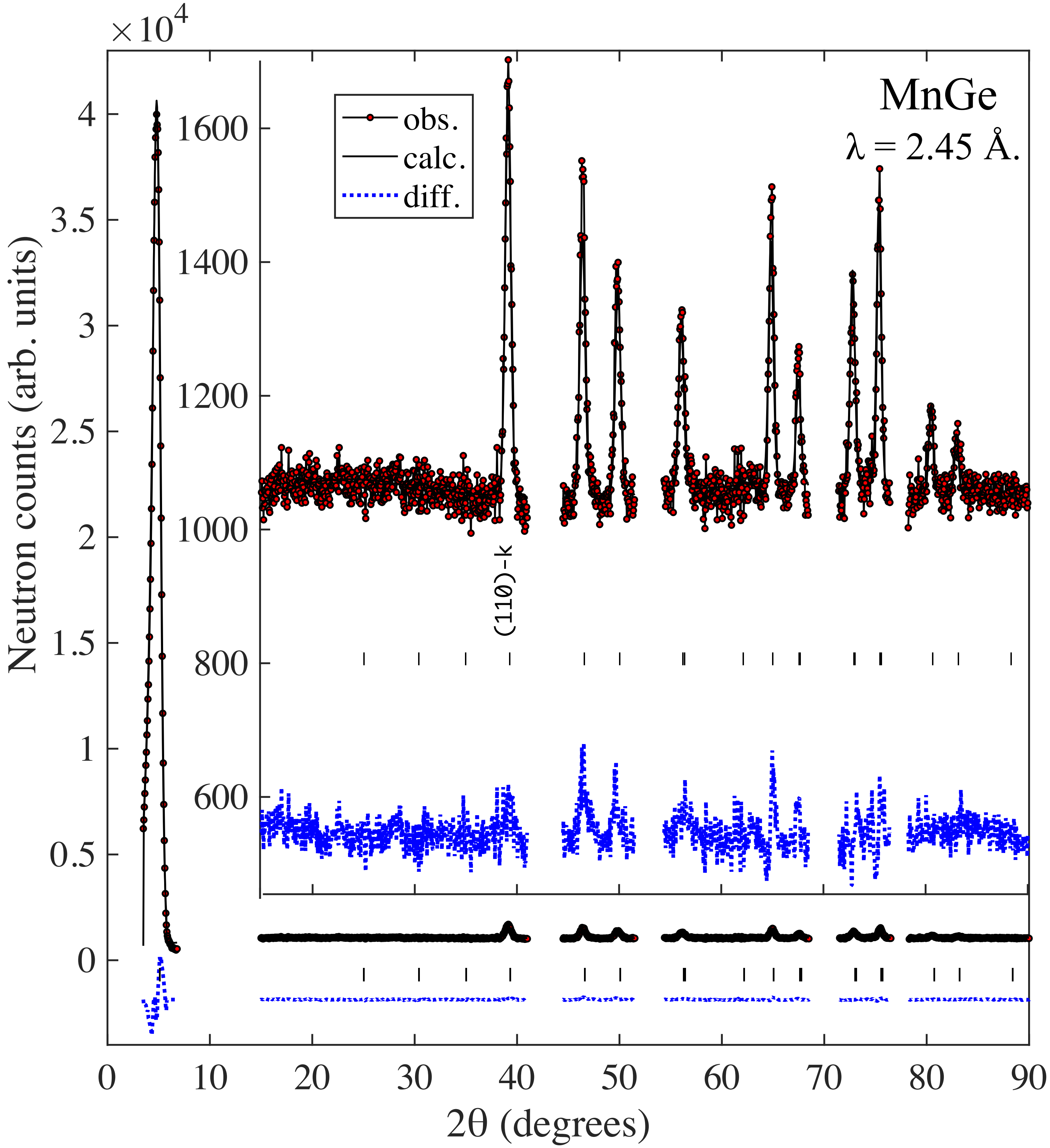

cubic P2_13

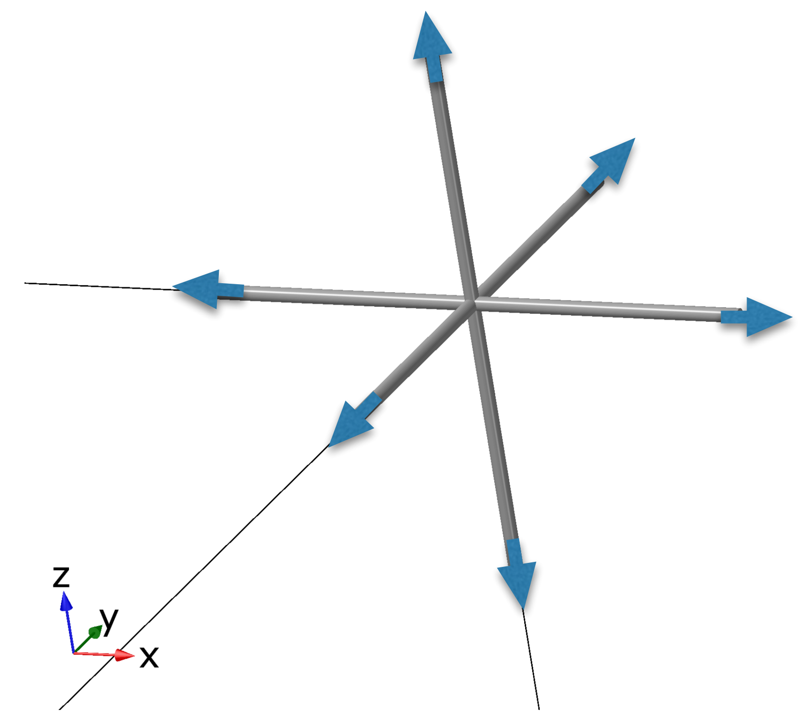

propagation vector star
3*2-arms **k** = [0b0]
Two irreps DT1, DT2

b = 0.17 → magnetic period 30 Å

magnetic domain sizes: L ≃ 520 Å

Magnetic and crystal symmetry analysis for single- and multi-k structures

Harold T. Stokes, Dorian M. Hatch, and Branton J. Campbell

ISODISTORT: ISOTROPY Software Suite http://iso.byu.edu

ISOTROPY Software Suite

Harold T. Stokes, Dorian M. Hatch, and Branton J. Campbell, Department of Physics and Astronomy, Brigham Young University, Provo, Utah 84606, USA,

M. I. Aroyo, J. M. Perez-Mato, D. Orobengoa, E. Tasci, G. de la Flor, and A. Kirov

Bilbao Crystallographic Server http://www.cryst.ehu.es/

Two main web sites with a collection of software which applies group theoretical methods to the analysis of phase transitions in crystalline solids.

General tools for representation analysis, Shubnikov groups, 3D+n, and much more...

Magnetic SuperSpace subGroups for P2_13 [a,0,0]+[0,a,0]+[0,0,a]

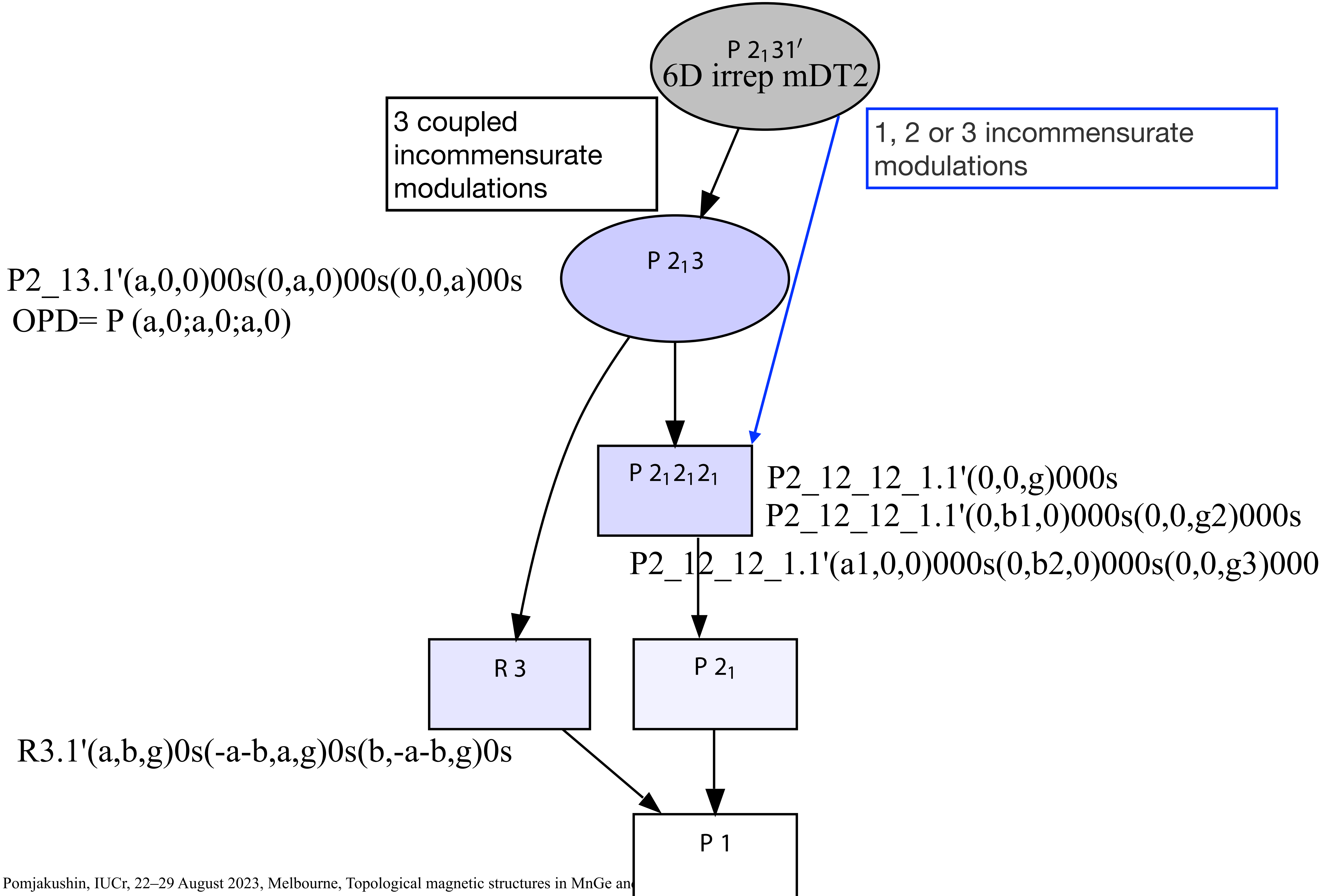

Magnetic SuperSpace subGroups for P2_13 [a,0,0]+[0,a,0]+[0,0,a]

<u>Data analysis★:</u>

1. Simulated annealing search for 3D+3, 3D+2 and 3D+1 MSSG
2. standard LSQ fit

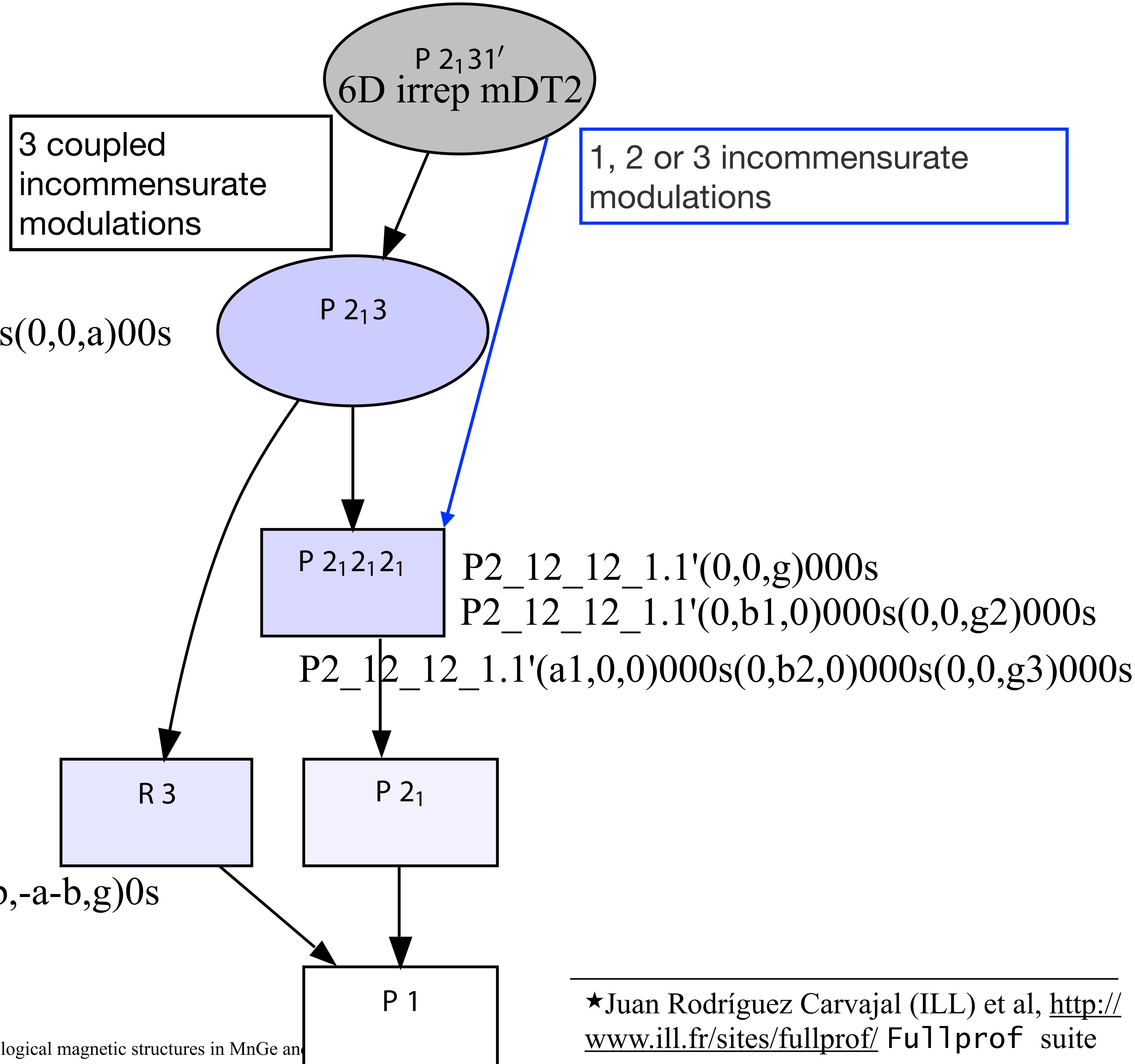

P2_13.1'(a,0,0)00s(0,a,0)00s(0,0,a)00s

OPD= P (a,0;a,0;a,0)

R3.1'(a,b,g)0s(-a-b,a,g)0s(b,-a-b,g)0s

★Juan Rodríguez Carvajal (ILL) et al, <u>http://www.ill.fr/sites/fullprof/</u> `Fullprof` suite

3D+3 General formula for magnetic moments

Magnetic moments on four Mn (4a) (x,x,x) - six parameters to find: m_1, m_2, m_3 , α_1 , α_2 , α_3

P2_13.1'(a,0,0)00s(0,a,0)00s(0,0,a)00s

$$
\begin{array}{rlll}
 & \text{1st arm} & \text{2nd arm} & \text{3rd arm} \\
[M_x, M_y, M_z]_1 = & [m_1\cos(\tilde y+\alpha_1) & + m_3\cos(\tilde z+\alpha_3) & + m_2\cos(\tilde x+\alpha_2), \leftarrow \text{Mx} \\
 & m_2\cos(\tilde y+\alpha_2) & + m_1\cos(\tilde z+\alpha_1) & + m_3\cos(\tilde x+\alpha_3), \leftarrow \text{My} \\
 & m_3\cos(\tilde y+\alpha_3) & + m_2\cos(\tilde z+\alpha_2) & + m_1\cos(\tilde x+\alpha_1)] \leftarrow \text{Mz} \\
[M_x, M_y, M_z]_2 = & [m_1\cos(\tilde y-\alpha_1) & + m_3\cos(\tilde z+\alpha_3) & - m_2\cos(\tilde x-\alpha_2), \\
 & m_2\cos(\tilde y-\alpha_2) & + m_1\cos(\tilde z+\alpha_1) & - m_3\cos(\tilde x-\alpha_3), \\
 & -m_3\cos(\tilde y-\alpha_3) & - m_2\cos(\tilde z+\alpha_2) & + m_1\cos(\tilde x-\alpha_1)] \\
[M_x, M_y, M_z]_3 = & [m_1\cos(\tilde y+\alpha_1) & - m_3\cos(\tilde z-\alpha_3) & + m_2\cos(\tilde x-\alpha_2), \\
 & -m_2\cos(\tilde y+\alpha_2) & + m_1\cos(\tilde z-\alpha_1) & - m_3\cos(\tilde x-\alpha_3), \\
 & m_3\cos(\tilde y+\alpha_3) & - m_2\cos(\tilde z-\alpha_2) & + m_1\cos(\tilde x-\alpha_1)] \\
[M_x, M_y, M_z]_4 = & [m_1\cos(\tilde y-\alpha_1) & - m_3\cos(\tilde z-\alpha_3) & - m_2\cos(\tilde x+\alpha_2), \\
 & -m_2\cos(\tilde y-\alpha_2) & + m_1\cos(\tilde z-\alpha_1) & + m_3\cos(\tilde x+\alpha_3), \\
 & -m_3\cos(\tilde y-\alpha_3) & + m_2\cos(\tilde z-\alpha_2) & + m_1\cos(\tilde x+\alpha_1)]
\end{array}
$$

$$\tilde y = 2\pi k y$$

Usually in crystallography one uses sin and cos-components:

$$
\begin{aligned}
m_1\cos(\tilde y+\alpha_1) &= m_1\cos\alpha_1 \cos\tilde y - m_1\sin\alpha_1 \sin\tilde y \\
&= m_c \cos\tilde y + m_s \sin\tilde y
\end{aligned}
$$

Models 3D+3, 3D+2

TABLE II. Magnetic structure parameters for MnGe for the different 3+3 and 3+2 models explained in Sec. IV D. See caption of Table I for details. The total moment amplitude, which is a sum over all k-vector components, is $\sqrt{6}$ and 2 times larger than the component given for a single k-vector for hedgehog and skyrmion structures, respectively. For the 3+2 structure, m_5 and m_6, are not given, because they are constrained to be equal to m 0 in formula (3).

Model	m_{xc}, m_{xs}, μ_B	m_{yc}, m_{ys}, μ_B	m_{zc}, m_{zs}, μ_B	M, μ_B
3+3 (F) SA	−0.8616, −0.0217	0.0028, 0.0711	0.1653, 1.2014	
3+3 (F) hedgehog	1.048(1), 0	0, 0	0, −1.048(1)	2.567(3)
R_{wp}, R_{exp}, χ^2, R_B		3.67, 1.63, 5.08, 0.634		
3+3 (1) hedgehog	0.950(1), 0	0, 0	0, −0.950(1)	2.327(3)
R_{wp}, R_{exp}, χ^2, R_B		7.60, 3.37, 5.07, 2.22		
3+3 (1) x	1.344(2), 0.14(12)	0, 0	0, 0	2.328(3)
R_{wp}, R_{exp}, χ^2, R_B		7.60, 3.37, 5.07, 2.17		
3+3 (F) xz	1.42(5), 0	0, 0	0.28(3), 0.41(2)	2.56(6)
R_{wp}, R_{exp}, χ^2, R_B		3.62, 1.63, 4.95, 0.589		
3+3 (F) x	1.481(2), 0.19(3)	0, 0	0, 0	2.58(3)
R_{wp}, R_{exp}, χ^2, R_B		3.64, 1.63, 5.01, 0.569		
3+2 (F) skyrmion	1.283(1), 0	0, 0	0, −1.283(1)	2.566(2)
R_{wp}, R_{exp}, χ^2, R_B		3.67, 1.63, 5.08 , 0.643		

Models 3D+3, 3D+2

TABLE II. Magnetic structure parameters for MnGe for the different 3+3 and 3+2 models explained in Sec. IV D. See caption of Table I for details. The total moment amplitude, which is a sum over all k-vector components, is $\sqrt{6}$ and 2 times larger than the component given for a single k-vector for hedgehog and skyrmion structures, respectively. For the 3+2 structure, m_5 and m_6, are not given, because they are constrained to be equal to m … 0 in formula (3).

Model	m_{xc}, m_{xs}, μ_B	m_{yc}, m_{ys}, μ_B	m_{zc}, m_{zs}, μ_B	M, μ_B
3+3 (F) SA	−0.8616, −0.0217	0.0028, 0.0711	0.1653, 1.2014	
3+3 (F) hedgehog	1.048(1), 0	0, 0	0, −1.048(1)	2.567(3)
R_{wp}, R_{exp}, χ^2, R_B		3.67, 1.63, 5.08, 0.634		
3+3 (1) hedgehog	0.950(1), 0	0, 0	0, −0.950(1)	2.327(3)
R_{wp}, R_{exp}, χ^2, R_B		7.60, 3.37, 5.07, 2.22		
3+3 (1) x	1.344(2), 0.14(12)	0, 0	0, 0	2.328(3)
R_{wp}, R_{exp}, χ^2, R_B		7.60, 3.37, 5.07, 2.17		
3+3 (F) xz	1.42(5), 0	0, 0	0.28(3), 0.41(2)	2.56(6)
R_{wp}, R_{exp}, χ^2, R_B		3.62, 1.63, 4.95, 0.589		
3+3 (F) x	1.481(2), 0.19(3)	0, 0	0, 0	2.58(3)
R_{wp}, R_{exp}, χ^2, R_B		3.64, 1.63, 5.01, 0.569		
3+2 (F) skyrmion	1.283(1), 0	0, 0	0, −1.283(1)	2.566(2)
R_{wp}, R_{exp}, χ^2, R_B		3.67, 1.63, 5.08 , 0.643		

Models 3D+3, 3D+2

TABLE II. Magnetic structure parameters for MnGe for the different 3+3 and 3+2 models explained in Sec. IV D. See caption of Table I for details. The total moment amplitude, which is a sum over all k-vector components, is $\sqrt{6}$ and 2 times larger than the component given for a single k-vector for hedgehog and skyrmion structures, respectively. For the 3+2 structure, m_5 and m_6, are not given, because they are constrained to be equal to m … 0 in formula (3).

Model	m_{xc}, m_{xs}, μ_B	m_{yc}, m_{ys}, μ_B	m_{zc}, m_{zs}, μ_B	M, μ_B
3+3 (F) SA	−0.8616, −0.0217	0.0028, 0.0711	0.1653, 1.2014	
3+3 (F) hedgehog	1.048(1), 0	0, 0	0, −1.048(1)	2.567(3)
R_{wp}, R_{exp}, χ^2, R_B		3.67, 1.63, 5.08, 0.634		
3+3 (1) hedgehog	0.950(1), 0	0, 0	0, −0.950(1)	2.327(3)
R_{wp}, R_{exp}, χ^2, R_B		7.60, 3.37, 5.07, 2.22		
3+3 (1) x	1.344(2), 0.14(12)	0, 0	0, 0	2.328(3)
R_{wp}, R_{exp}, χ^2, R_B		7.60, 3.37, 5.07, 2.17		
3+3 (F) xz	1.42(5), 0	0, 0	0.28(3), 0.41(2)	2.56(6)
R_{wp}, R_{exp}, χ^2, R_B		3.62, 1.63, 4.95, 0.589		
3+3 (F) x	1.481(2), 0.19(3)	0, 0	0, 0	2.58(3)
R_{wp}, R_{exp}, χ^2, R_B		3.64, 1.63, 5.01, 0.569		
3+2 (F) skyrmion	1.283(1), 0	0, 0	0, −1.283(1)	2.566(2)
R_{wp}, R_{exp}, χ^2, R_B		3.67, 1.63, 5.08 , 0.643		

Models 3D+3, 3D+2

TABLE II. Magnetic structure parameters for MnGe for the different 3+3 and 3+2 models explained in Sec. IV D. See caption of Table I for details. The total moment amplitude, which is a sum over all k-vector components, is $\sqrt{6}$ and 2 times larger than the component given for a single k-vector for hedgehog and skyrmion structures, respectively. For the 3+2 structure, m_5 and m_6, are not given, because they are constrained to be equal to m … 0 in formula (3).

Model	m_{xc}, m_{xs}, μ_B	m_{yc}, m_{ys}, μ_B	m_{zc}, m_{zs}, μ_B	M, μ_B
3+3 (F) SA	−0.8616, −0.0217	0.0028, 0.0711	0.1653, 1.2014	
3+3 (F) hedgehog	1.048(1), 0	0, 0	0, −1.048(1)	2.567(3)
R_{wp}, R_{exp}, χ^2, R_B		3.67, 1.63, 5.08, 0.634		
3+3 (1) hedgehog	0.950(1), 0	0, 0	0, −0.950(1)	2.327(3)
R_{wp}, R_{exp}, χ^2, R_B		7.60, 3.37, 5.07, 2.22		
3+3 (1) x	1.344(2), 0.14(12)	0, 0	0, 0	2.328(3)
R_{wp}, R_{exp}, χ^2, R_B		7.60, 3.37, 5.07, 2.17		
3+3 (F) xz	1.42(5), 0	0, 0	0.28(3), 0.41(2)	2.56(6)
R_{wp}, R_{exp}, χ^2, R_B		3.62, 1.63, 4.95, 0.589		
3+3 (F) x	1.481(2), 0.19(3)	0, 0	0, 0	2.58(3)
R_{wp}, R_{exp}, χ^2, R_B		3.64, 1.63, 5.01, 0.569		
3+2 (F) skyrmion	1.283(1), 0	0, 0	0, −1.283(1)	2.566(2)
R_{wp}, R_{exp}, χ^2, R_B		3.67, 1.63, 5.08 , 0.643		

Note on continuous limit of modulated structures

"true" topological charge $Q = (1/4\pi) \int \vec{n}(\partial\vec{n}/\partial x \times \partial\vec{n}/\partial y) dxdy$

there is a principal difficulty in the realisation of the continuous limit related to the crystallographic symmetries like rotations by the large crystallographic angles, such as 180, 120, 90, or 60 deg.

Note on continuous limit of modulated structures

k=0.3 one atom in unit cell

$$y = 1, 2, 3...$$

$$M(y) = m\cos(2\pi k y)$$

$$\tilde{y} = 2\pi k y$$

Note on continuous limit of modulated structures

k=0.3 one atom in unit cell k=0.03

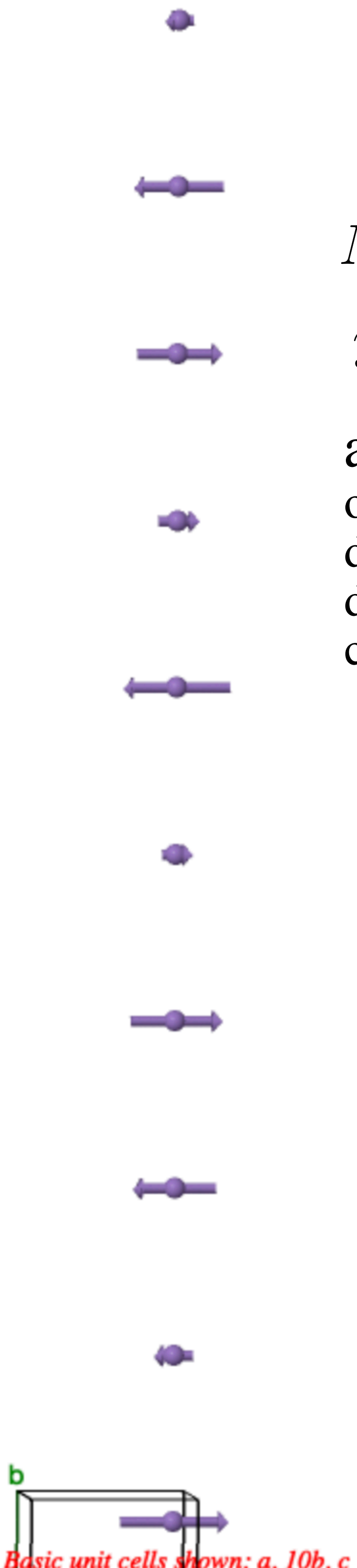

$$y = 1, 2, 3...$$

$$M(y) = m\cos(2\pi k y)$$

$$\tilde{y} = 2\pi k y$$

and in the limit of k $\rightarrow$ 0
one can approximate the distribution of the magnetization density to be spatially continuous.

derivatives $\dfrac{\partial \mathbf{n}}{\partial \tilde{y}}$ are no problem!

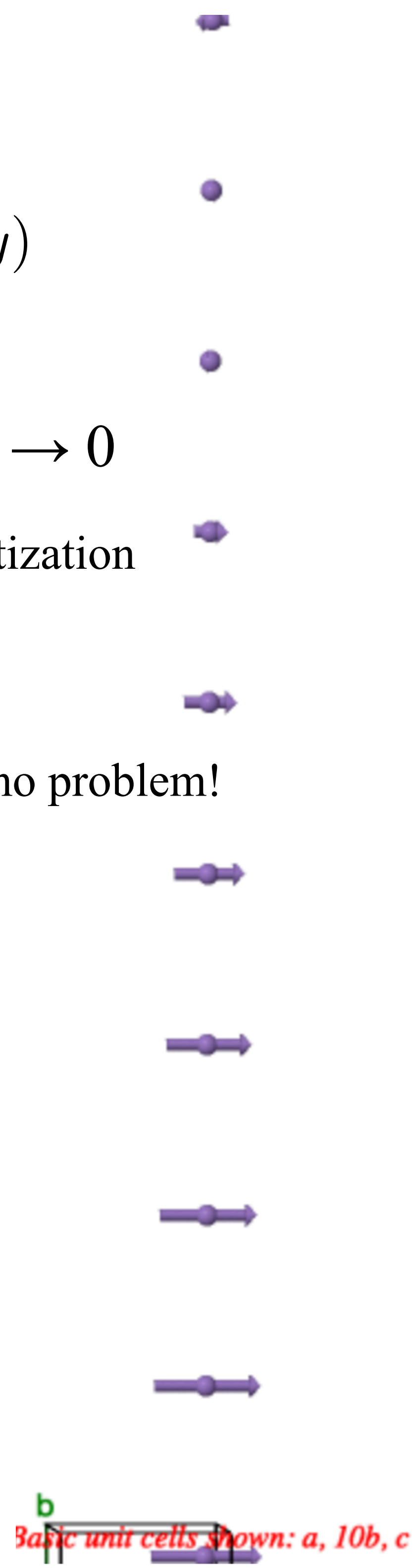

Note on continuous limit of modulated structures

k=0.3 one atom in unit cell k=0.03

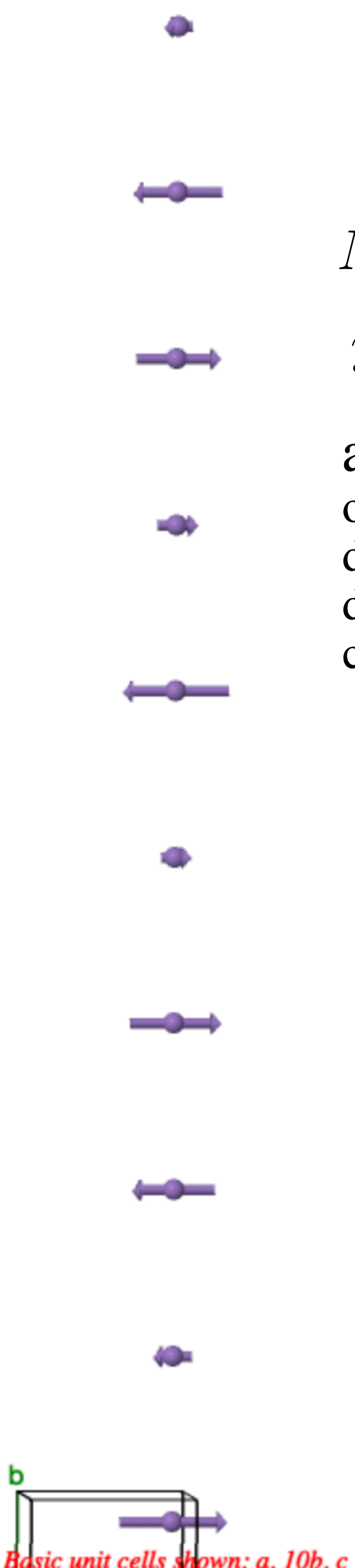

$$y = 1, 2, 3 \ldots$$

$$M(y) = m \cos(2\pi k y)$$

$$\tilde{y} = 2\pi k y$$

and in the limit of k → 0
one can approximate the distribution of the magnetization density to be spatially continuous.

derivatives $\dfrac{\partial \mathbf{n}}{\partial \tilde{y}}$ are no problem!

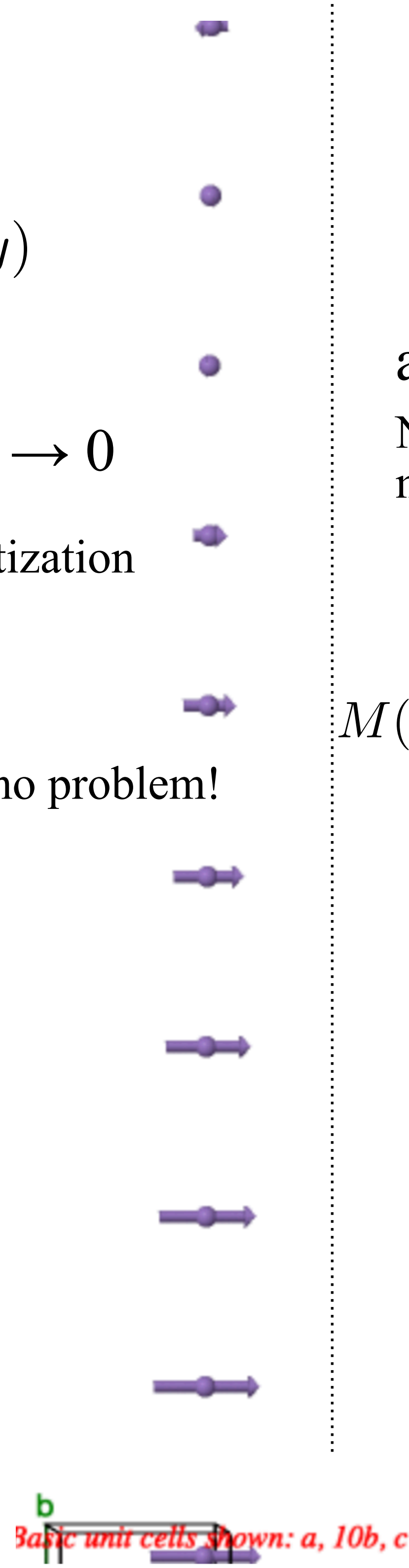

MnGe with artificially small k

k=0.03 four atoms in unit cell, related by 2_x 2_y 2_z

$\alpha_1 = \pi/2$

and in the limit of k → 0
NO spatially continuous magnetization density

$$M(y) = \begin{array}{l} m_1 \cos(\tilde{y} + \alpha_1) = -\sin\tilde{y} \\ m_1 \cos(\tilde{y} - \alpha_1) = +\sin\tilde{y} \\ m_1 \cos(\tilde{y} + \alpha_1) \\ m_1 \cos(\tilde{y} - \alpha_1) \end{array}$$

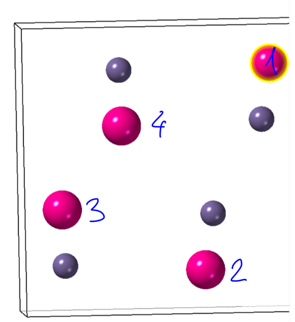

$$\tilde{y} = 2\pi k y$$

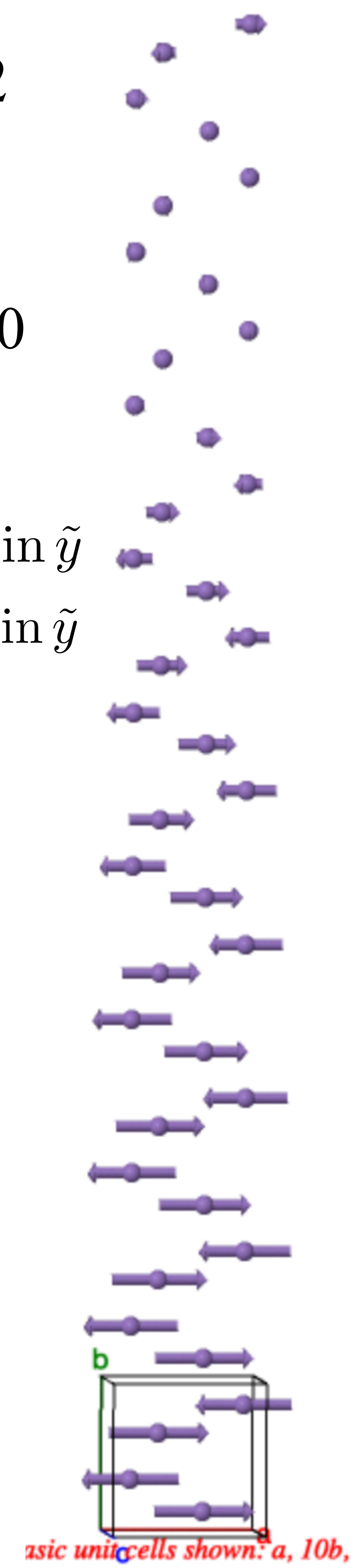

Note on continuous limit of modulated structures

k=0.3 one atom in unit cell k=0.03

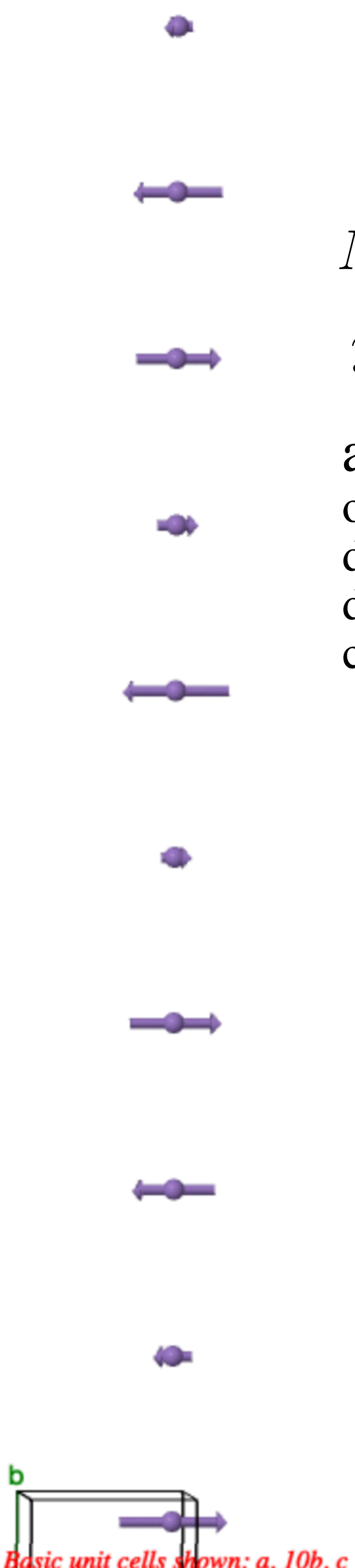

$$y = 1, 2, 3\ldots$$

$$M(y) = m\cos(2\pi k y)$$

$$\tilde{y} = 2\pi k y$$

and in the limit of k → 0
one can approximate the distribution of the magnetization density to be spatially continuous.

derivatives $\dfrac{\partial \mathbf{n}}{\partial \tilde{y}}$ are no problem!

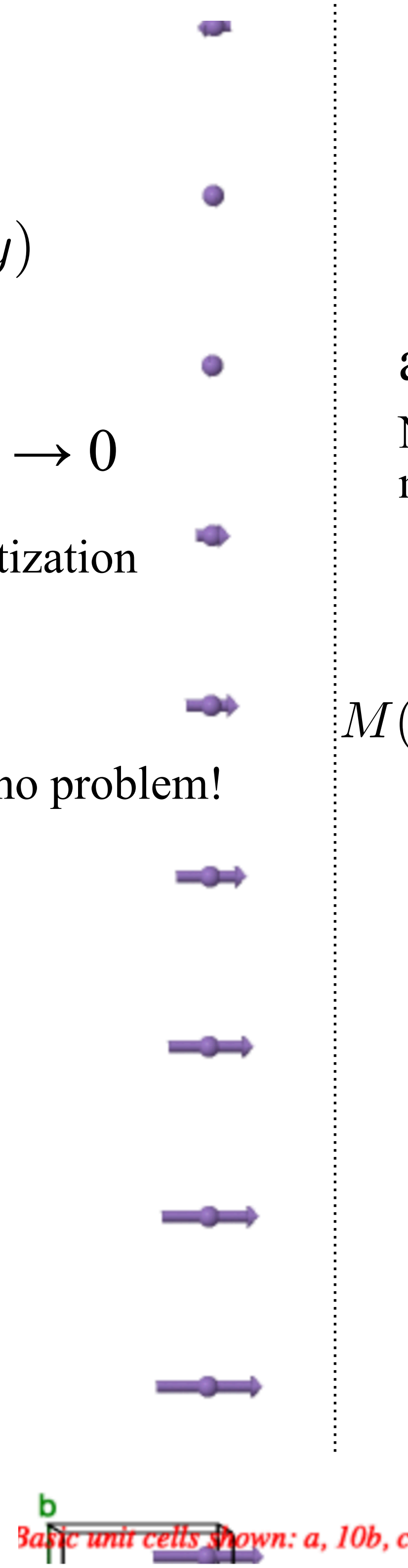

MnGe with artificially small k

k=0.03 four atoms in unit cell, related by 2_x 2_y 2_z

$\alpha_1=\pi/2$ $\alpha_1=0$

and in the limit of k → 0
NO spatially continuous magnetization density

$$M(y) = \begin{cases} m_1\cos(\tilde{y}+\alpha_1) = -\sin\tilde{y} \\ m_1\cos(\tilde{y}-\alpha_1) = +\sin\tilde{y} \\ m_1\cos(\tilde{y}+\alpha_1) \\ m_1\cos(\tilde{y}-\alpha_1) \end{cases}$$

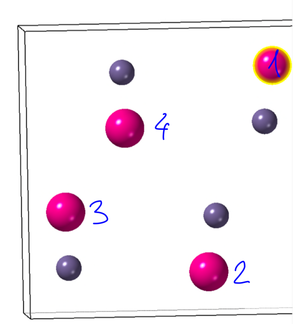

$$\tilde{y} = 2\pi k y$$

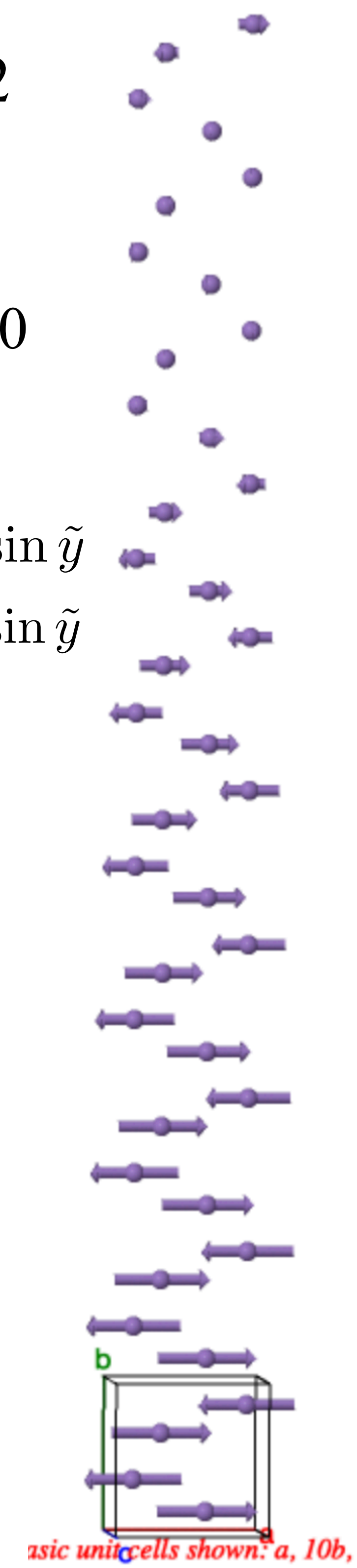

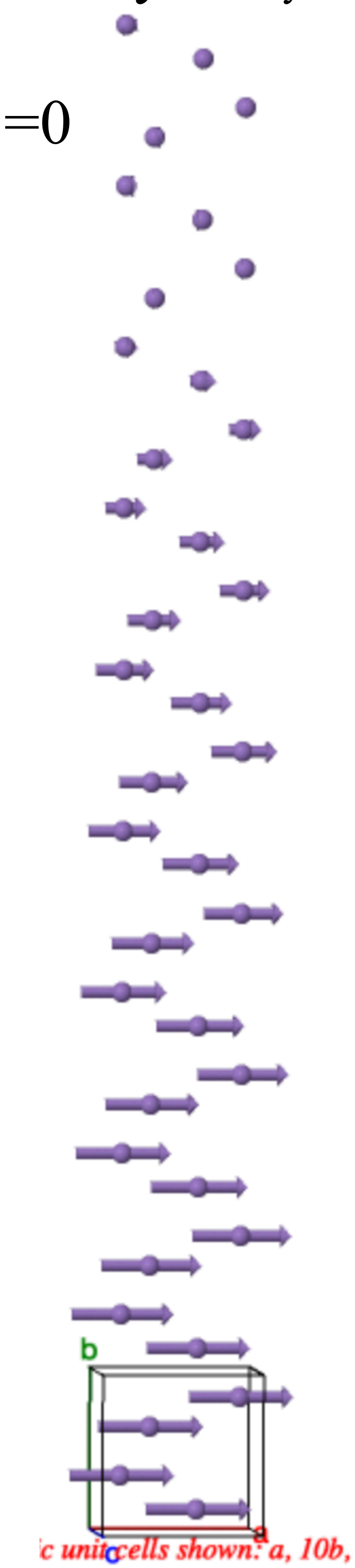

3D+3 Hedgehog model

all parameters are zero except:
m1 =m3=0.950(1)μ_B , α3 =π/2

or with sin/cos

m_{xcos}=0.950(1), m_{xsin}=0

m_{zcos}=0, m_{zsin}=-0.950(1)

P2_13.1'(a,0,0)00s(0,a,0)00s(0,0,a)00s

M_{total}=2.327(3)

1st arm 2nd arm 3rd arm

$$[M_x, M_y, M_z]_1 = \begin{bmatrix} m_1 \cos(\tilde{y}+\alpha_1) \\ m_2 \cos(\tilde{y}+\alpha_2) \\ m_3 \cos(\tilde{y}+\alpha_3) \end{bmatrix} \begin{matrix} \leftarrow \text{Mx} \\ \leftarrow \text{My} \\ \leftarrow \text{Mz} \end{matrix}$$

$$[M_x, M_y, M_z]_2 = \begin{bmatrix} m_1 \cos(\tilde{y}-\alpha_1) \\ m_2 \cos(\tilde{y}-\alpha_2) \\ -m_3 \cos(\tilde{y}-\alpha_3) \end{bmatrix}$$

$$[M_x, M_y, M_z]_3 = \begin{bmatrix} m_1 \cos(\tilde{y}+\alpha_1) \\ -m_2 \cos(\tilde{y}+\alpha_2) \\ m_3 \cos(\tilde{y}+\alpha_3) \end{bmatrix}$$

$$[M_x, M_y, M_z]_4 = \begin{bmatrix} m_1 \cos(\tilde{y}-\alpha_1) \\ -m_2 \cos(\tilde{y}-\alpha_2) \\ -m_3 \cos(\tilde{y}-\alpha_3) \end{bmatrix}$$

$\tilde{y} = 2\pi k y$

3D+3 Hedgehog model

all parameters are zero except:
$m1 = m3 = 0.950(1)\mu_B$, $\alpha 3 = \pi/2$

or with sin/cos

$m_{xcos}=0.950(1)$, $m_{xsin}=0$

$m_{zcos}=0$, $m_{zsin}=-0.950(1)$

$M_{total}=2.327(3)$

P2_13.1'(a,0,0)00s(0,a,0)00s(0,0,a)00s

1st arm 2nd arm 3rd arm

$$[M_x, M_y, M_z]_1 = \boxed{\begin{array}{r} [m_1\cos(\tilde{y}+\alpha_1) \\ m_2\cos(\tilde{y}+\alpha_2) \\ m_3\cos(\tilde{y}+\alpha_3) \end{array}}$$

← Mx

← My

← Mz

$$[M_x, M_y, M_z]_2 = \boxed{\begin{array}{r} [m_1\cos(\tilde{y}-\alpha_1) \\ m_2\cos(\tilde{y}-\alpha_2) \\ -m_3\cos(\tilde{y}-\alpha_3) \end{array}}$$

$$[M_x, M_y, M_z]_3 = \boxed{\begin{array}{r} [m_1\cos(\tilde{y}+\alpha_1) \\ -m_2\cos(\tilde{y}+\alpha_2) \\ m_3\cos(\tilde{y}+\alpha_3) \end{array}}$$

$$[M_x, M_y, M_z]_4 = \boxed{\begin{array}{r} [m_1\cos(\tilde{y}-\alpha_1) \\ -m_2\cos(\tilde{y}-\alpha_2) \\ -m_3\cos(\tilde{y}-\alpha_3) \end{array}}$$

$$\tilde{y} = 2\pi k y$$

Continuous limit is possible only for:
m2=0, α1 =0, α3 =π/2

3D+3 Hedgehog model

P2_13.1'(a,0,0)00s(0,a,0)00s(0,0,a)00s

	1st arm	2nd arm	3rd arm	
$[M_x, M_y, M_z]_1 =$	$m_1 \cos \tilde{y}$	$-m_1 \sin \tilde{z}$		← Mx
		$m_1 \cos \tilde{z}$	$-m_1 \sin \tilde{x}$	← My
	$-m_1 \sin \tilde{y}$		$m_1 \cos \tilde{x}$	← Mz
$[M_x, M_y, M_z]_2 =$	$m_1 \cos \tilde{y}$	$-m_1 \sin \tilde{z}$		
		$m_1 \cos \tilde{z}$	$-m_1 \sin \tilde{x}$	
	$-m_1 \sin \tilde{y}$		$m_1 \cos \tilde{x}$	
$[M_x, M_y, M_z]_3 =$				
	$\ldots$			
$[M_x, M_y, M_z]_4 =$				

$\tilde{y} = 2\pi k y$

m_{xcos}=0.950(1), m_{xsin}=0

m_{zcos}=0, m_{zsin}=-0.950(1)

M_{total}=2.327(3)

$$[M_x, M_y, M_z] = 0.95[\cos \tilde{y} - \sin \tilde{z}, \cos \tilde{z} - \sin \tilde{x}, \cos \tilde{x} - \sin \tilde{y}]\mu_B$$

Hedgehog 3D+3 magnetic structure - one refined parameter

cubic MSSG 198.3.206.1.m10.2 P2_13.1′ (a,0,0)00s(0,a,0)00s(0,0,a)00s

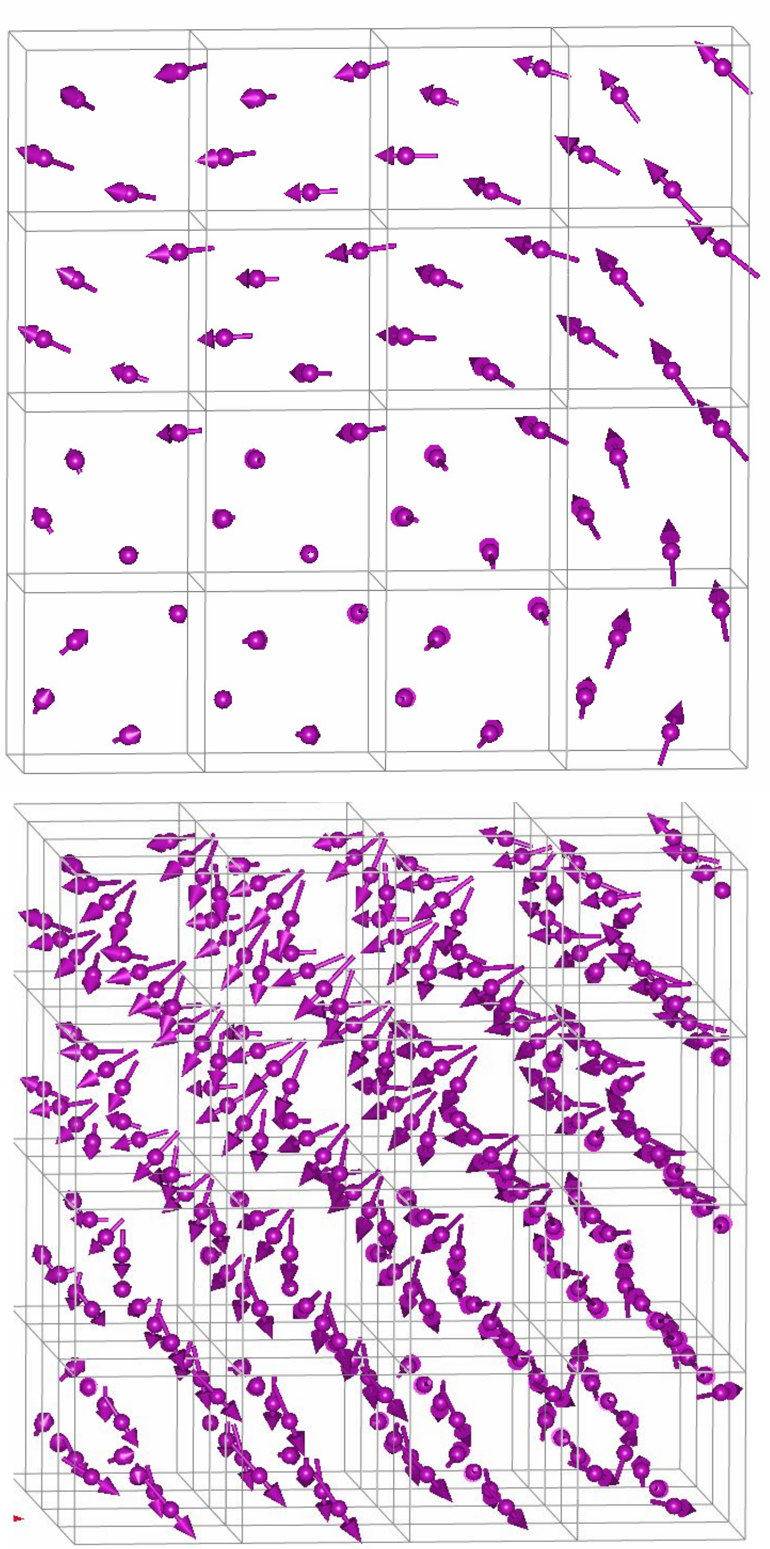

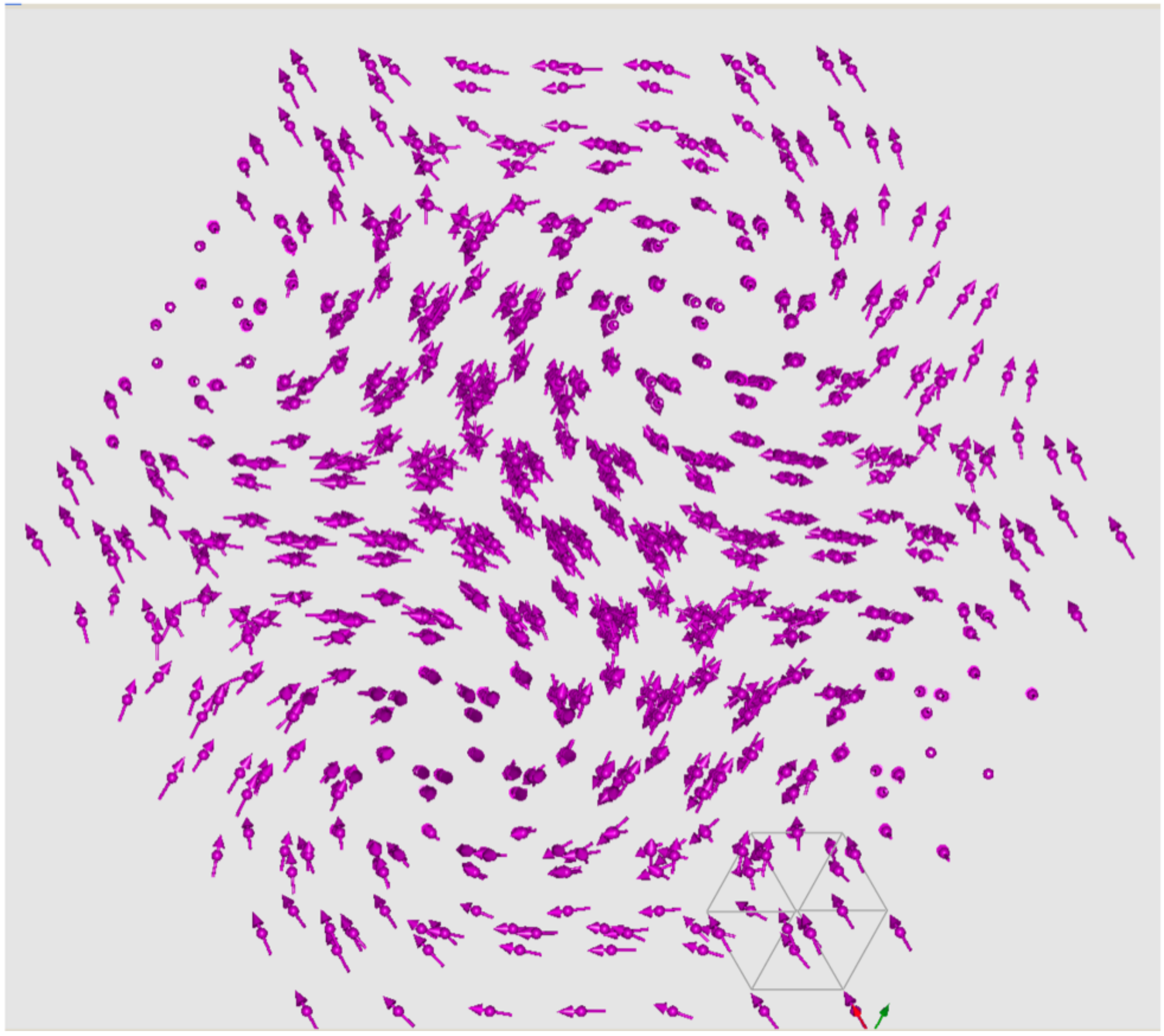

Skyrmion★ and topological charges Q

Artificial normalised magnetisation $\mathbf{n}(x,y)=\mathbf{M}(x,y)/M$

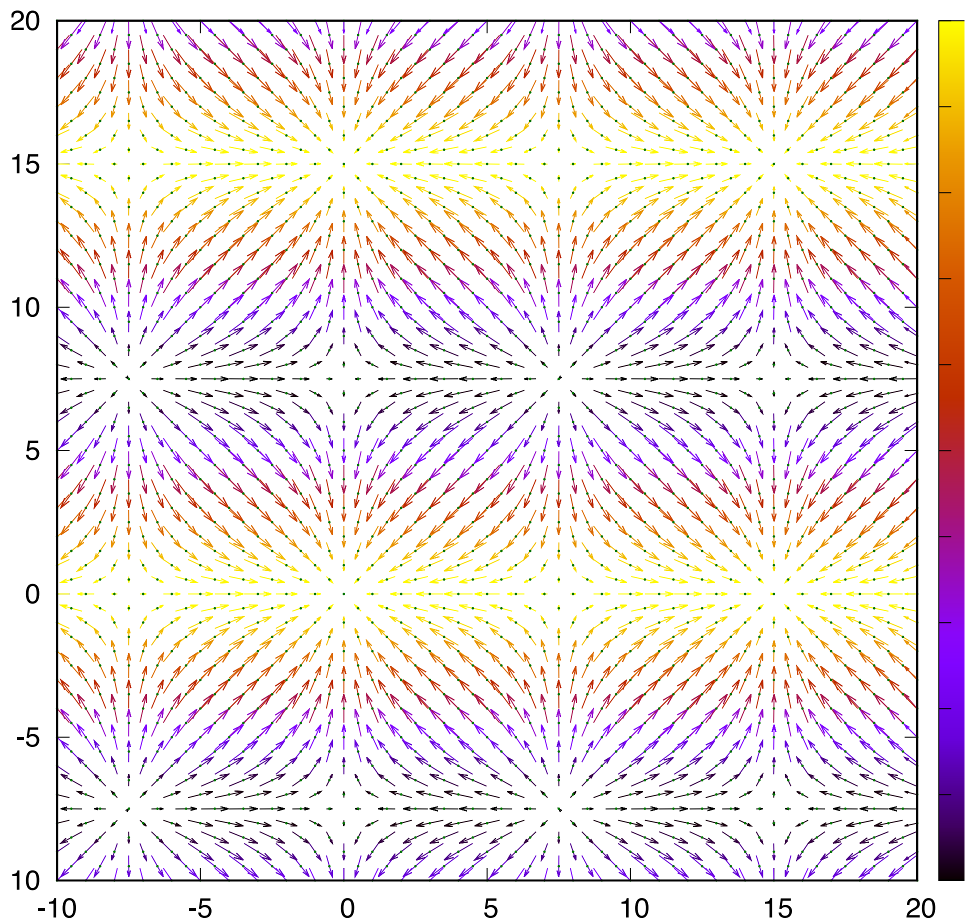

topological density/winding ~ solid angle

$$w(x,y) = \frac{1}{4\pi}(\mathbf{n}\cdot[\frac{\partial \mathbf{n}}{\partial x}\times\frac{\partial \mathbf{n}}{\partial y}]),\ \mathbf{n} = \mathbf{M}/M$$

Topological number/charge

$$Q = \int\int w(x,y)dxdy$$

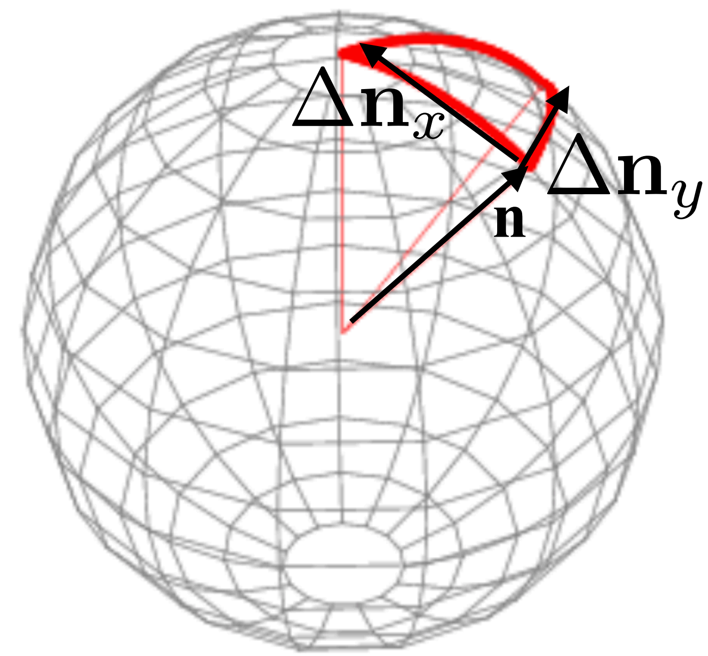

Topological skyrmion (Q=-1),
antiskyrmion (Q=+1) and
antimeron-meron (Q = ±1/2) for magnetization textures.

★ T Skyrme was a British physicist. In 1962 he proposed topological soliton to model a particle like neutron or proton. These entities would later in 1982 became known as skyrmions.

- Now it is established that proton is made of quarks… But in solid state physics we have such objects: magnetic skyrmions.

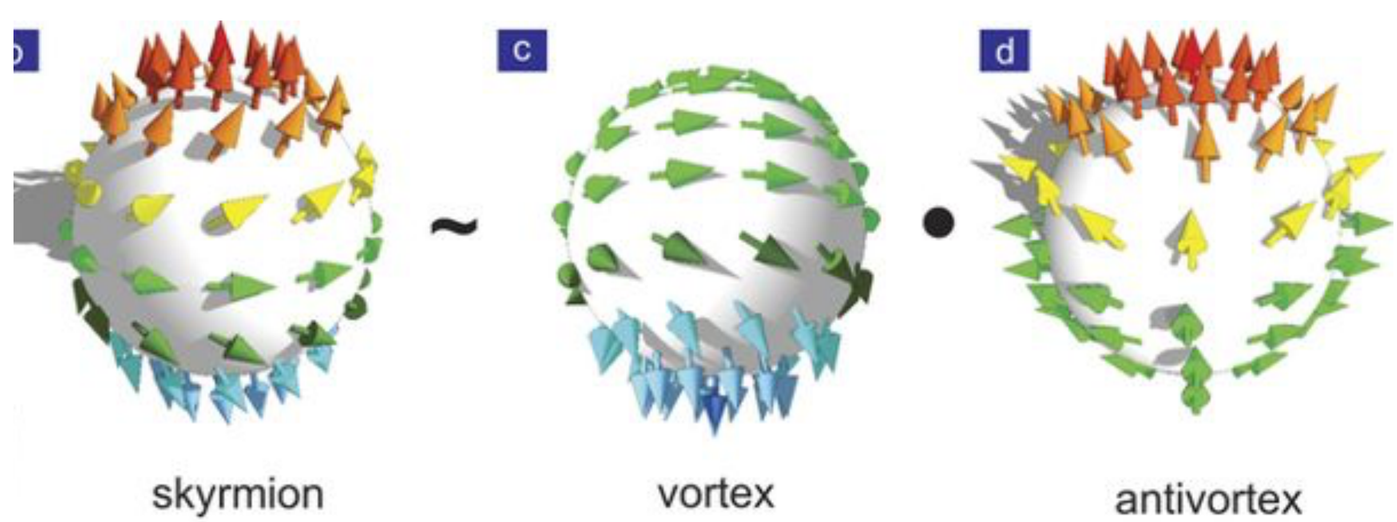

Stereographic-projection view of the magnetisation distribution of a single magnetic skyrmion *Scientific Reports* ***5****, Article number: 15773 (2015)*

Hedgehog 3D+3 magnetic cell contains 8 monopoles

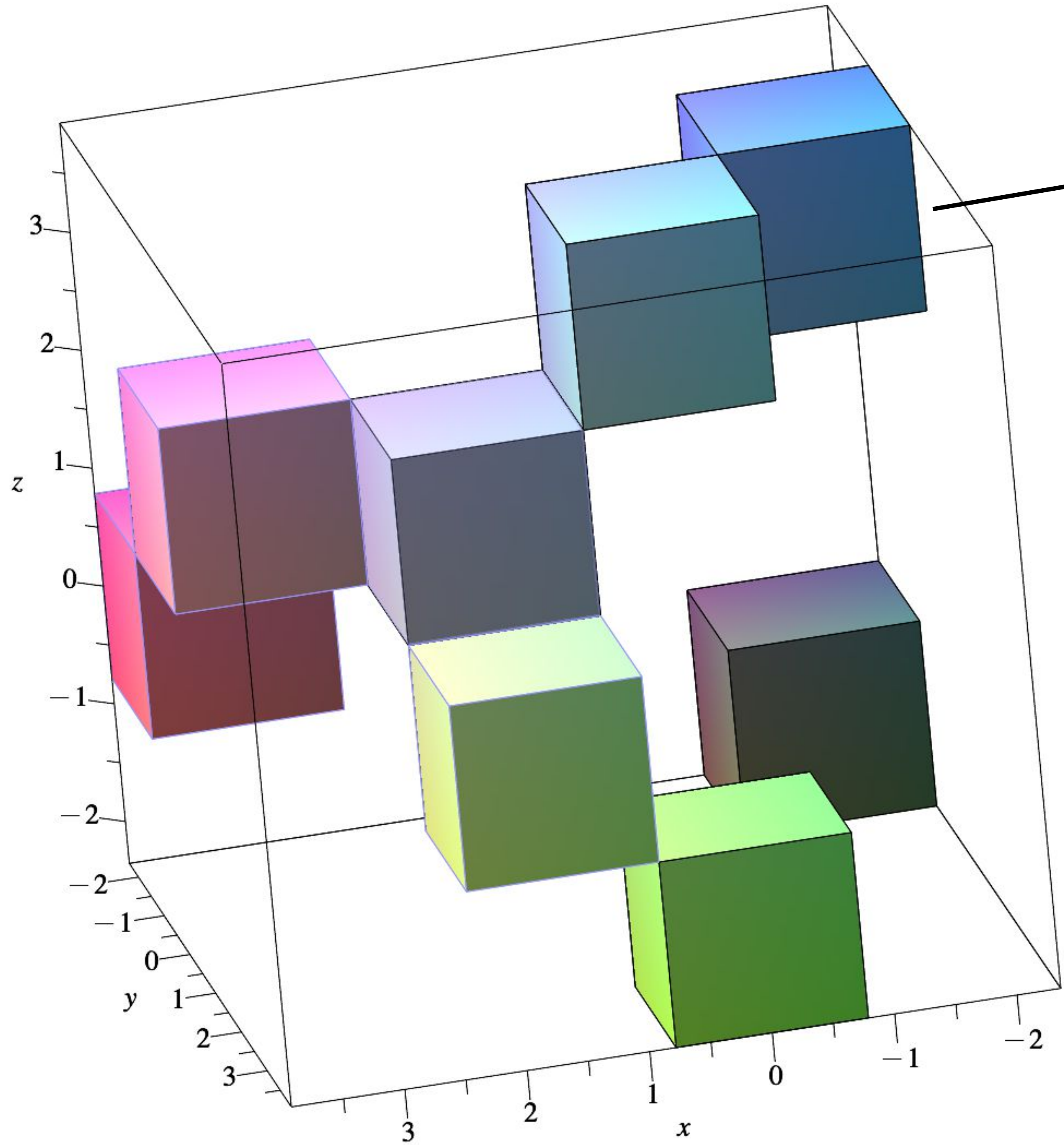

V. Pomjakushin, IUCr, 22–29 August 2023, Melbourne, Topological magnetic structures in MnGe and CeAlGe.

Hedgehog 3D+3 magnetic cell contains 8 monopoles

cubic MSSG 198.3.206.1.m10.2 P2_13.1′ (a,0,0)00s(0,a,0)00s(0,0,a)00s

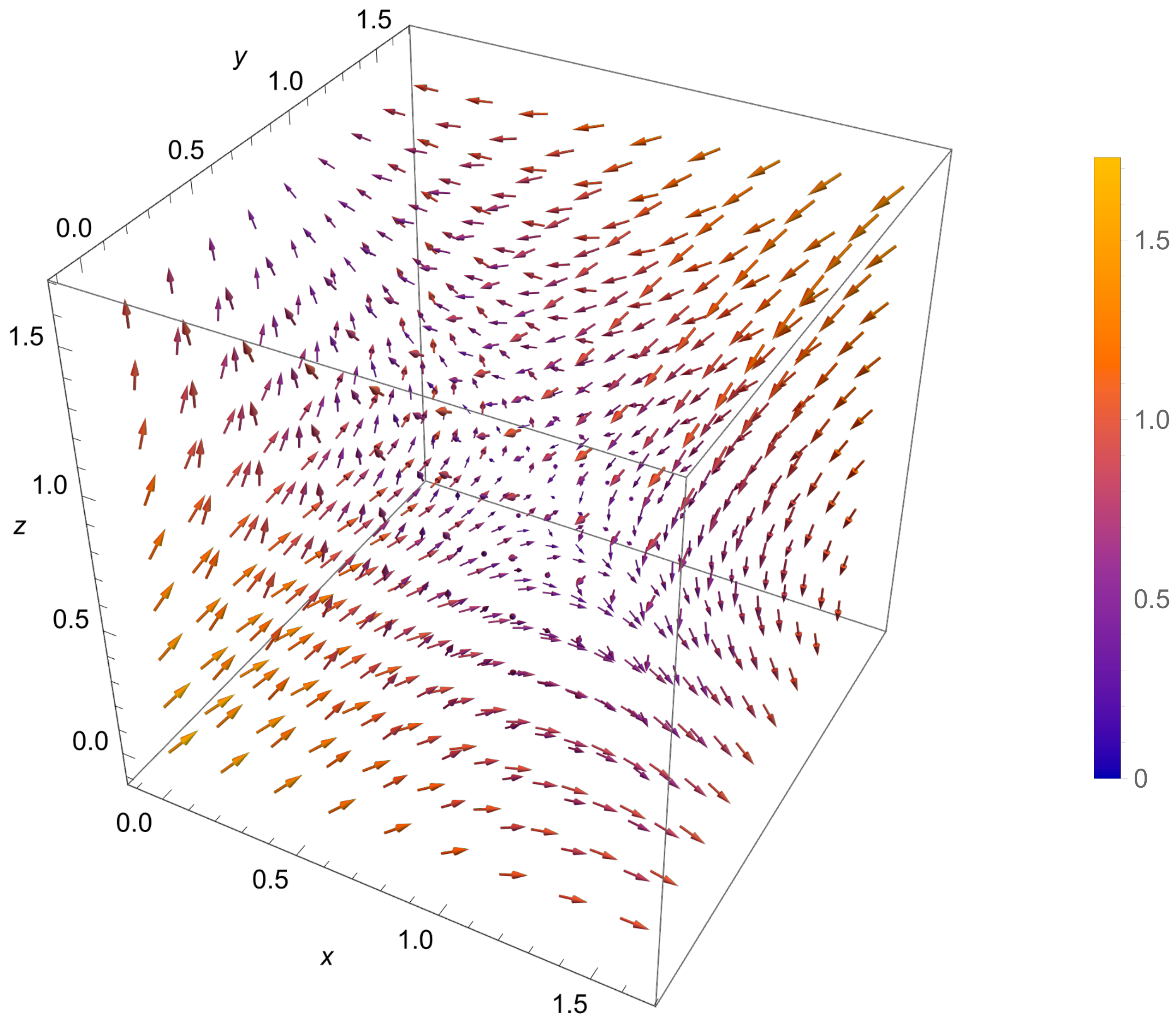

Fragment of magnetization (edge π /2 around the center π/4,π/4,π/4). The total solid angle spanned on the cube faces is Q = −1 in 4π units. The color indicates the size of the magnetization.

Normalized Linearized Magnetization on unity sphere

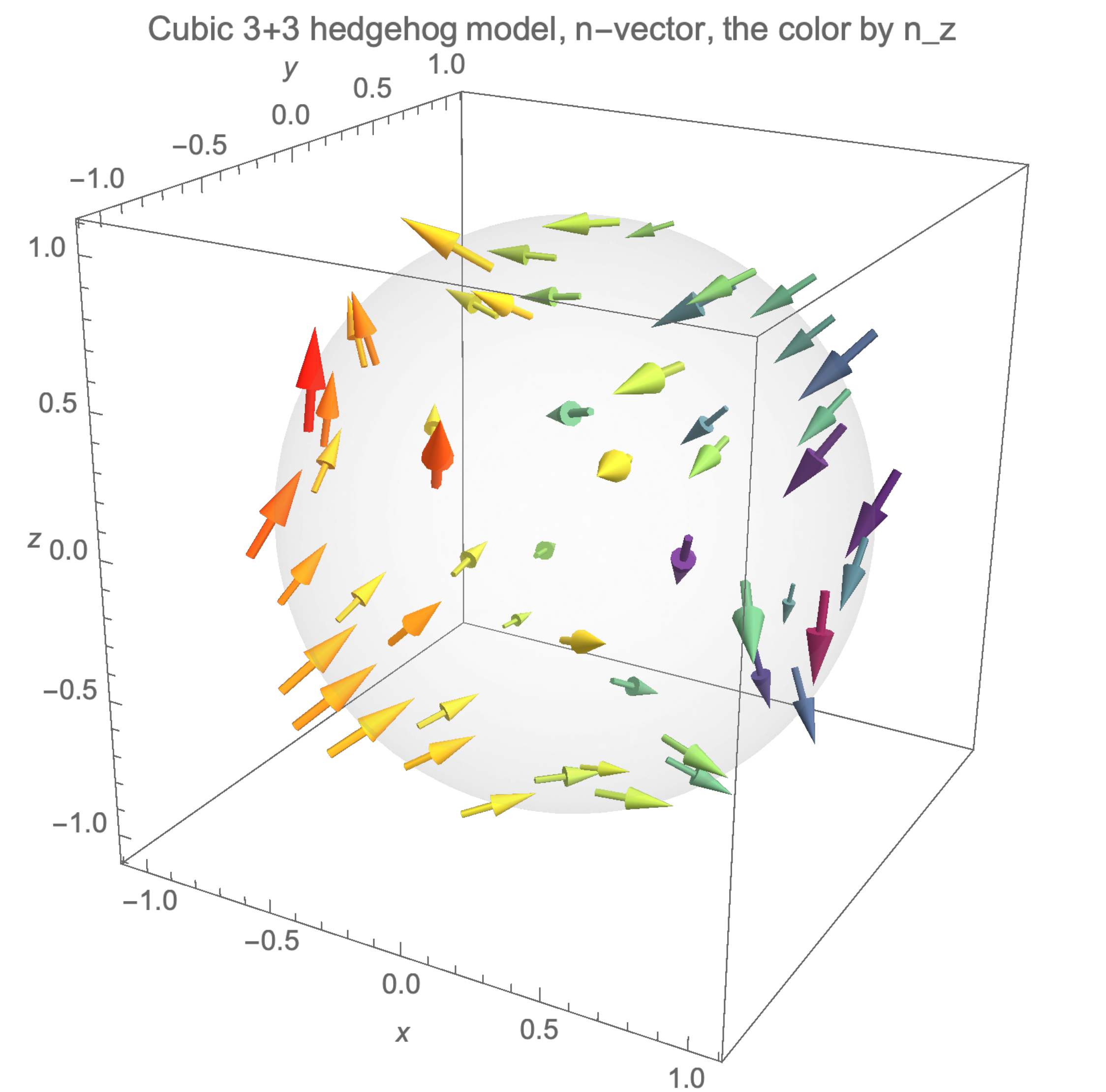

"Bloch" skyrmion (meron) 3D+2 magnetic structure

orthorhombic MSSG 19.2.29.2.m26.3 P2_12_12_1.1′ (0,b1,0)000s(0,0,g2)000s

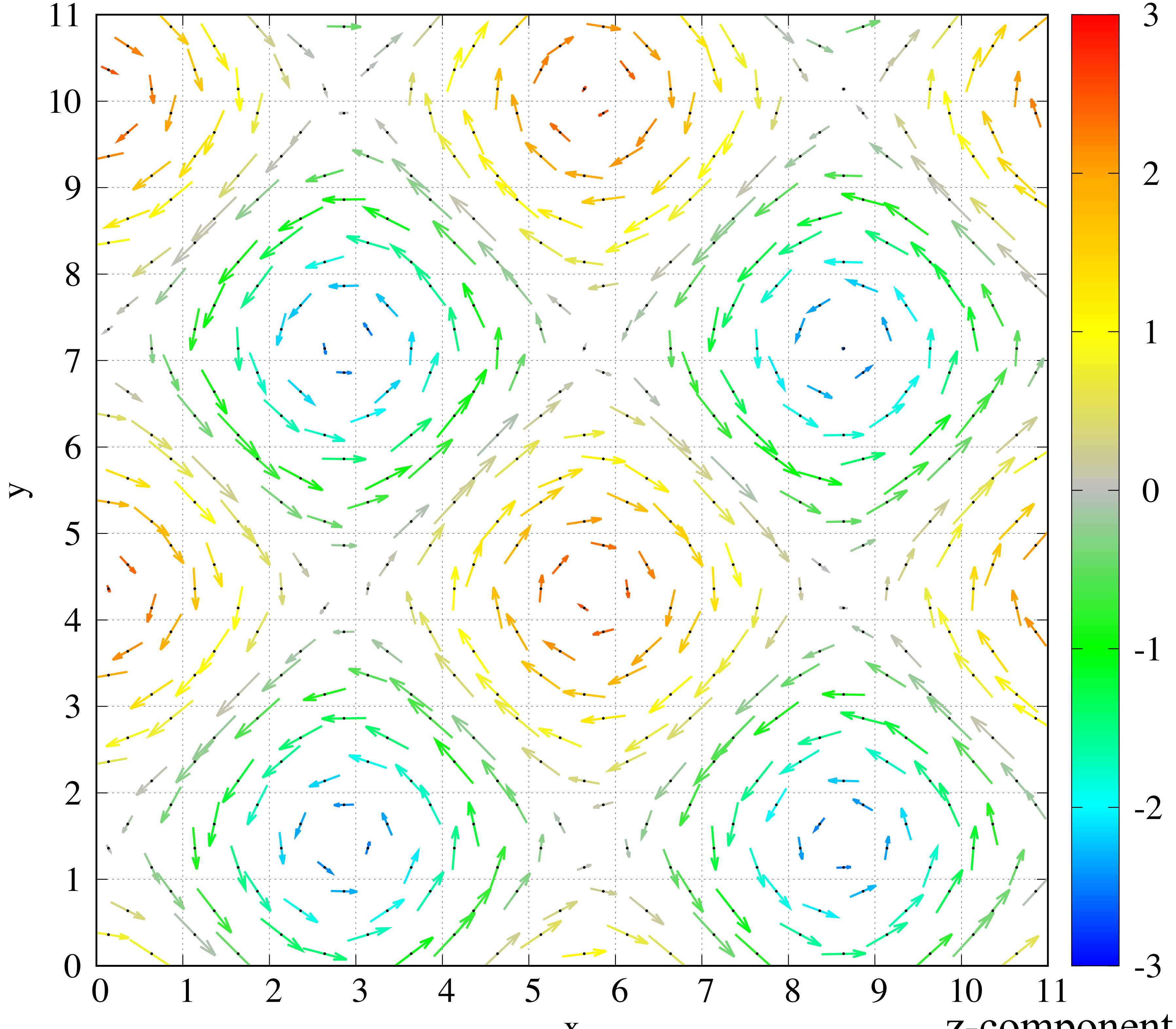

z-component by color

$$w(x,y) = \frac{1}{4\pi}\left(\mathbf{n}\cdot\left[\frac{\partial \mathbf{n}}{\partial x}\times\frac{\partial \mathbf{n}}{\partial y}\right]\right)$$

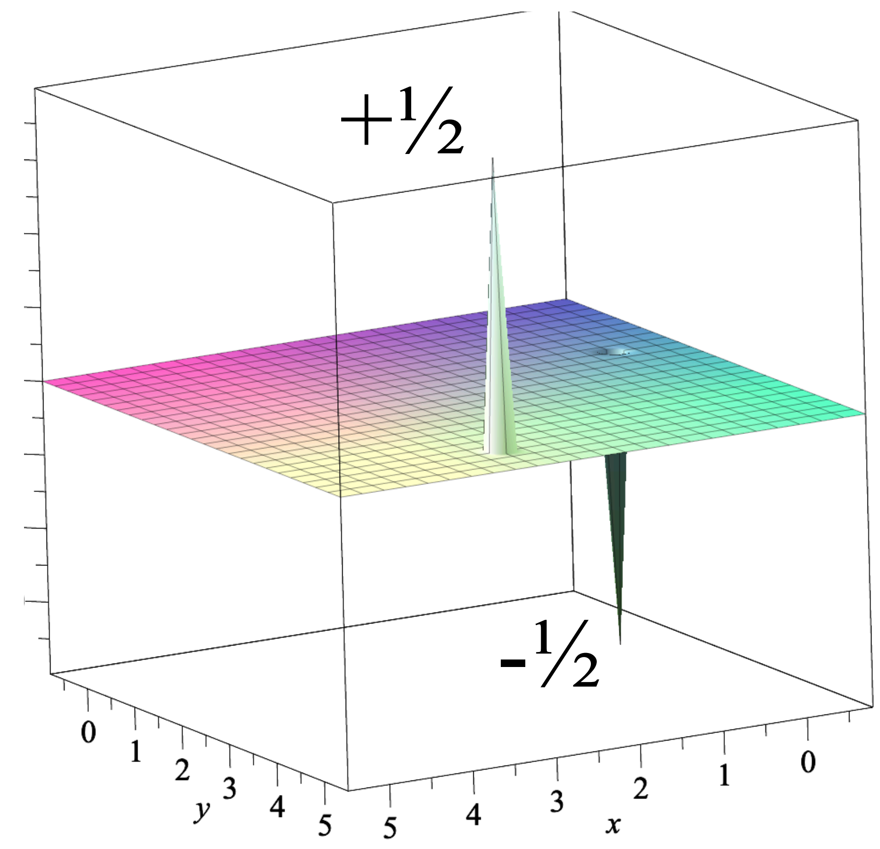

The total topo-charge Q = 0 in zero field.

“Bloch” skyrmion (meron) 3D+2 magnetic structure

orthorhombic MSSG 19.2.29.2.m26.3 P2_12_12_1.1′ (0,b1,0)000s(0,0,g2)000s

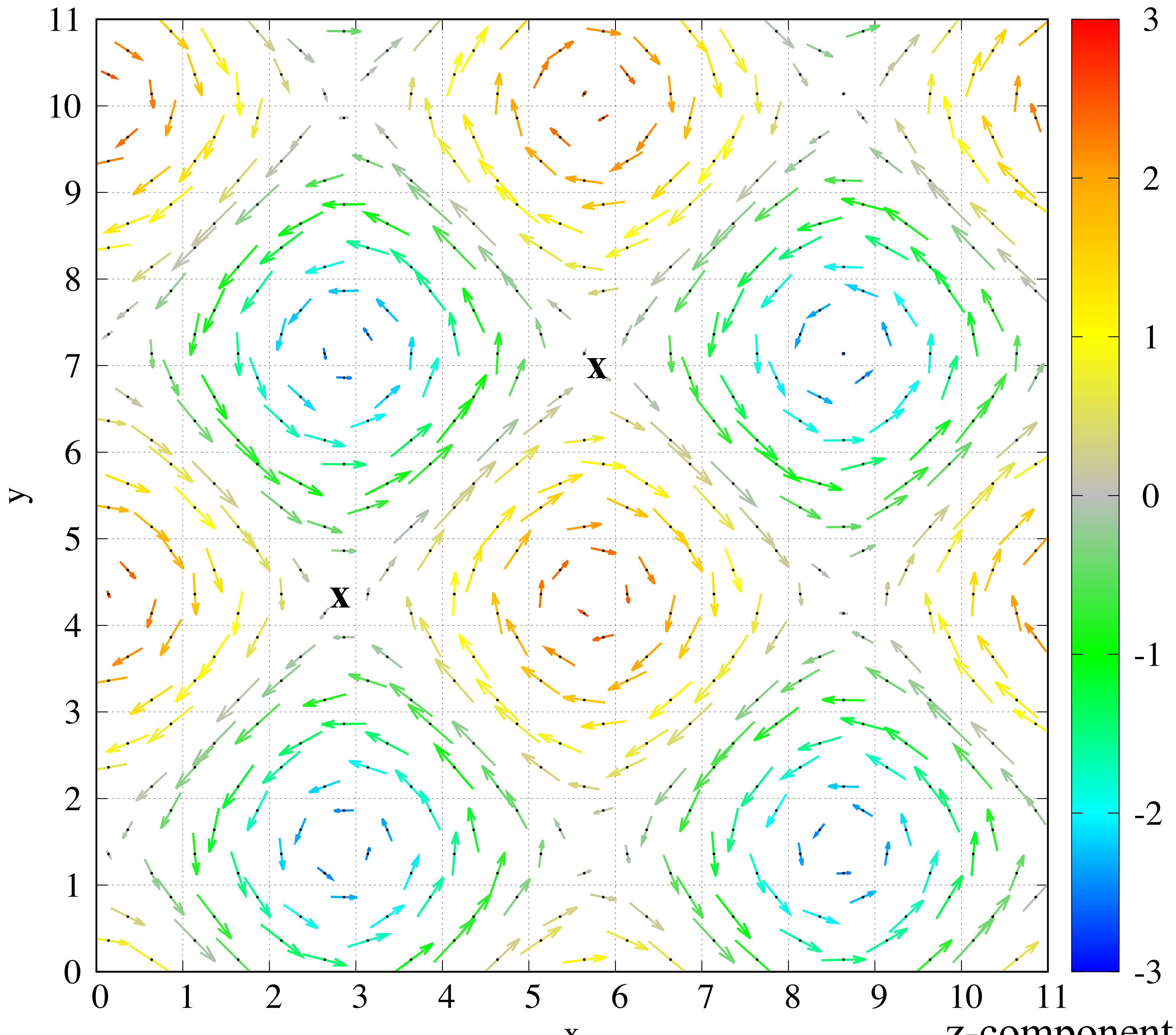

z-component by color

$$w(x,y) = \frac{1}{4\pi}\left(\mathbf{n}\cdot\left[\frac{\partial \mathbf{n}}{\partial x}\times\frac{\partial \mathbf{n}}{\partial y}\right]\right)$$

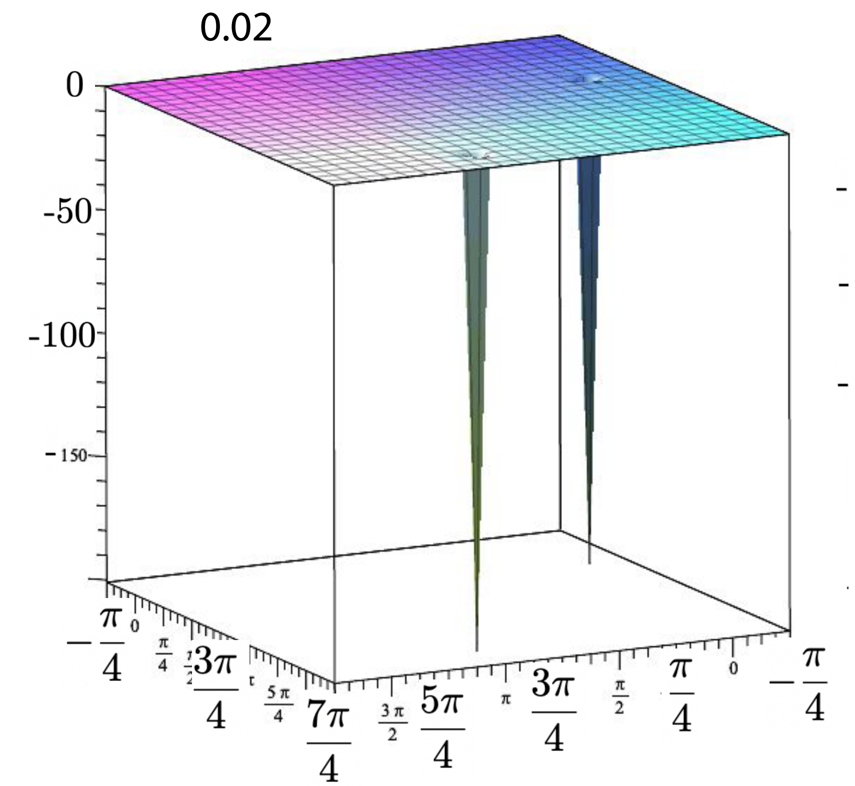

The total topo-charge Q = −1 in infinitesimal field.

Field plot, singularities and Bloch/Neel

{Mx , My} vs. {x,y}, Mz by color

Extrema can be only in |M|=0

```
:= {fig1, fig2} // Row
```

]=

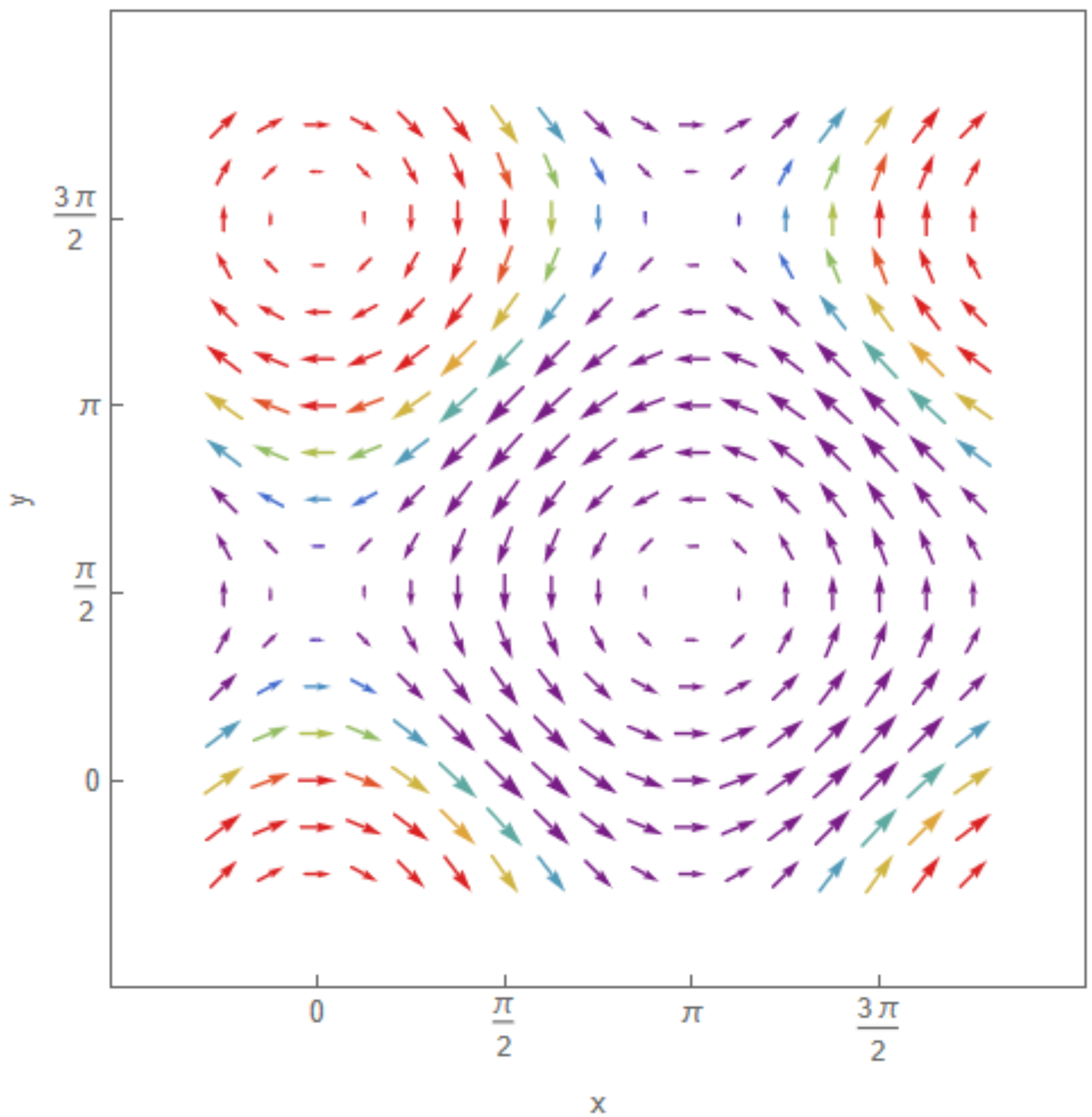

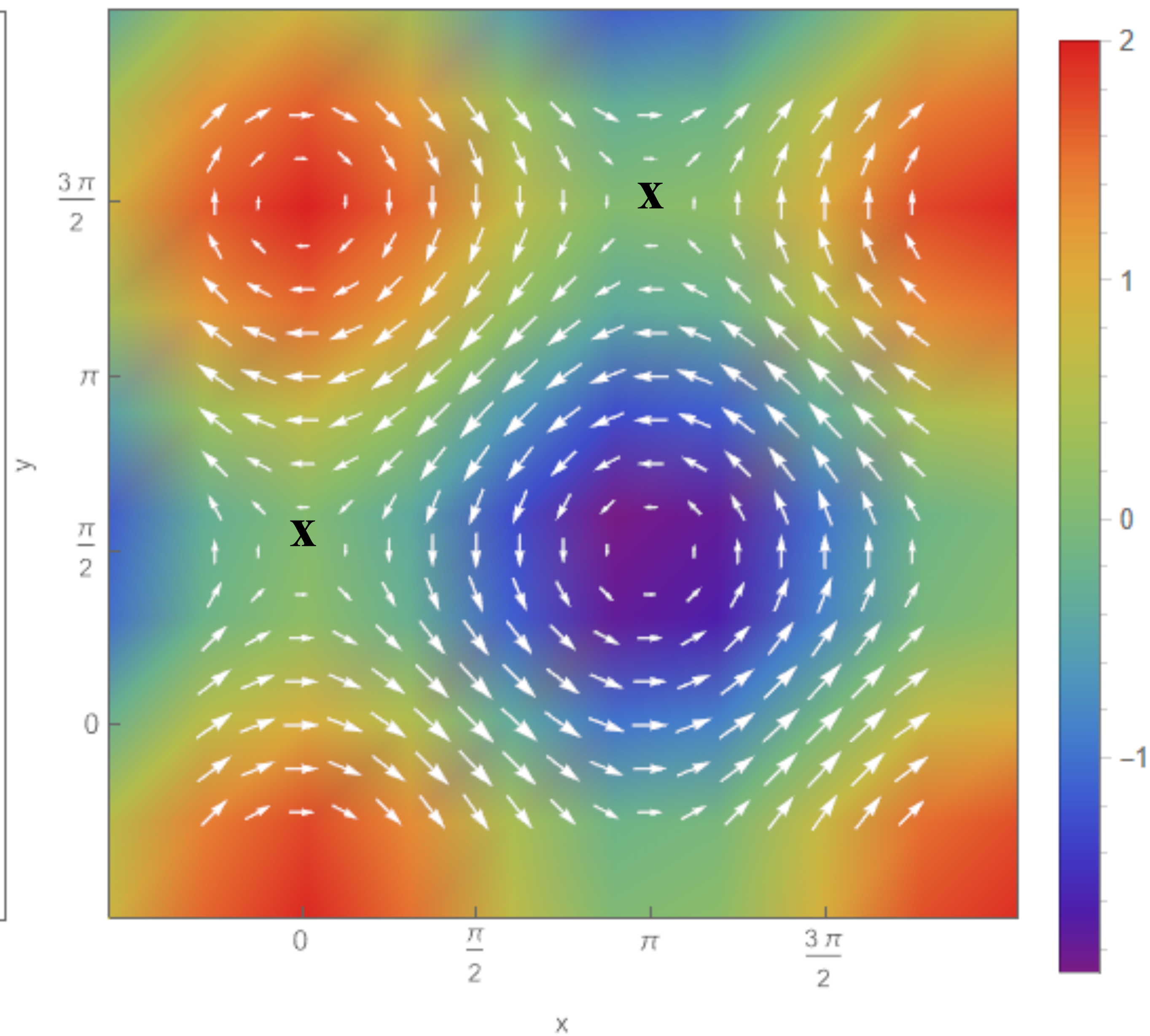

$$(mx, my, mz) = (\cos y, -\sin x, -\sin y + 1.001\cos x).$$

in CeAlGe for Ce1 $(mx, my, mz) = [\sin y,\ \sin x, 0.5(0.11 \cos x + 0.11\cos y)]$.

“Neel” skyrmion does not fit the data!

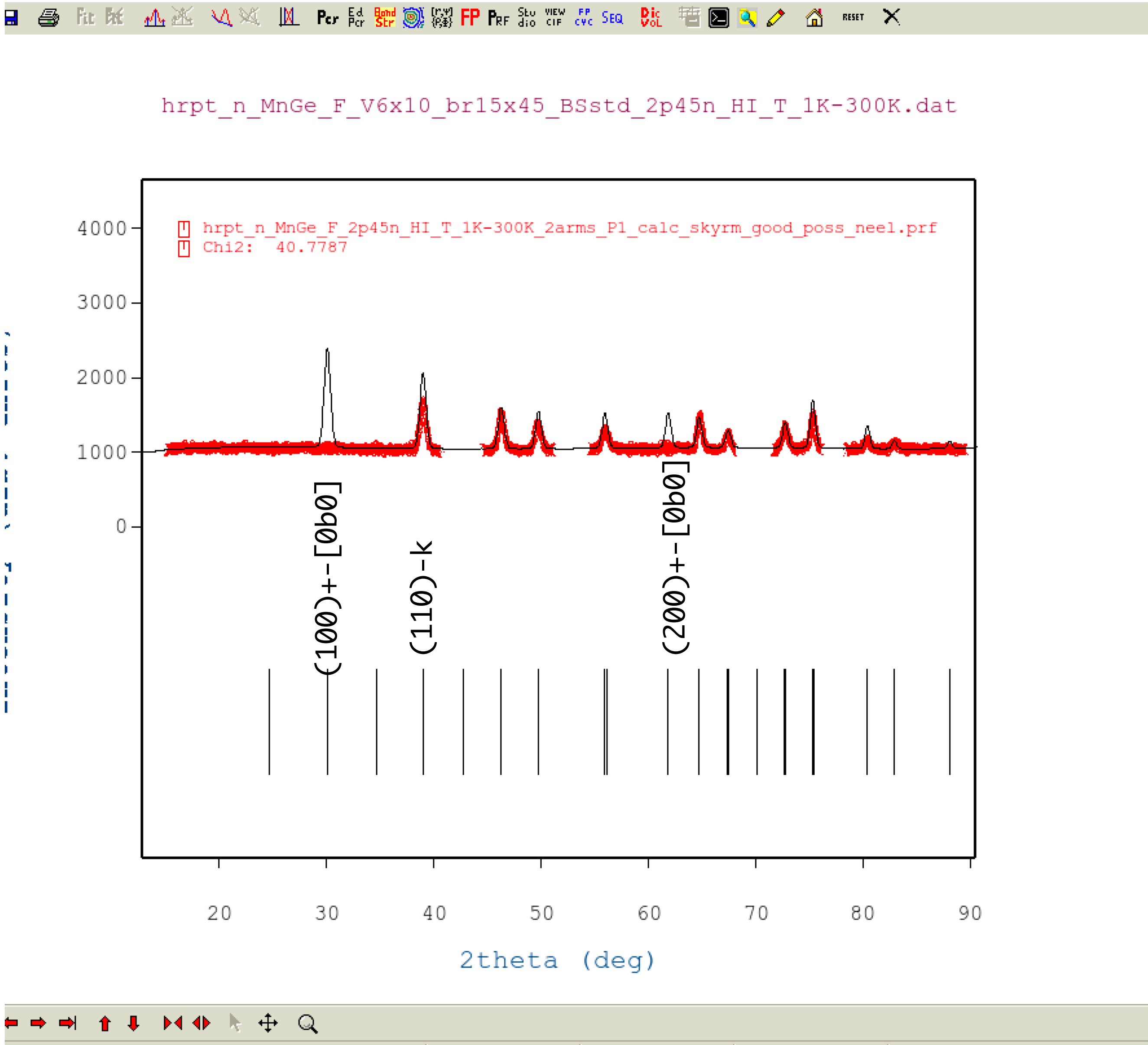

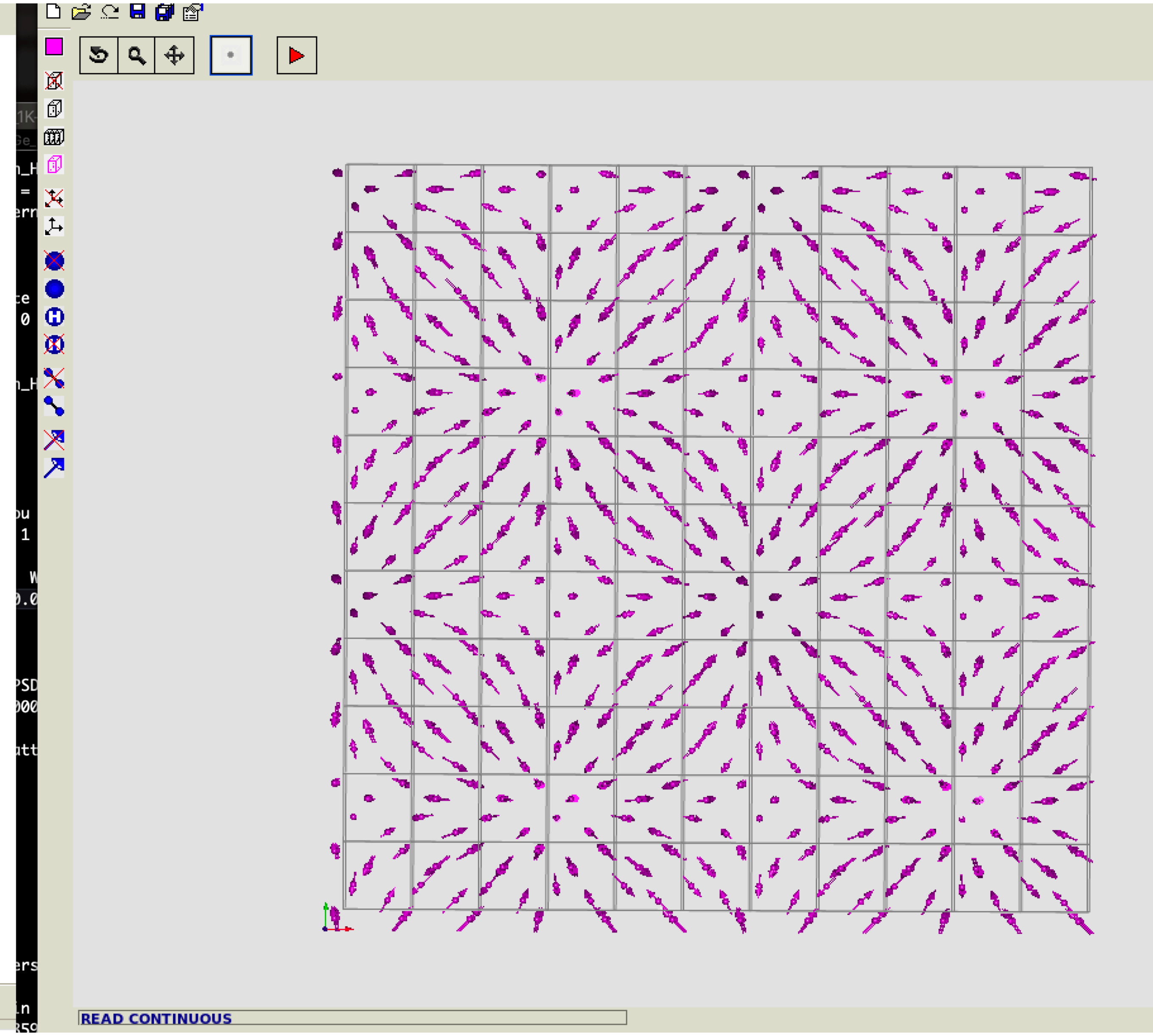

m1=1,m3=1,m4=-1 α3=α4=π/2 in (3)

Néel skyrmion

(mx, my, mz) = (sin x, cos y, − sin y + cos x).

the one in the paper is Bloch:

(mx, my, mz) = (cos y, − sin x, − sin y + cos x).

$$\begin{aligned} M_1 = [&m_1\cos(\tilde{y}+\alpha_1)+m_4\cos(\tilde{x}+\alpha_4), \longleftarrow \text{mx}\\ &m_2\cos(\tilde{y}+\alpha_2)+m_5\cos(\tilde{x}+\alpha_5), \longleftarrow \text{my}\\ &m_3\cos(\tilde{y}+\alpha_3)+m_6\cos(\tilde{x}+\alpha_6)], \longleftarrow \text{mz}\end{aligned}$$

CeAlGe

Motivation to study CeAlGe

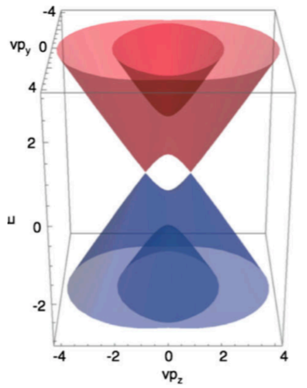

CeAlGe was predicted theoretically to be an easy-plane FM type-II Weyl semimetal (WSM)*.

It is still not clear if it is WSM… Instead, we have found that CeAlGe is an antiferromagnet with rich phase diagram

It has topologically nontrivial magnetization textures in real-space ==> topological Hall effect (THE).

* G. Chang, B. Singh, S.-Y. Xu, G. Bian, S.-M. Huang, C.-H. Hsu, I. Belopolski, N. Alidoust, D. S. Sanchez, H. Zheng, et a
Physical Review B 97 (2018).

Superspace magnetic structure in Weyl semimetal CeAlGe. Multi arm antiferromagnetic order.

BULK SINGLE-CRYSTAL GROWTH OF THE … PHYSICAL REVIEW MATERIALS 3, 024204 (2019)

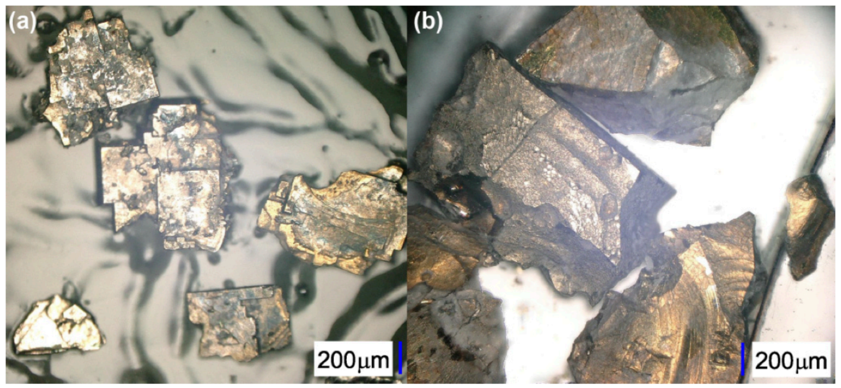

FIG. 2. Pictures of the flux-grown crystals of (a) CeAlGe and (b) PrAlGe right after flux removal using NaOH-H_2O, and before subsequent annealing

FIG. 3. Photos of (a) the cast CeAlGe rod, and the floating-zone-grown crystals of (b) CeAlGe and (c) PrAlGe.

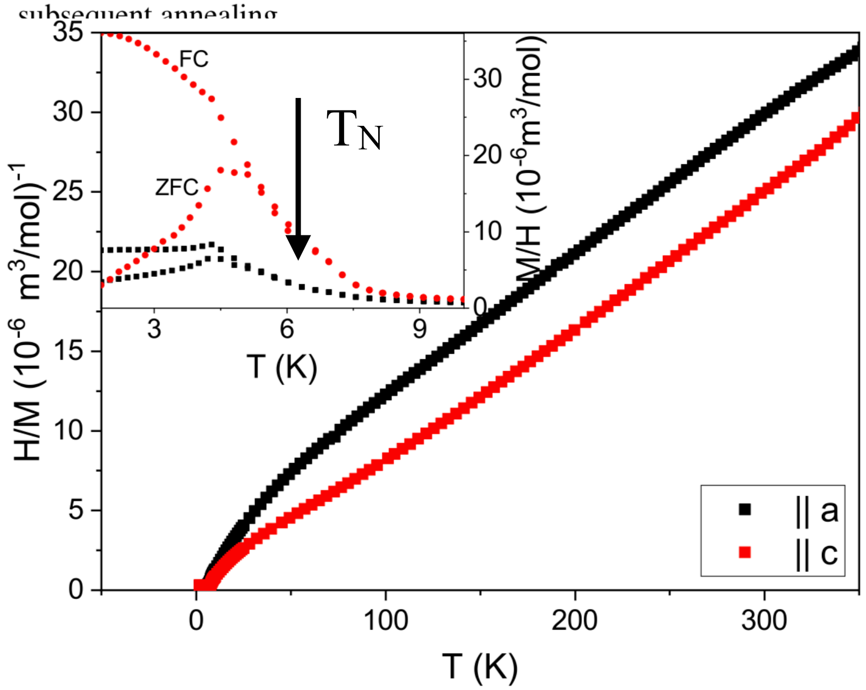

FIG. 8. Magnetic data obtained on a floating-zone-grown CeAlGe single crystal with a mass of 125.4 mg. The magnetic

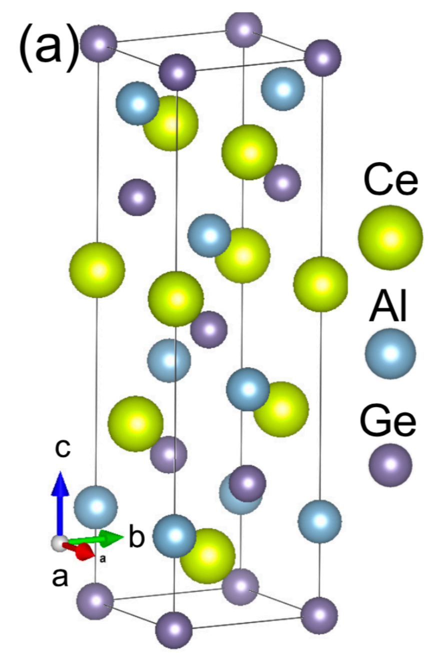

Space Group: 109 I4_1md C4v-11
non-centrosymmetric
Lattice parameters:
a=4.25717, c=14.64520

Ce1 4a (0,0,z), z=-0.41000 single magnetic Ce site

Neutron diffraction experiments: HRPT and DMC, SANS at PSI Switzerland, D33, at ILL France
Resistivity: Topologicall Hall Effect in University of Tokyo

Samples: both powder and single crystals of CeAlGe grown at PSI in Solid State Chemistry group

P. Puphal, et al, Physical Review Letters, 124, 017202 (2020)

Magnetic peaks are well seen from both powder and s.c. neutron diffraction

CeAlGe

k1=[g,0,0], SM point of BZ, g=0.06503(22) ~65Å

Magnetic NPD difference profile taken between T = 1.7 K and 10 K

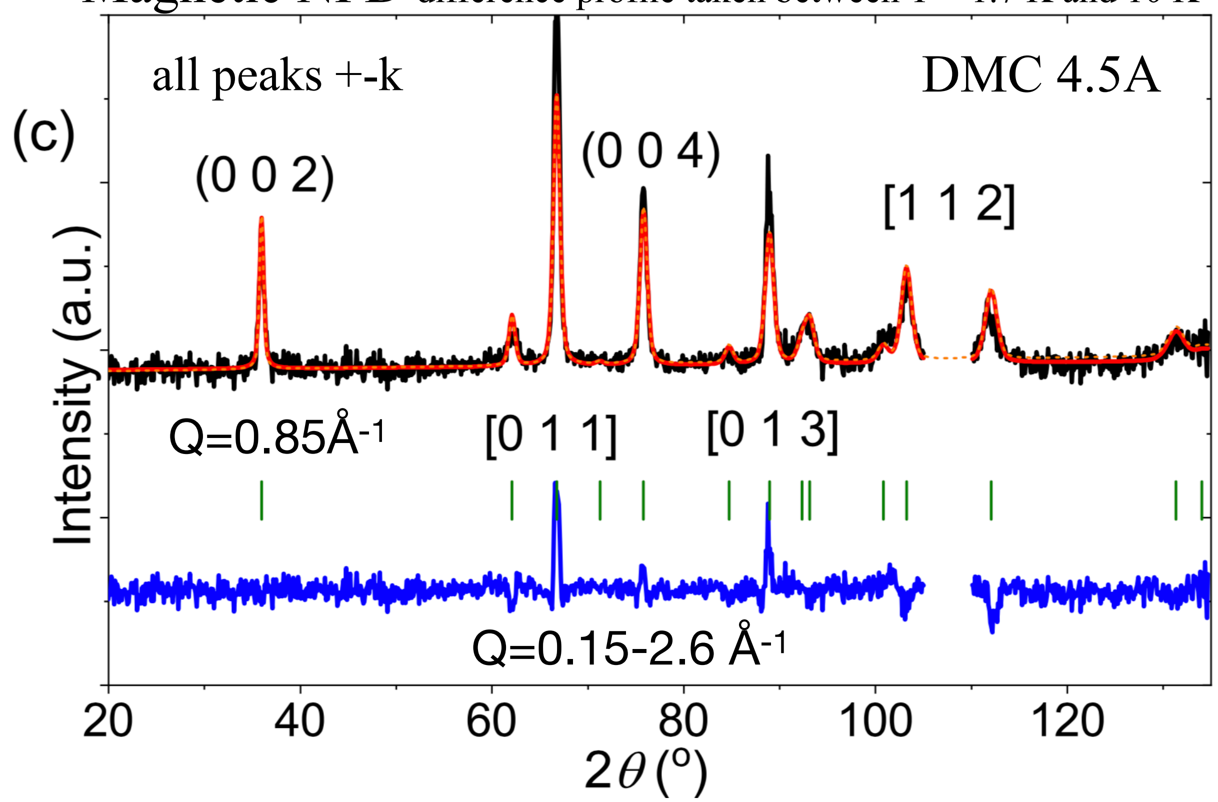

Gamma point k=0 does not fit NPD

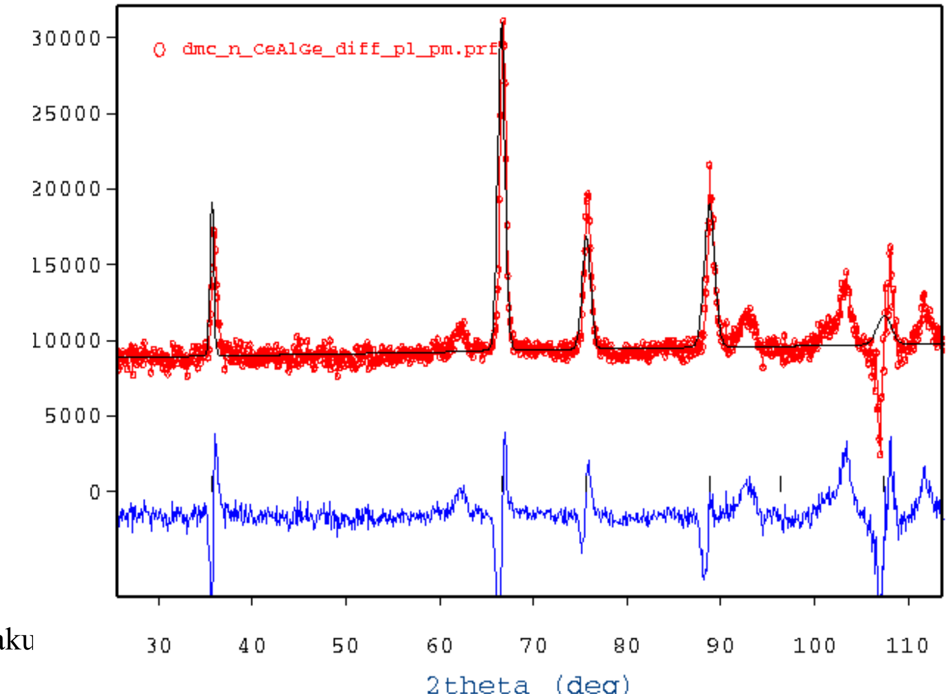

P. Puphal, et al, Physical Review Letters, 124, 017202 (2020)

Magnetic peaks are well seen from both powder and s.c. neutron diffraction

CeAlGe

k1=[g,0,0], SM point of BZ, g=0.06503(22) ~65Å

Magnetic NPD difference profile taken between T = 1.7 K and 10 K

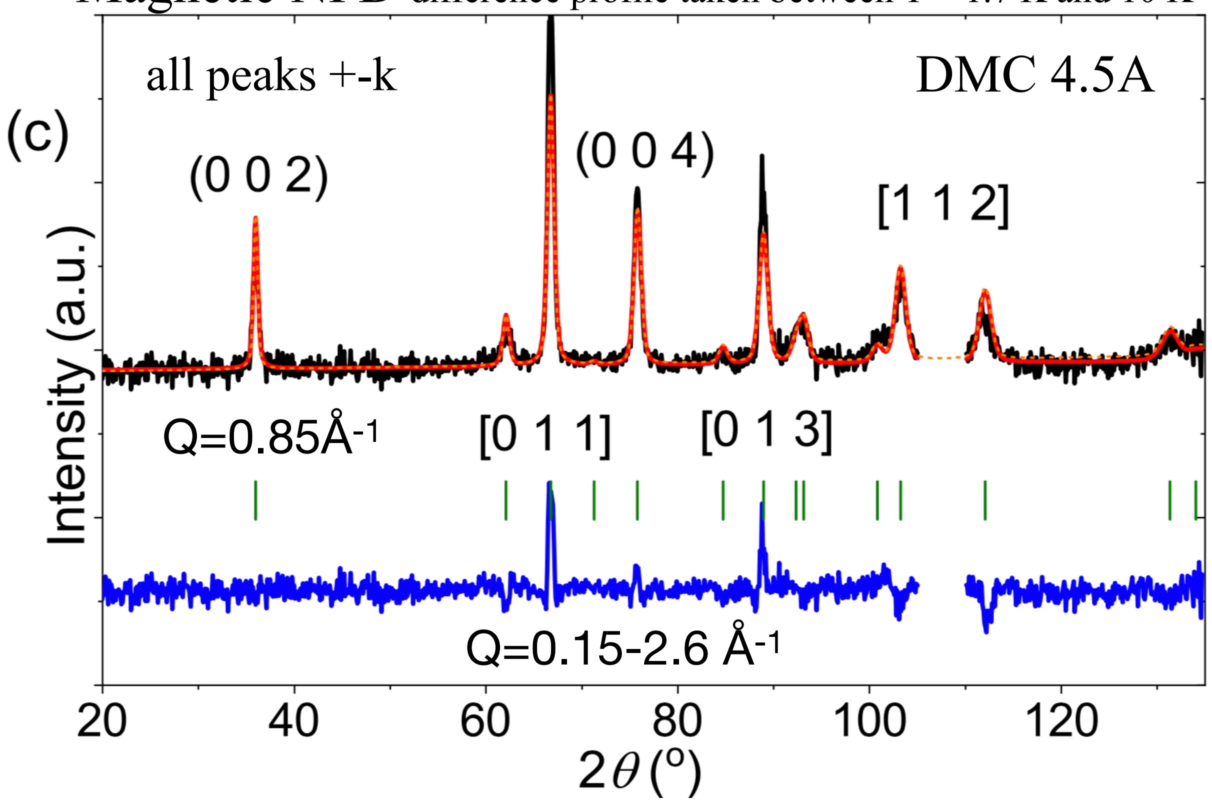

Gamma point k=0 does not fit NPD

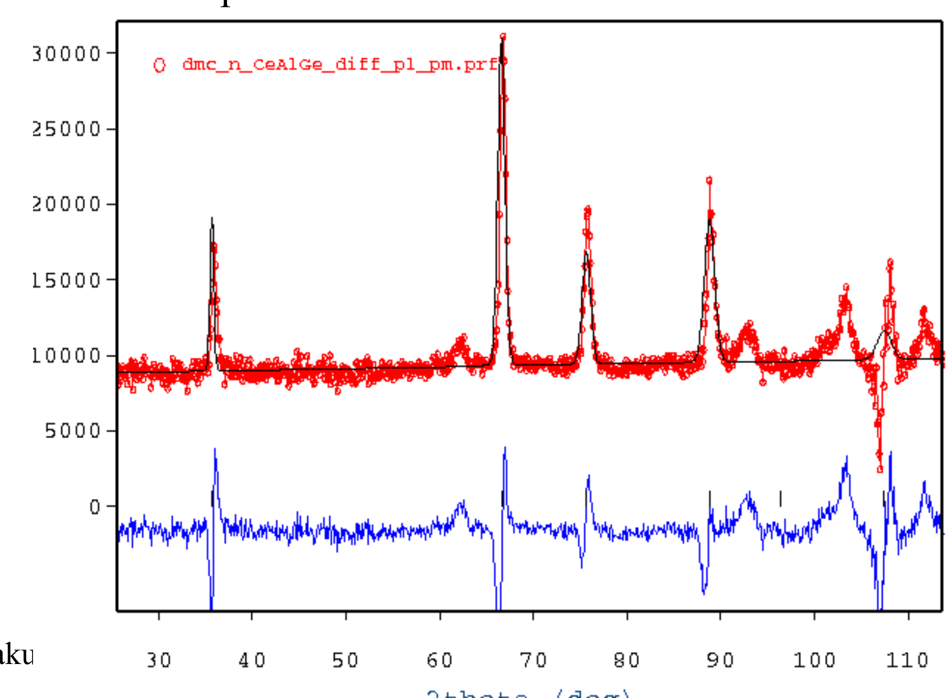

k1=[g,0,0], k2=[0,g,0]

Single crystal

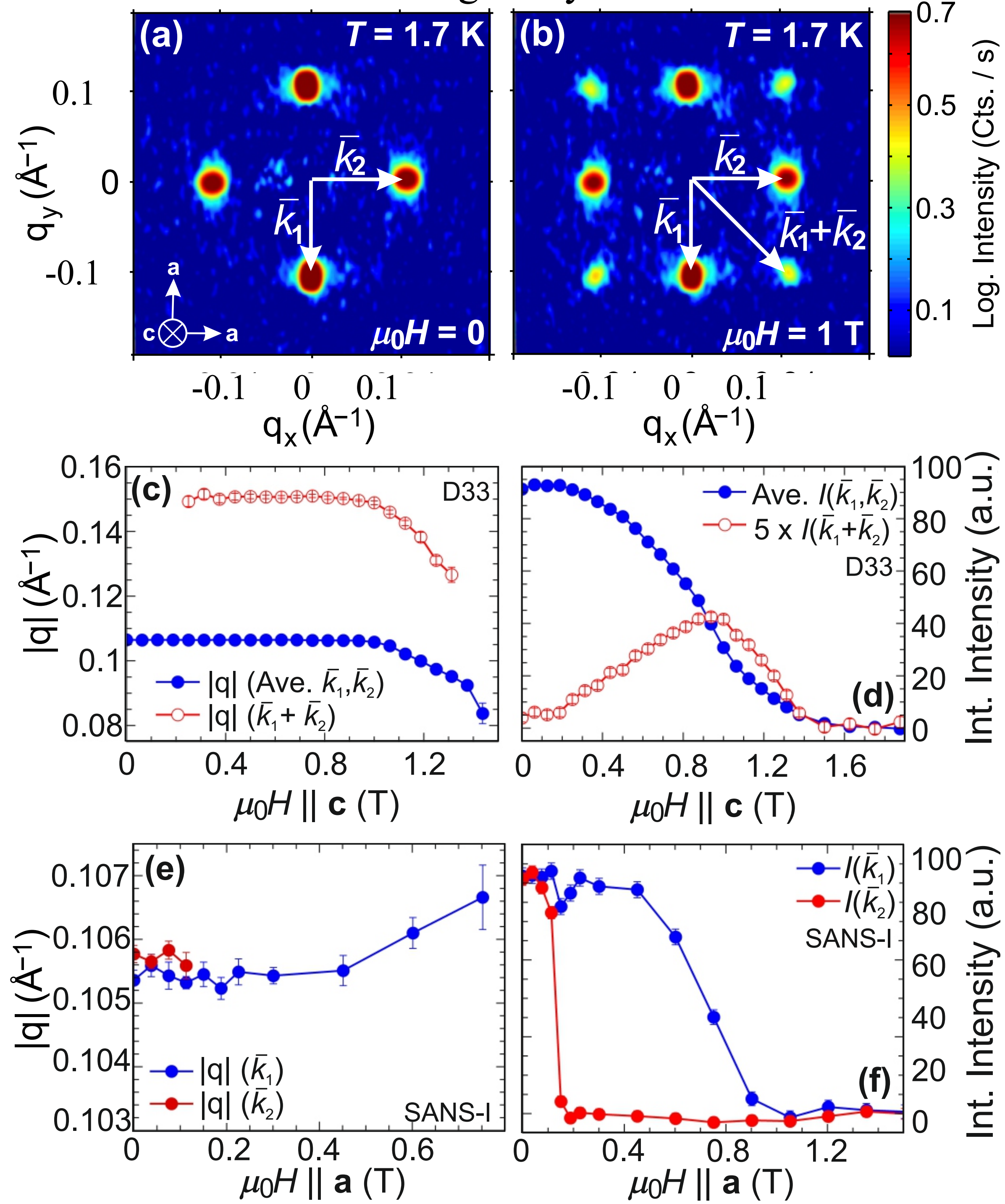

P. Puphal, et al, Physical Review Letters, 124, 017202 (2020)

One k-case, standard representation analysis without magnetic group symmetry arguments.

Space group $I4_1md$:
8 symops & I-centering,
Ce 4a (0,0,z) single magnetic Ce site: 4 atoms per cell

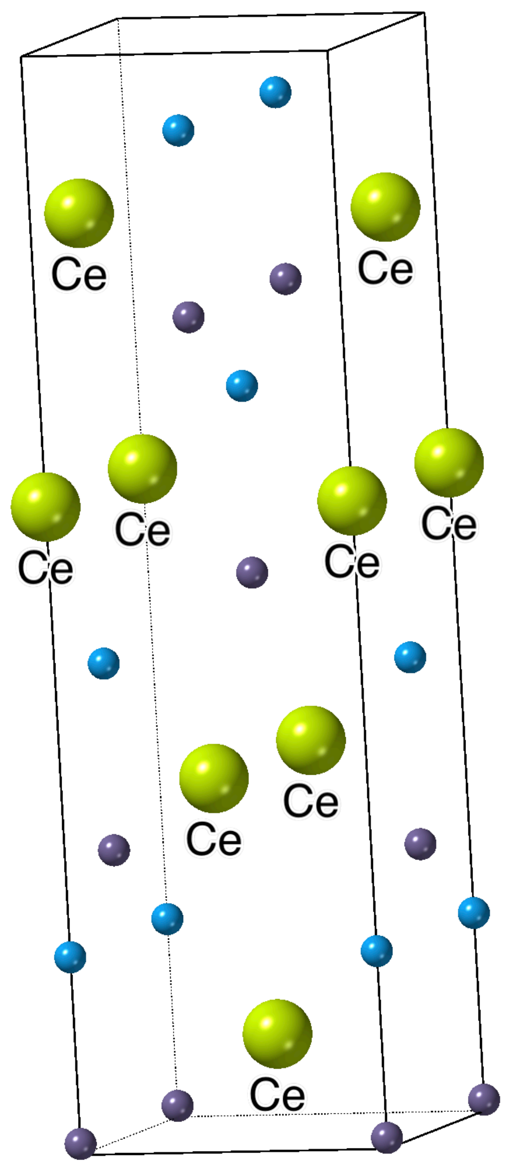

One k-case, standard representation analysis without magnetic group symmetry arguments.

Space group $I4_1md$:
8 symops & I-centering,
Ce 4a (0,0,z) single magnetic Ce site: 4 atoms per cell

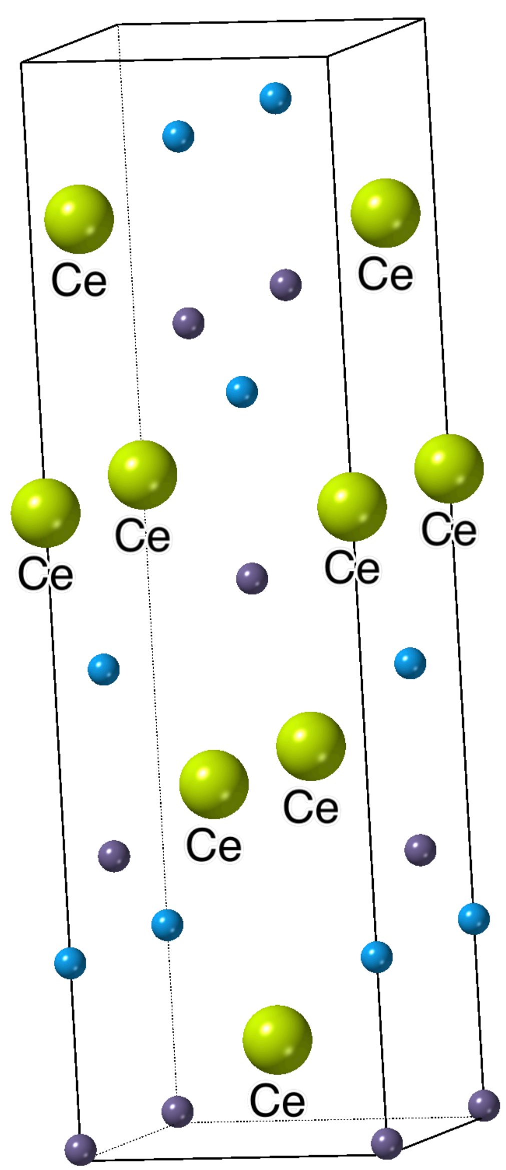

$$4(a)\quad \begin{array}{l} \mathrm{Ce1}(0,0,z) \\ \mathrm{Ce2}(0,\frac{1}{2},z+\frac{1}{4}) \end{array} \qquad \bar{y}, x+\frac{1}{2}, z+\frac{1}{4}$$

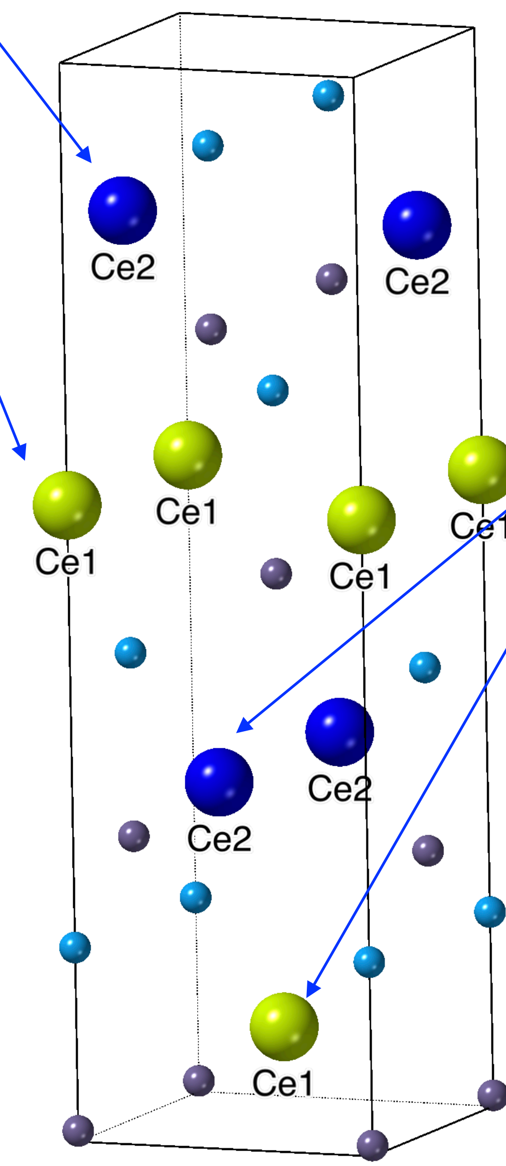

Two other Ce's are generated b
I-centering translations (½, ½, ½)+

subgroup tree for I4_1md [u,0,0]+[0,u,0]

I4_1md1’

4D irrep SM2

1 incommensurate modulation

OPD=(a,0;0,0)

I2mm.1'(0,0,g)0s0s

OPD=(a,b;0,0)

Bm.1'(a,b,0)ss

irrep OPD

$$\begin{pmatrix} 1 & 0 & 0 & 0 \\ 0 & -1 & 0 & 0 \\ 0 & 0 & 1 & 0 \\ 0 & 0 & 0 & -1 \end{pmatrix}\begin{pmatrix} a \\ b \\ c \\ d \end{pmatrix}$$

$$\left.\begin{matrix} 0 & 0 & 1 & 0 \\ 0 & 0 & 0 & -1 \\ \mathrm{Cos}(\pi u) & \mathrm{Sin}(\pi u) & 0 & 0 \\ \mathrm{Sin}(\pi u) & \mathrm{Cos}(\pi u) & 0 & 0 \end{matrix}\right)$$

$$\left.\begin{matrix} 0 & 0 & 1 & 0 \\ 0 & 0 & 0 & 1 \\ \mathrm{Cos}(\pi u) & -\mathrm{Sin}(\pi u) & 0 & 0 \\ \mathrm{Sin}(\pi u) & -\mathrm{Cos}(\pi u) & 0 & 0 \end{matrix}\right)$$

$$\begin{pmatrix} -1 & 0 & 0 & 0 \\ 0 & -1 & 0 & 0 \\ 0 & 0 & -1 & 0 \\ 0 & 0 & 0 & 1 \end{pmatrix}$$

subgroup tree for I4_1md [u,0,0]+[0,u,0]

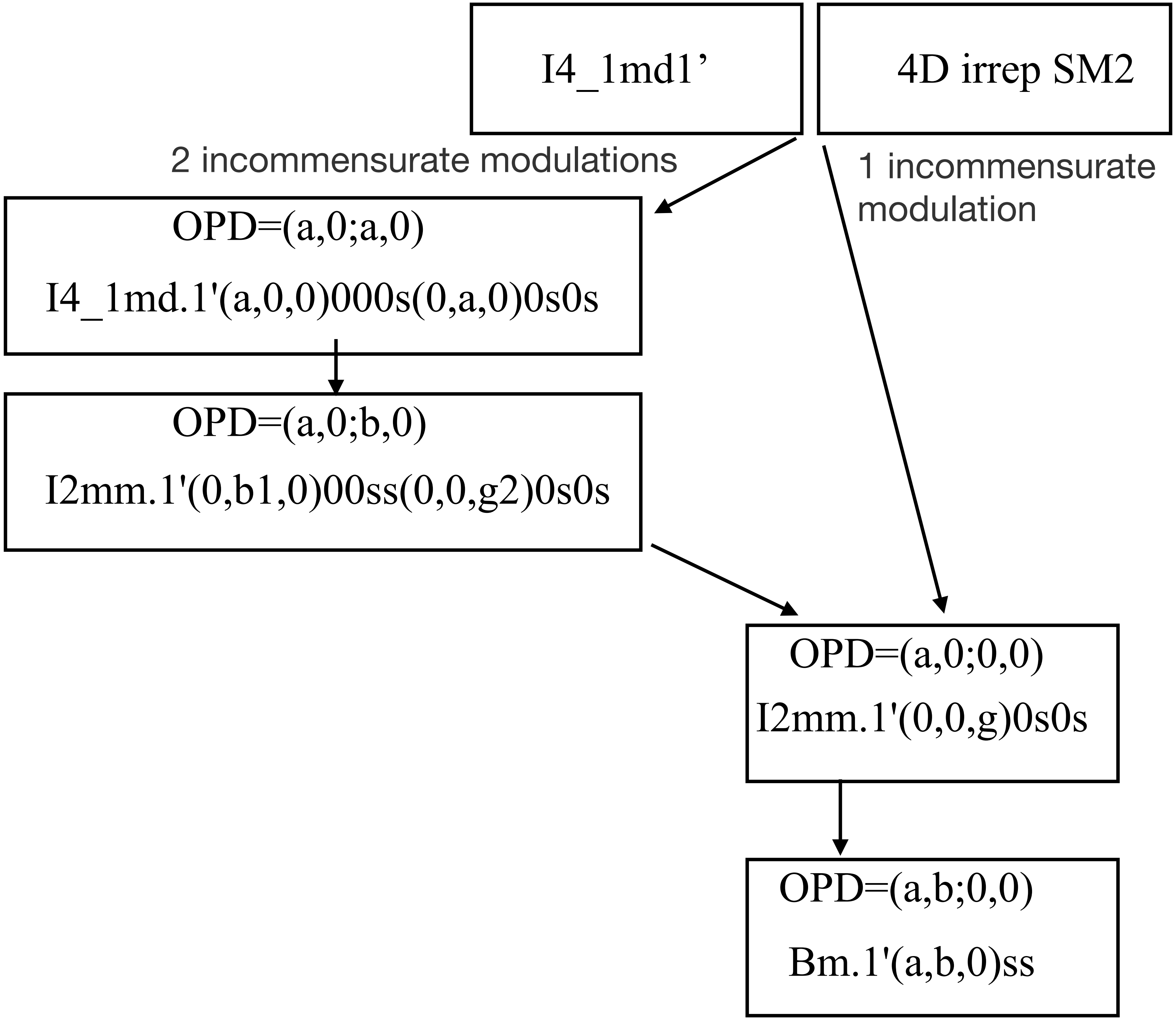

irrep OPD

$$\begin{pmatrix} 1 & 0 & 0 & 0 \\ 0 & -1 & 0 & 0 \\ 0 & 0 & 1 & 0 \\ 0 & 0 & 0 & -1 \end{pmatrix} \begin{pmatrix} a \\ b \\ c \\ d \end{pmatrix}$$

$$\begin{matrix} 0 & 0 & 1 & 0 \\ 0 & 0 & 0 & -1 \\ \mathrm{Cos}(\pi u) & \mathrm{Sin}(\pi u) & 0 & 0 \\ \mathrm{Sin}(\pi u) & \mathrm{Cos}(\pi u) & 0 & 0 \end{matrix} \Bigg)$$

$$\begin{matrix} 0 & 0 & 1 & 0 \\ 0 & 0 & 0 & 1 \\ \mathrm{Cos}(\pi u) & -\mathrm{Sin}(\pi u) & 0 & 0 \\ \mathrm{Sin}(\pi u) & -\mathrm{Cos}(\pi u) & 0 & 0 \end{matrix} \Bigg)$$

$$\begin{pmatrix} -1 & 0 & 0 & 0 \\ 0 & -1 & 0 & 0 \\ 0 & 0 & -1 & 0 \\ 0 & 0 & 0 & 1 \end{pmatrix}$$

CeAlGe: Maximal symmetry full star superspace 3D+2 magnetic group I4_1md1'(a00)000s(0a0)0s0s

$I4_1md1'$ IR: mSM2 , k-active= (g,0,0),(0,g,0)

I4_1md1'(a,0,0)000s(0,a,0)0s0s
single Ce site: Ce1 and Ce2 equivalent

View along the z-(c-)axis of the magnetic structure of CeAlGe. The x- and y-axes are in units of in-plane lattice parameter a.

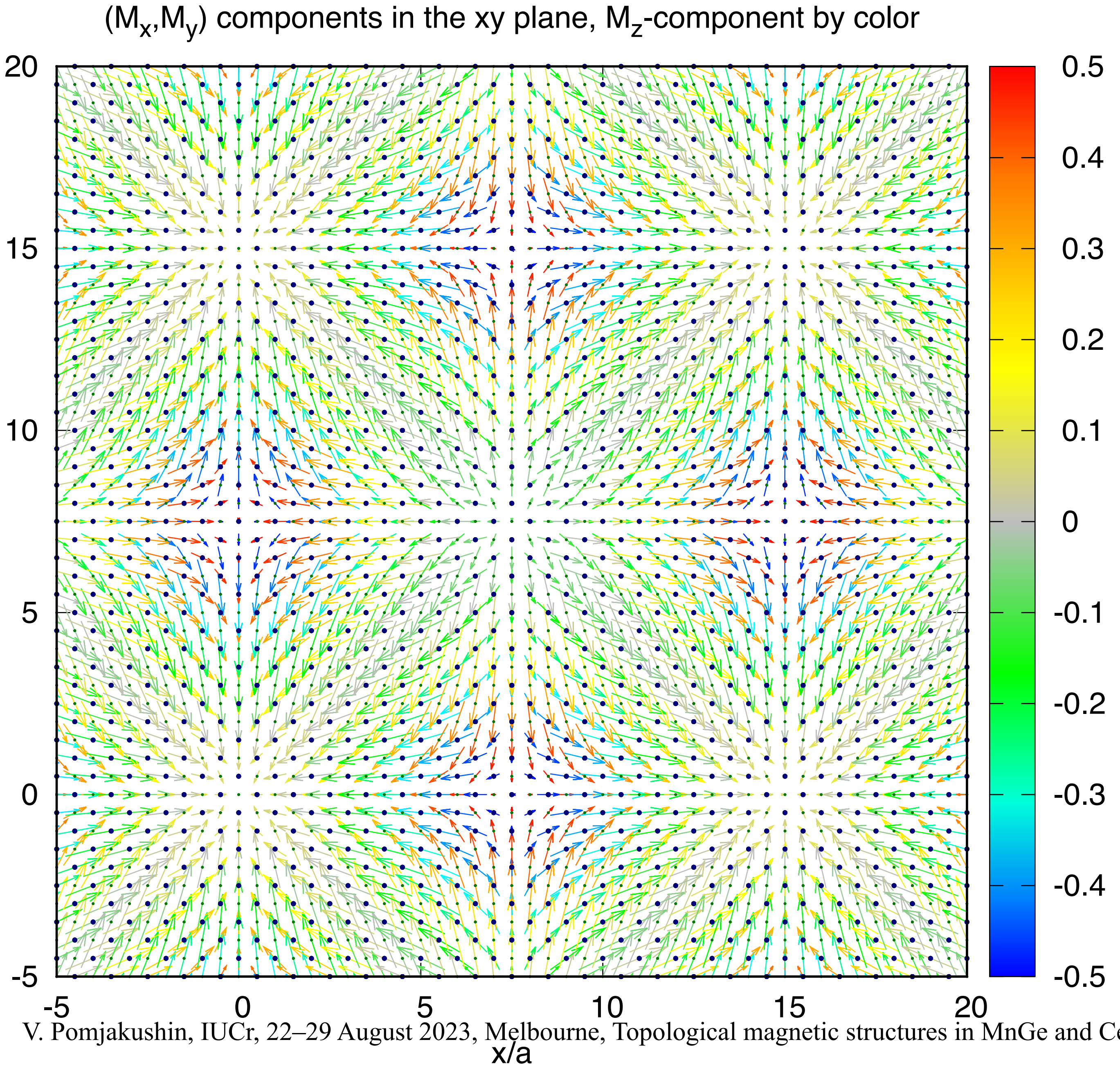

k1=[g,0,0], SM point of BZ, g=0.06503(22): four arms

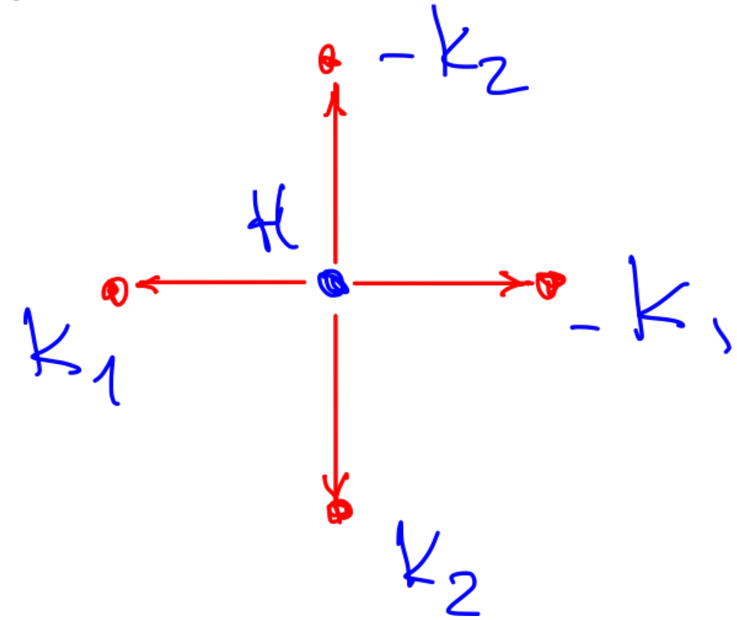

CeAlGe: Maximal symmetry full star superspace 3D+2 magnetic group I4_1md1'(a00)000s(0a0)0s0s

$I4_1md1'$ IR: mSM2 , k-active= (g,0,0),(0,g,0)

I4_1md1'(a,0,0)000s(0,a,0)0s0s
single Ce site: Ce1 and Ce2 equivalent

k1=[g,0,0], SM point of BZ, g=0.06503(22): four arms

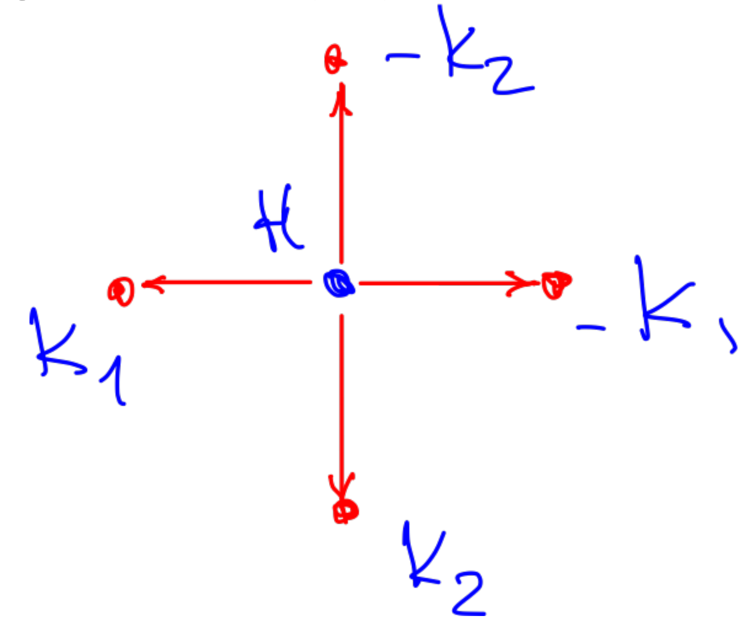

View along the z-(c-)axis of the magnetic structure of CeAlGe. The x- and y-axes are in units of in-plane lattice parameter a.

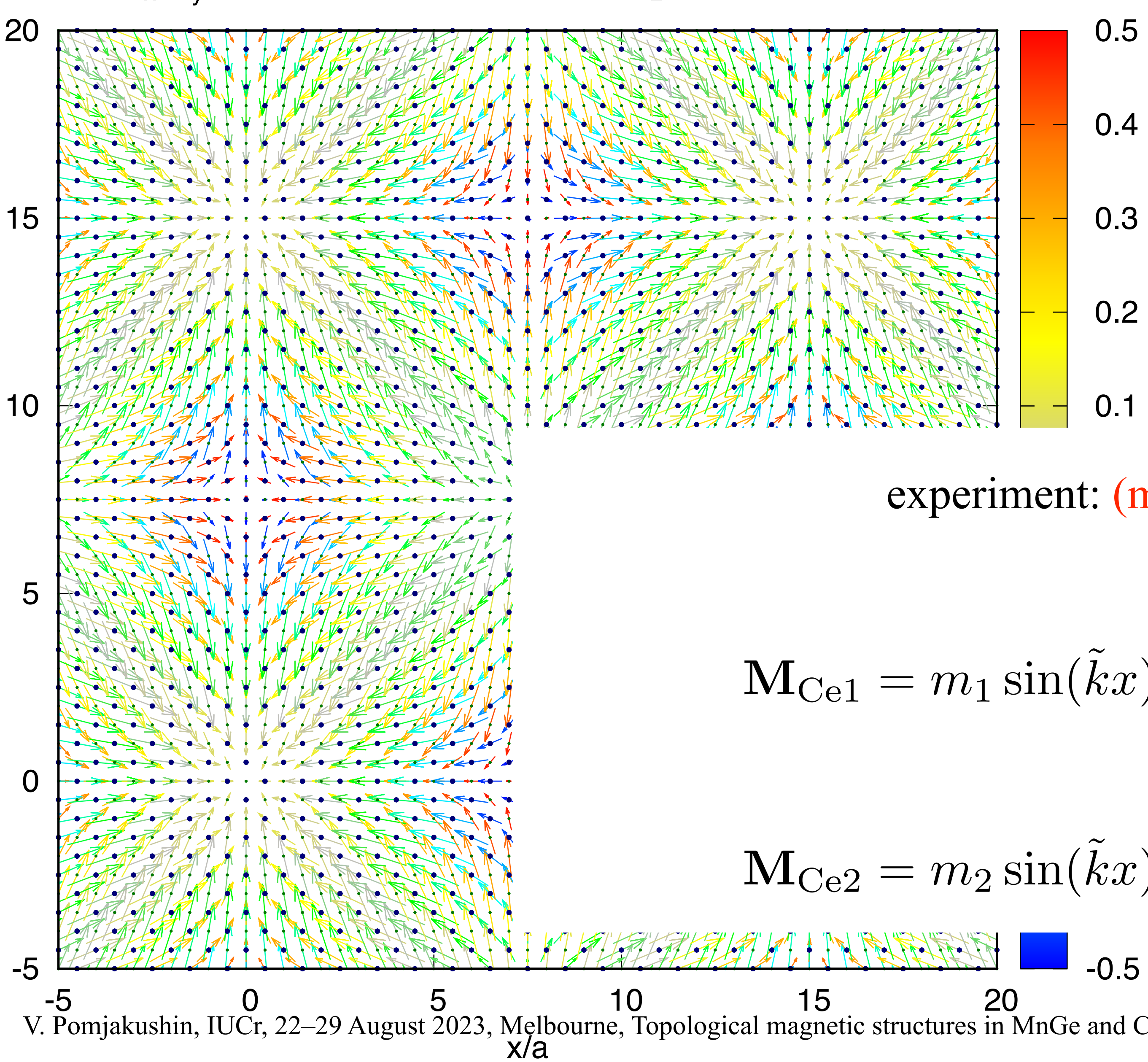

All Ce are equivalent and their moments are given symmetrically by 4 parameters

experiment: (m1,m2,m3,m4) = (0.44(1), 1.02(1), −0.21(5), 0.29(7)) μ_B.

$\tilde{k}=2\pi|\boldsymbol{k}_1|=2\pi|\boldsymbol{k}_2|=2\pi g$

$$\mathbf{M}_{\mathrm{Ce1}} = m_1 \sin(\tilde{k}x)\mathbf{e}_{\boldsymbol{x}} + m_2 \sin(\tilde{k}y)\mathbf{e}_{\boldsymbol{y}} + \Big(m_3 \cos(\tilde{k}x) + m_4 \cos(\tilde{k}y)\Big)\,\mathbf{e}_{\boldsymbol{z}}$$

$$\mathbf{M}_{\mathrm{Ce2}} = m_2 \sin(\tilde{k}x)\mathbf{e}_{\boldsymbol{x}} + m_1 \sin(\tilde{k}y)\mathbf{e}_{\boldsymbol{y}} + \Big(m_4 \cos(\tilde{k}x) + m_3 \cos(\tilde{k}y)\Big)\,\mathbf{e}_{\boldsymbol{z}}$$

CeAlGe: Maximal symmetry full star superspace 3D+2 magnetic group I4_1md1'(a00)000s(0a0)0s0s

$I4_1md1'$ IR: mSM2 , k-active= (g,0,0),(0,g,0)

↓

I4_1md1'(a,0,0)000s(0,a,0)0s0s
single Ce site: Ce1 and Ce2 equivalent

k1=[g,0,0], SM point of BZ, g=0.06503(22): four arms

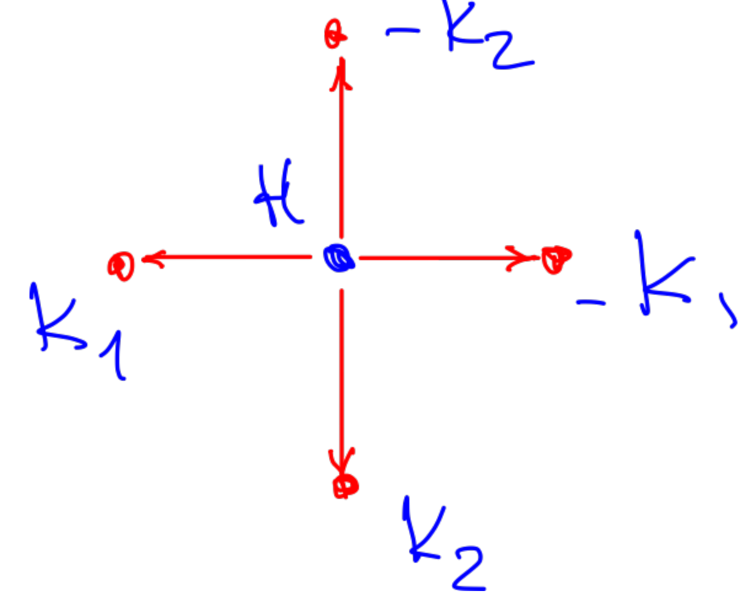

All Ce are equivalent and their moments are given symmetrically by 4 parameters

View along the z-(c-)axis of the magnetic structure of CeAlGe. The x- and y-axes are in units of in-plane lattice parameter a.

(M_x,M_y) components in the xy plane, M_z-component by color

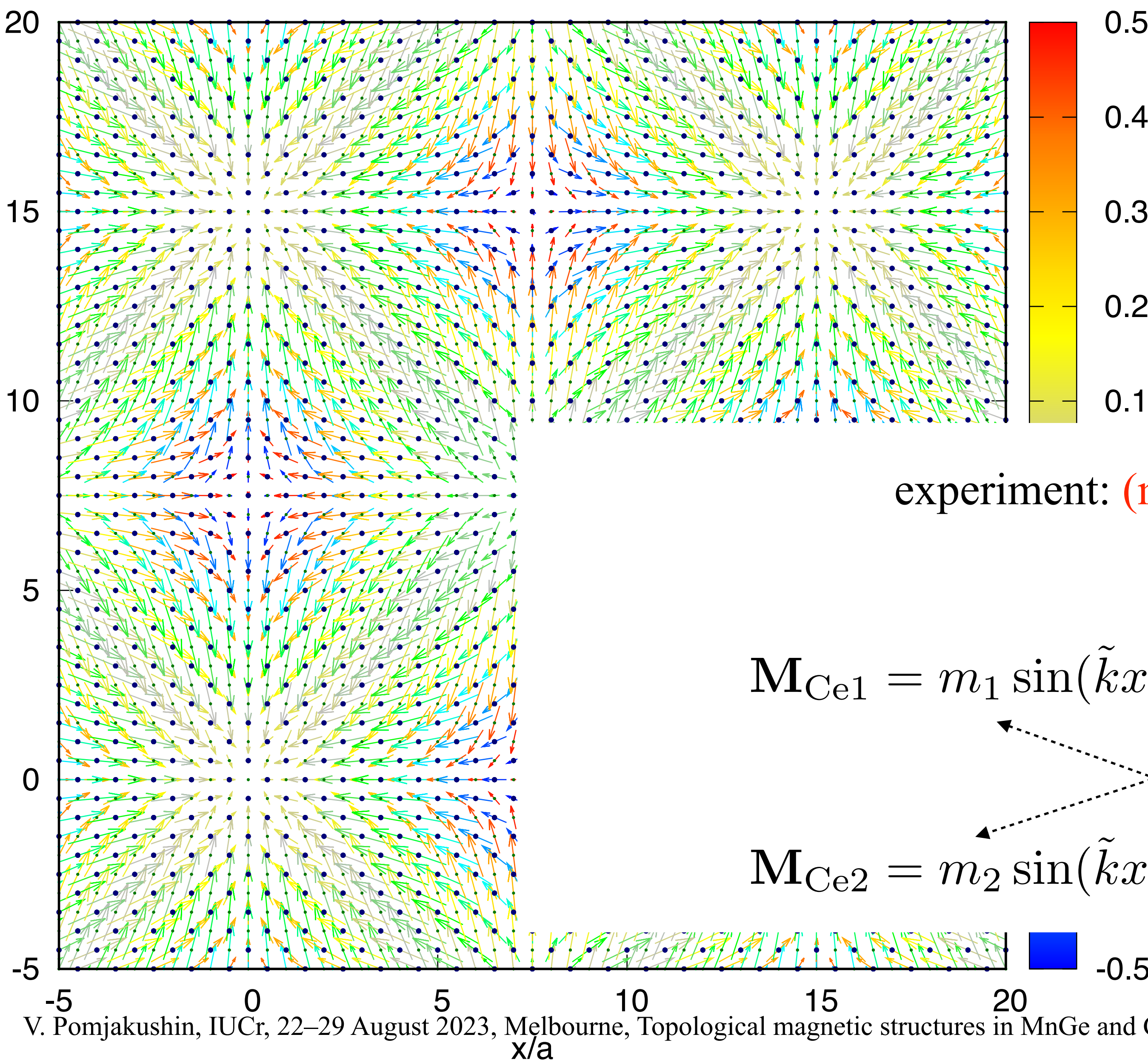

experiment: (m1,m2,m3,m4) = (0.44(1), 1.02(1), −0.21(5), 0.29(7)) μ_B.

$$\tilde{k}=2\pi|\boldsymbol{k}_1|=2\pi|\boldsymbol{k}_2|=2\pi g$$

$$\mathbf{M}_{\mathrm{Ce1}} = m_1 \sin(\tilde{k}x)\mathbf{e}_{\boldsymbol{x}} + m_2 \sin(\tilde{k}y)\mathbf{e}_{\boldsymbol{y}} + \left(m_3 \cos(\tilde{k}x) + m_4 \cos(\tilde{k}y)\right)\mathbf{e}_{\boldsymbol{z}}$$

$$\mathbf{M}_{\mathrm{Ce2}} = m_2 \sin(\tilde{k}x)\mathbf{e}_{\boldsymbol{x}} + m_1 \sin(\tilde{k}y)\mathbf{e}_{\boldsymbol{y}} + \left(m_4 \cos(\tilde{k}x) + m_3 \cos(\tilde{k}y)\right)\mathbf{e}_{\boldsymbol{z}}$$

CeAlGe: Maximal symmetry full star superspace 3D+2 magnetic group I4_1md1'(a00)000s(0a0)0s0s

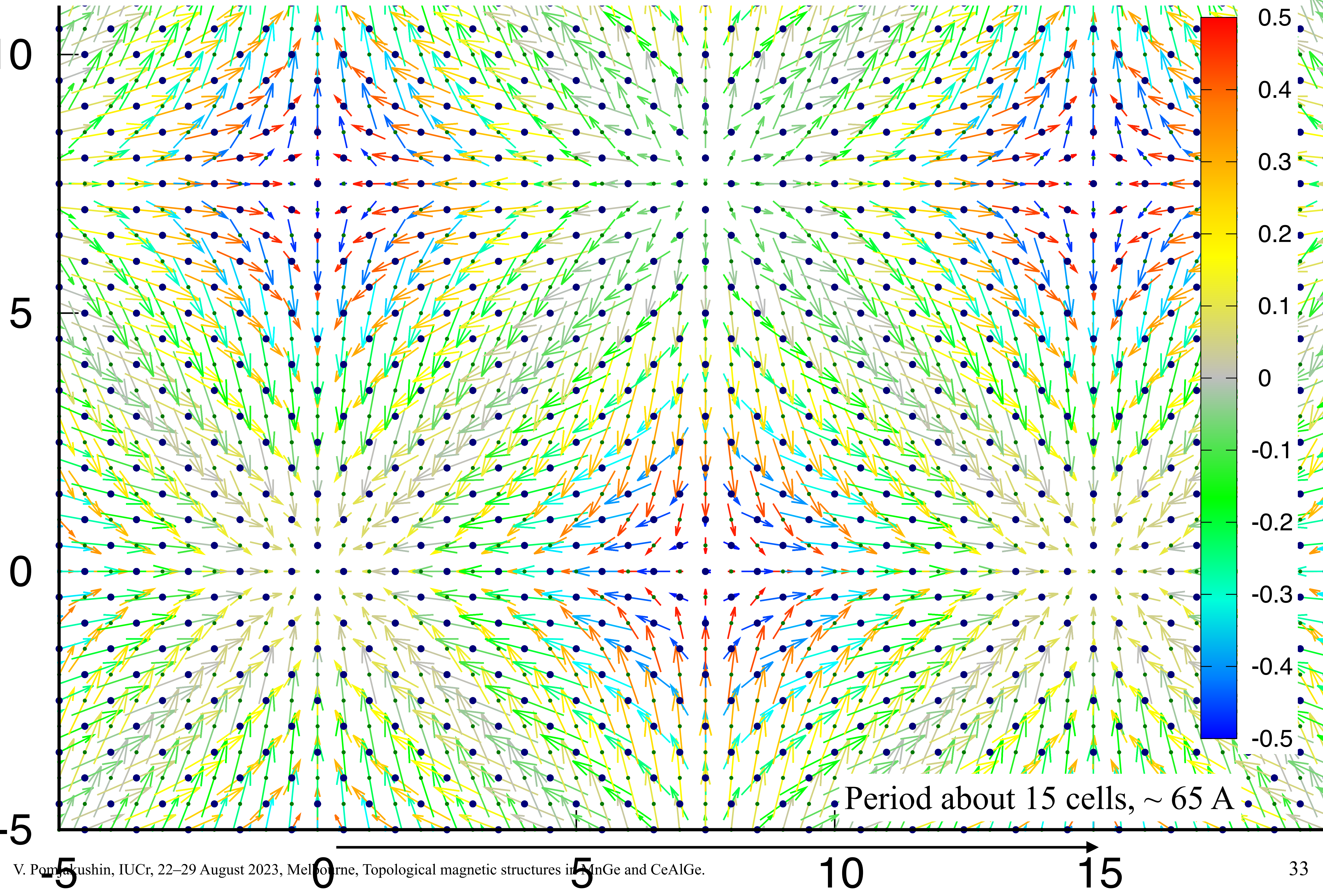

non-continuos case: magnetic merons in CeAlGe

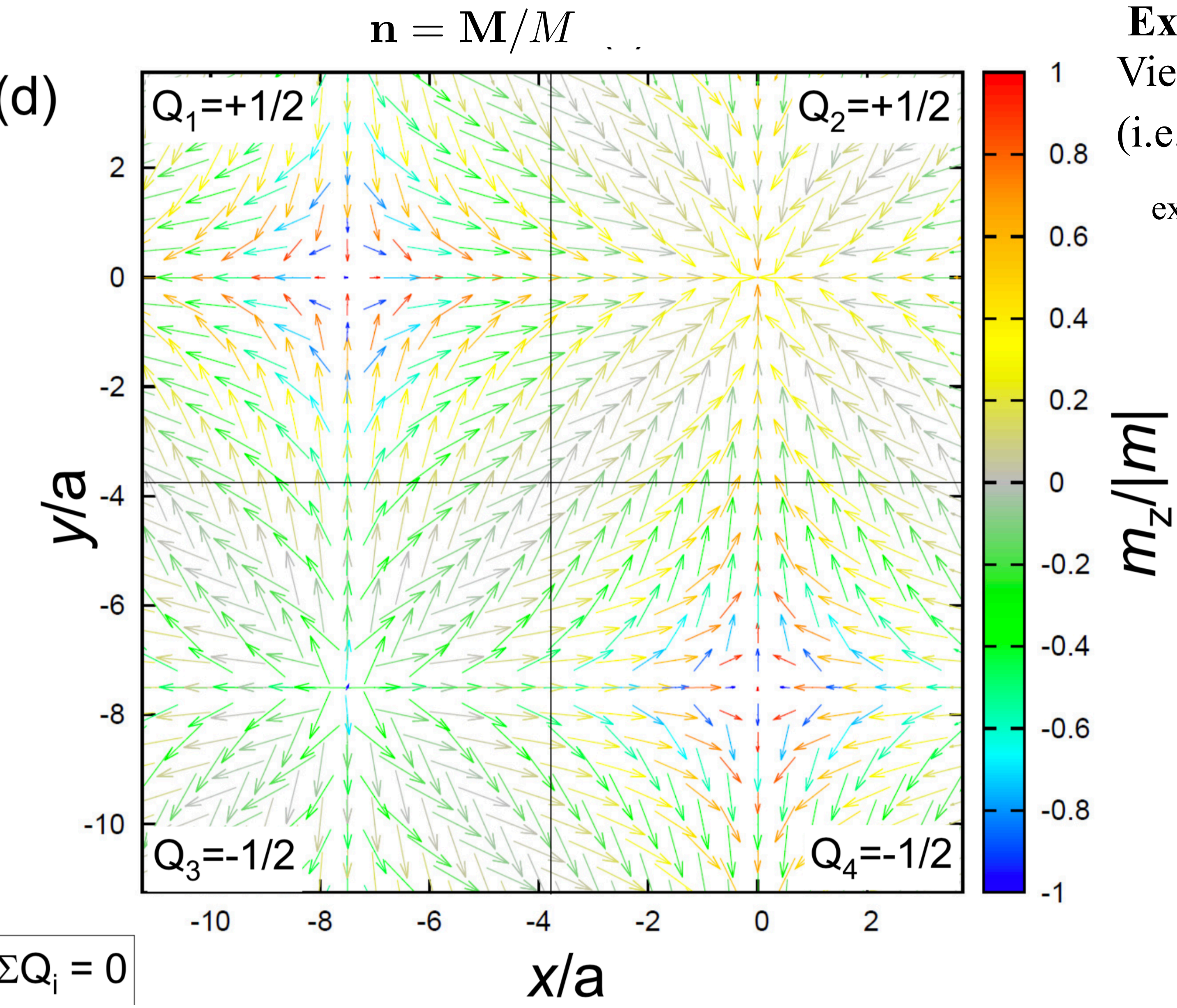

Experimentally observed multi-k magnetic structure.
View along the z-(c-)axis of the normalized
(i.e. $\vec{n} = \vec{M}/|\vec{M}|$, where $\vec{M}$ is the local Ce moment)

experiment: (m1,m2,m3,m4) = (0.44(1), 1.02(1), −0.21(5), 0.29(7)) μ_B.

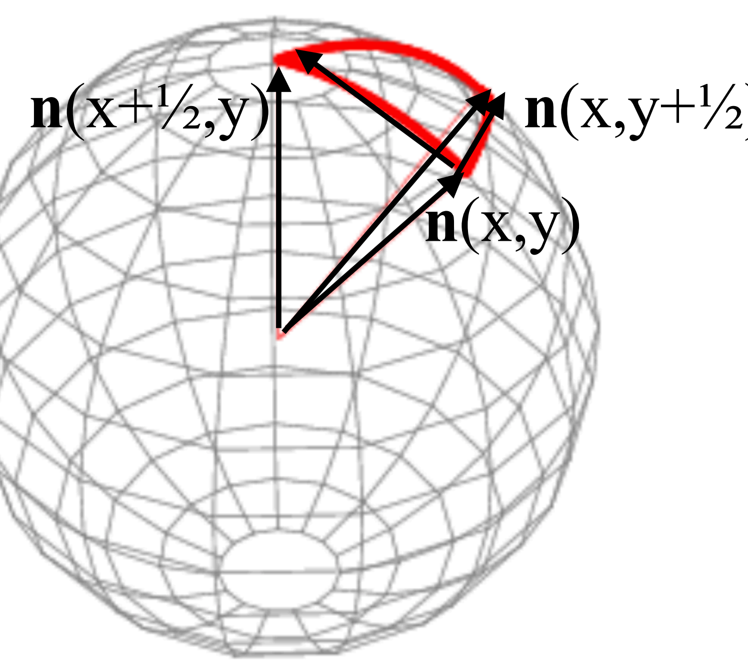

topological density/winding ~ solid angle

$$w(x,y) = \frac{1}{4\pi}(\mathbf{n}\cdot[\frac{\partial \mathbf{n}}{\partial x}\times\frac{\partial \mathbf{n}}{\partial y}]),\ \ \mathbf{n} = \mathbf{M}/M$$

Topological number/charge

$$Q = \int\int w(x,y)dxdy$$

non-continuos case: magnetic merons in CeAlGe

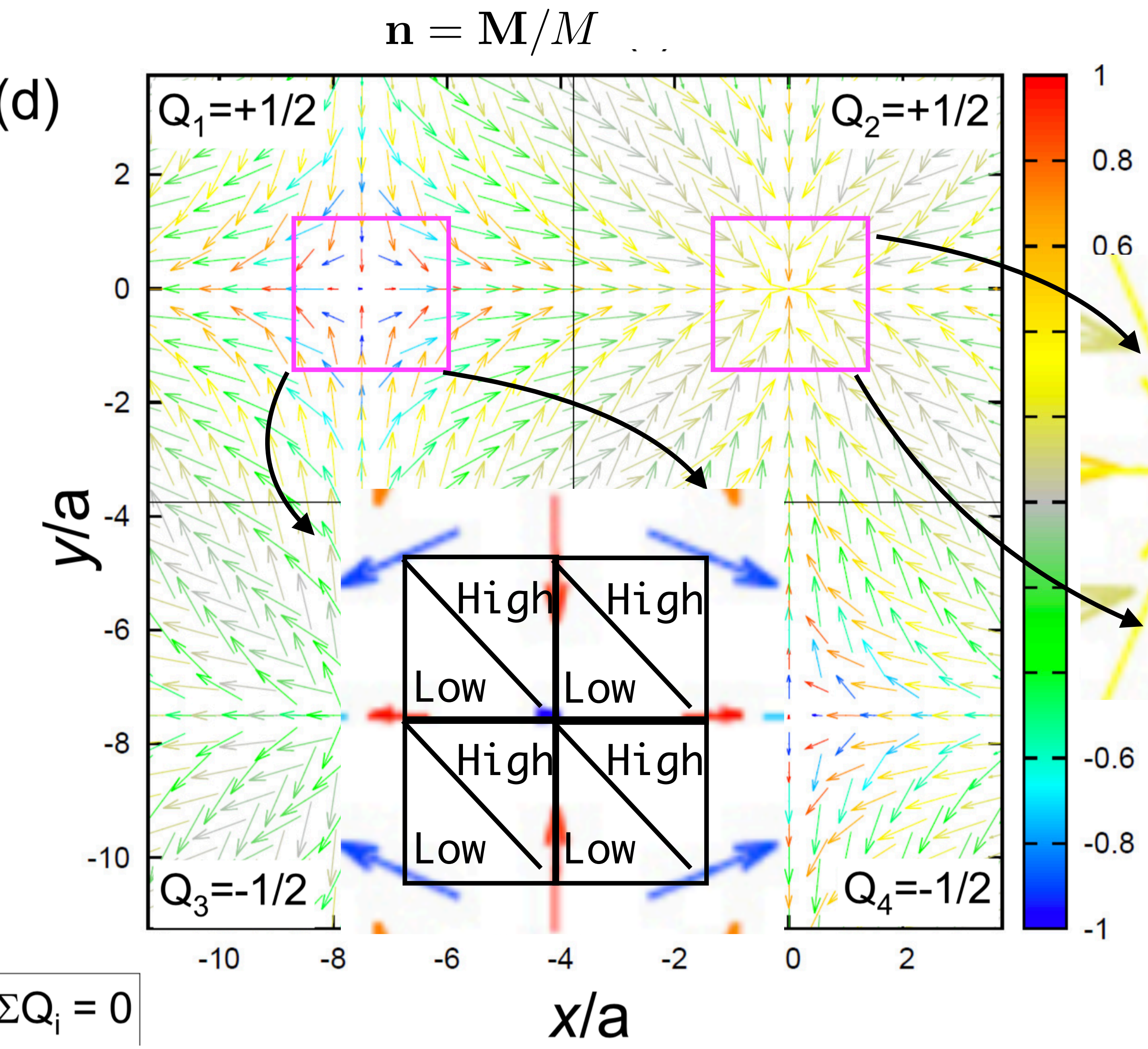

Experimentally observed multi-k magnetic structure.
View along the z-(c-)axis of the normalized
(i.e. $\vec{n} = \vec{M}/|\vec{M}|$, where $\vec{M}$ is the local Ce moment)

experiment: (m1,m2,m3,m4) = (0.44(1), 1.02(1), −0.21(5), 0.29(7)) μ_B.

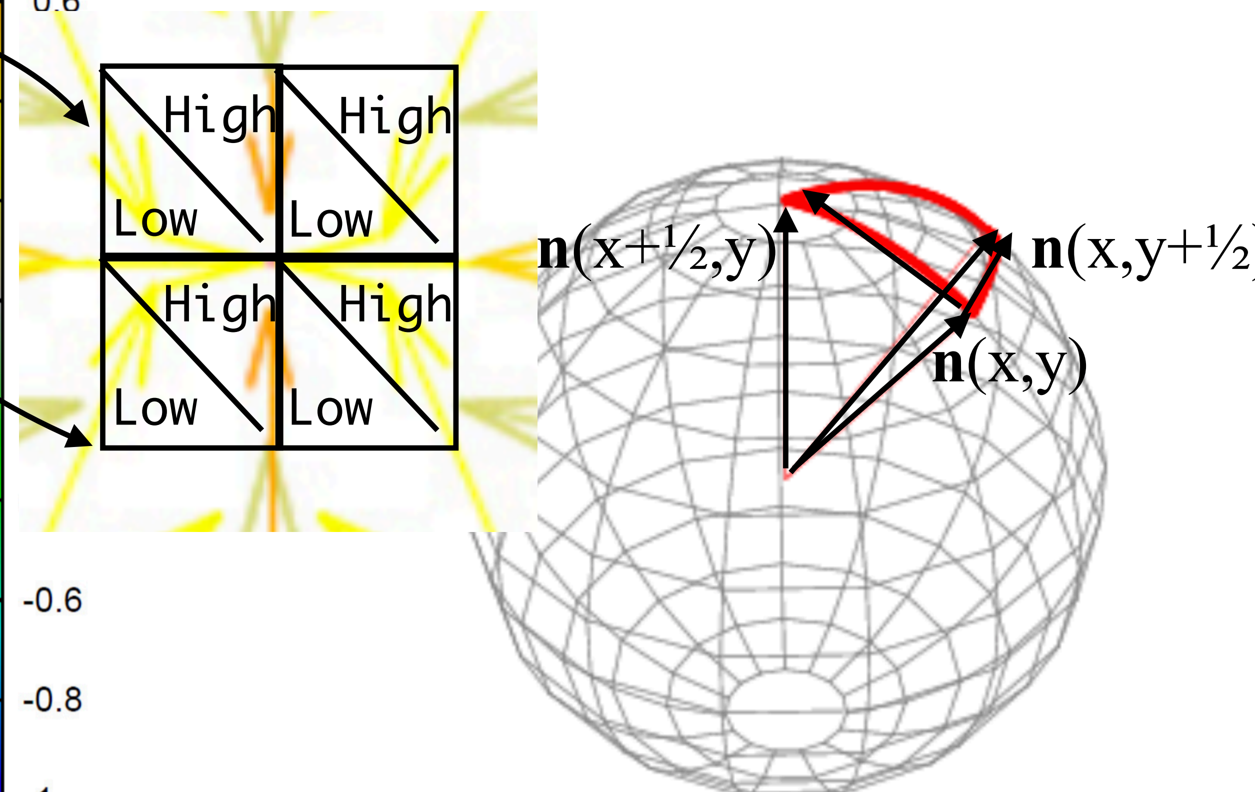

topological density/winding ~ solid angle

$$w(x,y) = \frac{1}{4\pi}(\mathbf{n}\cdot[\frac{\partial \mathbf{n}}{\partial x} \times \frac{\partial \mathbf{n}}{\partial y}]), \quad \mathbf{n} = \mathbf{M}/M$$

Topological number/charge

$$Q = \int\int w(x,y)dxdy$$

non-continuos case: magnetic merons in CeAlGe

$\mathbf{n} = \mathbf{M}/M$

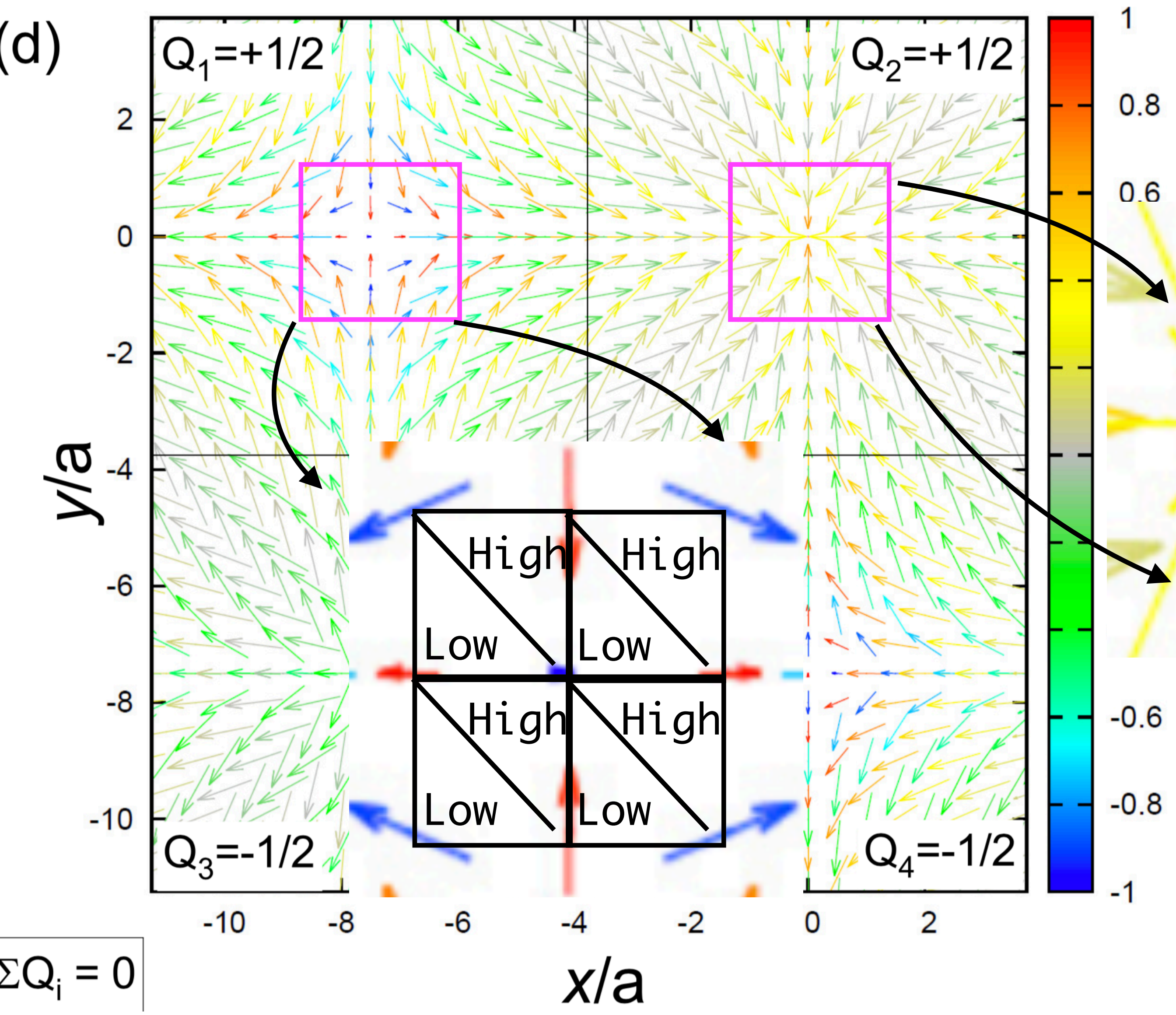

Experimentally observed multi-k magnetic structure.

View along the z-(c-)axis of the normalized (i.e. $\vec{n} = \vec{M}/|\vec{M}|$, where $\vec{M}$ is the local Ce moment)

experiment: (m1,m2,m3,m4) = (0.44(1), 1.02(1), −0.21(5), 0.29(7)) μ_B.

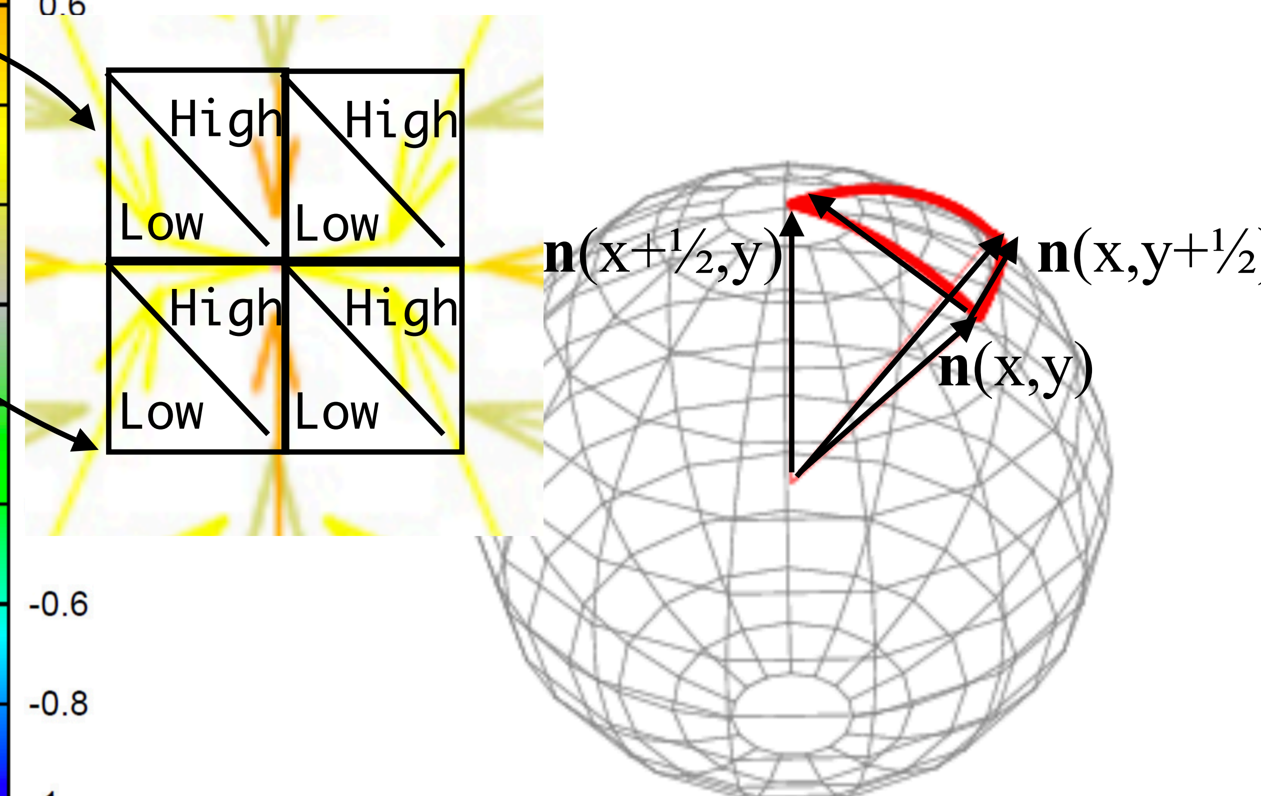

topological density/winding ~ solid angle

$$w(x,y) = \frac{1}{4\pi}(\mathbf{n}\cdot[\frac{\partial \mathbf{n}}{\partial x}\times\frac{\partial \mathbf{n}}{\partial y}]),\quad \mathbf{n} = \mathbf{M}/M$$

$$\longrightarrow \quad \Delta w(x,y) = \frac{1}{4\pi}\left(\Delta\Omega_{\mathrm{low}} + \Delta\Omega_{\mathrm{high}}\right)^{\star}$$

solid angle per square placket

Topological number/charge

$$Q = \int\int w(x,y)dxdy$$

$$\longrightarrow \quad Q = \sum_{x,y} \Delta w(x,y)$$

$$^{\star}\ \tan\left(\frac{1}{2}\Omega\right) = \frac{\mathbf{a}\cdot(\mathbf{b}\times\mathbf{c})}{abc + (\mathbf{a}\cdot\mathbf{b})\,c + (\mathbf{a}\cdot\mathbf{c})\,b + (\mathbf{b}\cdot\mathbf{c})\,a}$$

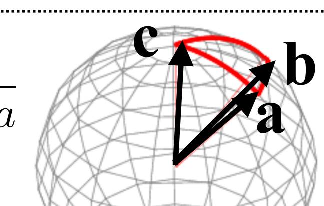

Topological density and charge. H=0

experiment: (m1,m2,m3,m4) = (0.44(1), 1.02(1), −0.21(5), 0.29(7)) μ_B.

$$\mathbf{n} = \mathbf{M}/M$$

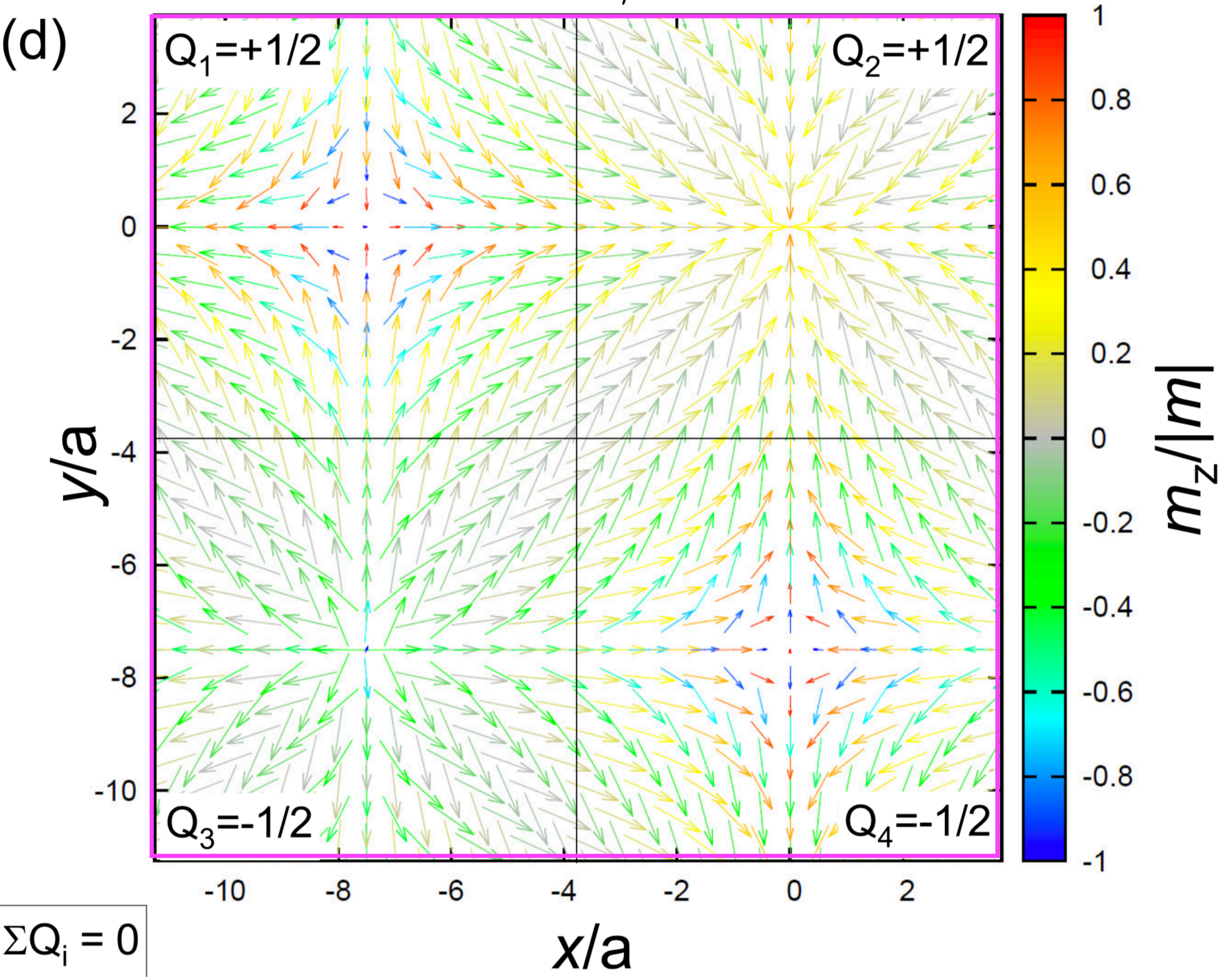

$\Sigma Q_i = 0$

$$\Delta w(x,y) = \frac{1}{4\pi}\left(\mathbf{n}\cdot[\Delta\mathbf{n}_x \times \Delta\mathbf{n}_y]\right)$$

solid angle per square placket

$$Q = \sum_{x,y} \Delta w(x,y)$$

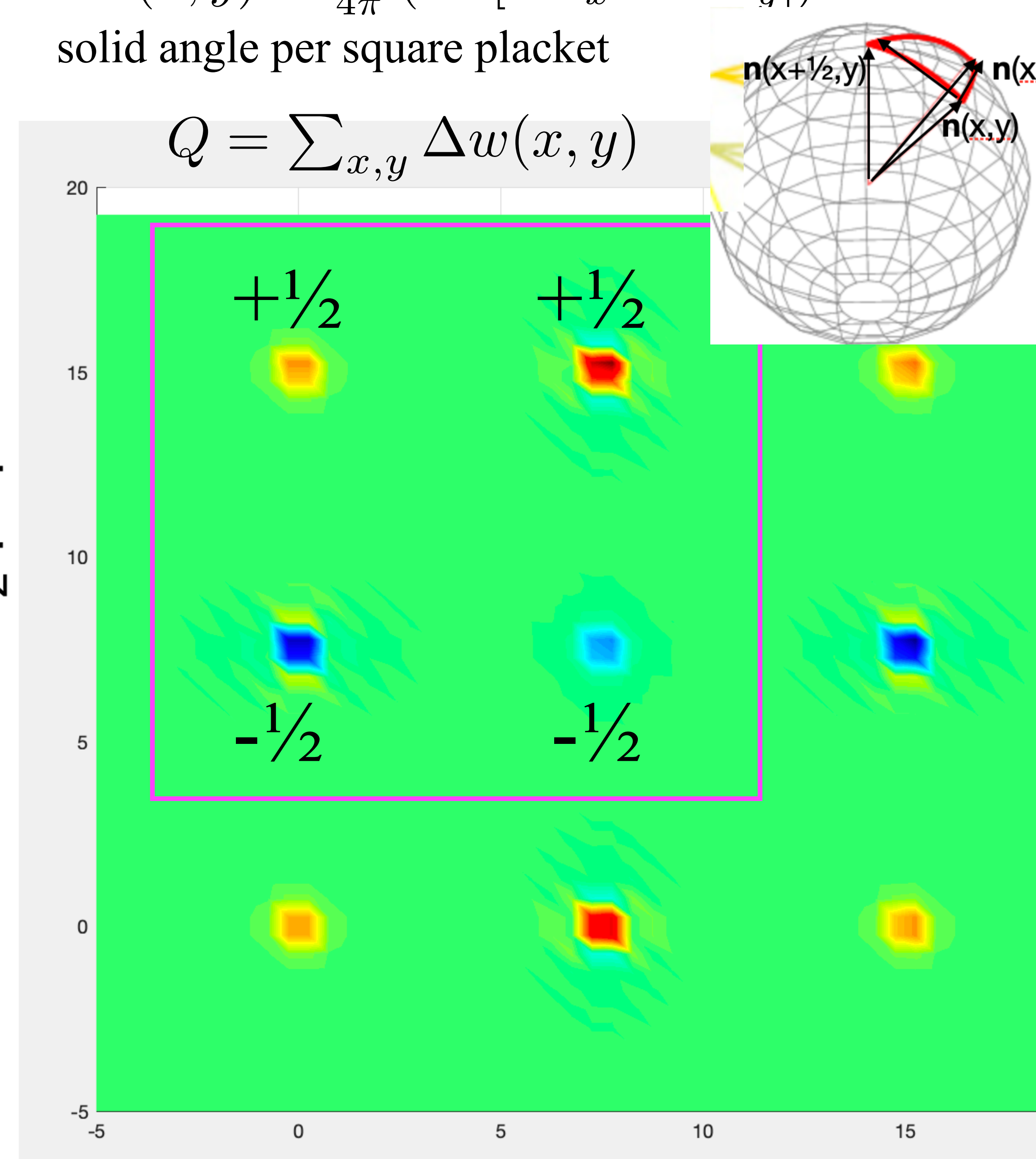

$$\mathbf{M}_{\mathrm{Ce2}} = m_2\sin(\tilde{k}x)\mathbf{e_x} + m_1\sin(\tilde{k}y)\mathbf{e_y} + \left(m_4\cos(\tilde{k}x) + m_3\cos(\tilde{k}y)\right)\mathbf{e_z}$$

$$\mathbf{M}_{\mathrm{Ce1}} = m_1\sin(\tilde{k}x)\mathbf{e_x} + m_2\sin(\tilde{k}y)\mathbf{e_y} + \left(m_3\cos(\tilde{k}x) + m_4\cos(\tilde{k}y)\right)\mathbf{e_z}$$

$\tilde{k} = 2\pi|\boldsymbol{k}_1| = 2\pi|\boldsymbol{k}_2| = 2\pi g$

Topological magnetic structures in MnGe: Neutron diffraction and symmetry analysis

<u>The motivation:</u> apply a state-of-the-art analysis of all possible magnetic superspace structures allowed by the crystal symmetry in metallic MnGe (P213) that are consistent with neutron diffraction data. *MnGe has been long-studied for its remarkable phenomena related to its topological magnetic order, but surprisingly, the detailed magnetic structure underlying such phenomena was not addressed before this study.*

Several maximal crystallographic symmetry magnetic structures are found to fit the data equally well. Among them: <u>Topological multi-**k**</u> 3**k**-hedgehog and 2**k**-meron structures that can account for the topological Hall effect should be preferable over the single-**k** helical- or AM-structures.

<u>New route</u> to synthesize MnGe at ambient pressures and moderate temperatures, in addition to the traditional high pressure synthesis.

$P2_13.1'(a,0,0)00s(0,a,0)00s(0,0,a)00s$

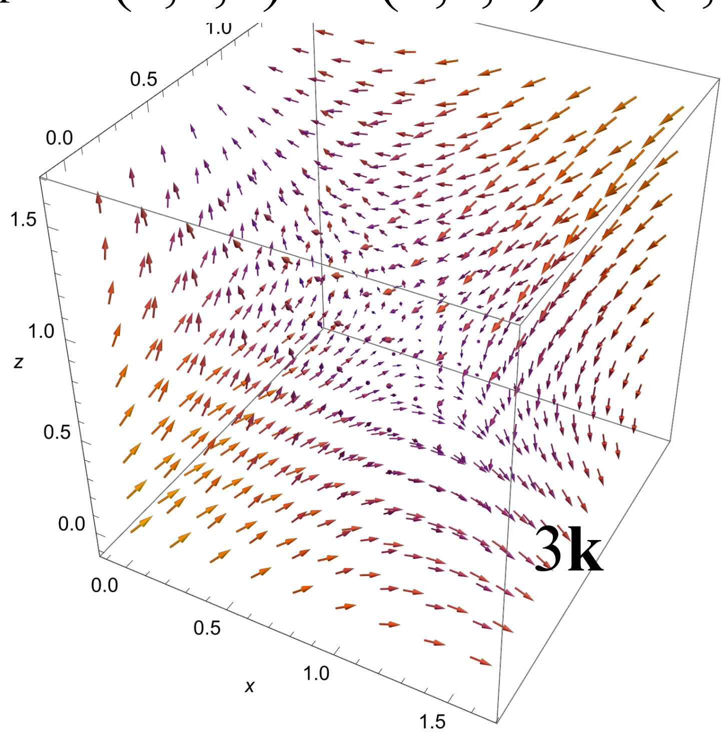

$P2_12_12_1.1'(0,b1,0)000s(0,0,g2)000s$

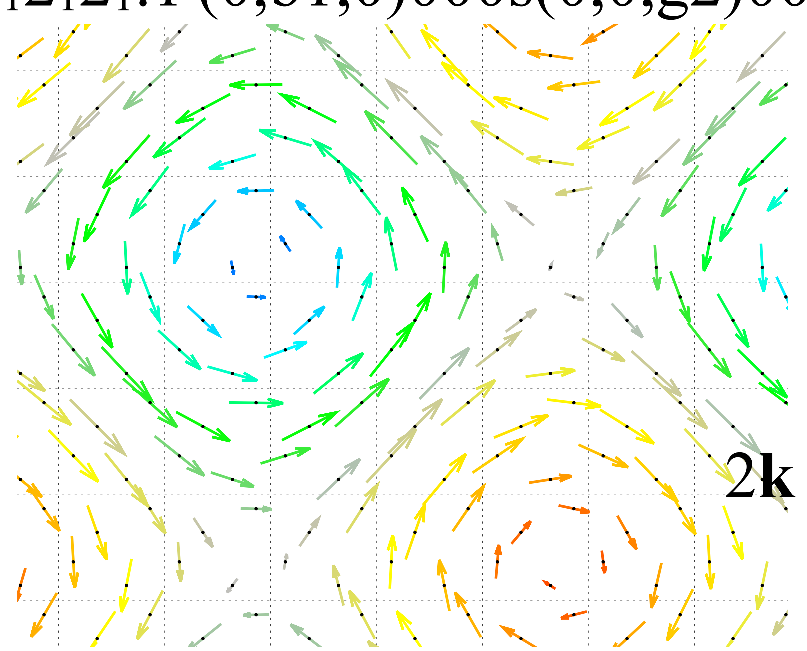

$P2_12_12_1.1'(0,0,g)000s$

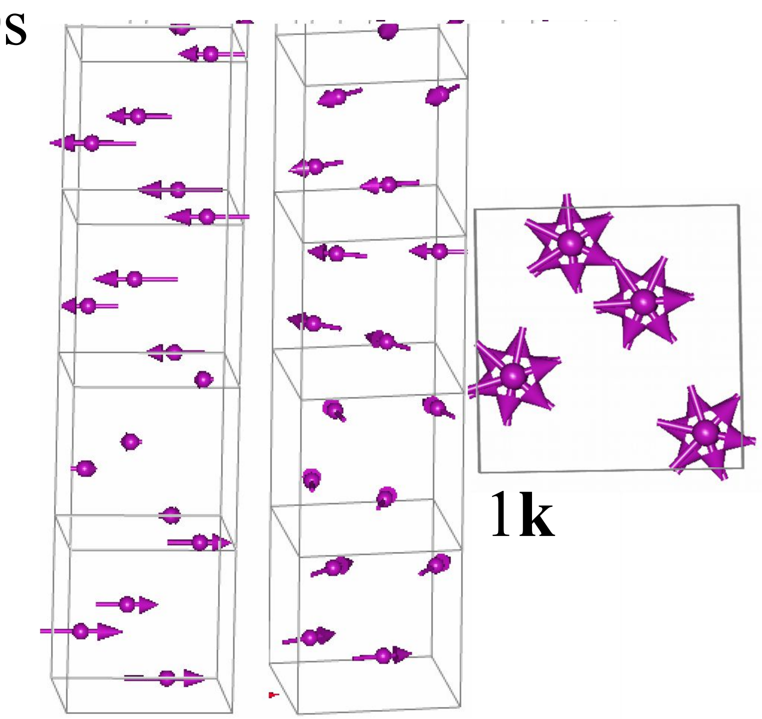

Summary on CeAlGe

- We report the discovery of topological magnetic order in the polar tetragonal magnetic Weyl semimetal candidate CeAlGe.

- CeAlGe has an incommensurate magnetic structure modulation length 70 Å [3D+2 group *I4_1md.1'(a,0,0)000s(0,a,0)0s0s*] hosting a lattice of magnetic particle-like objects called (anti)merons with half-integer topological numbers Q=±1/2. 1k-structure cycloid structure in *I2mm.1'(0,0,g)0s0s* fit the data as well

- At intermediate magnetic fields H parallel to the c-axis one of merons flips sign leading to total Q=±1 in accordance with the observation of a topological Hall effect (THE) in the same range of H.

Thank you!

Bloch vs. Neel

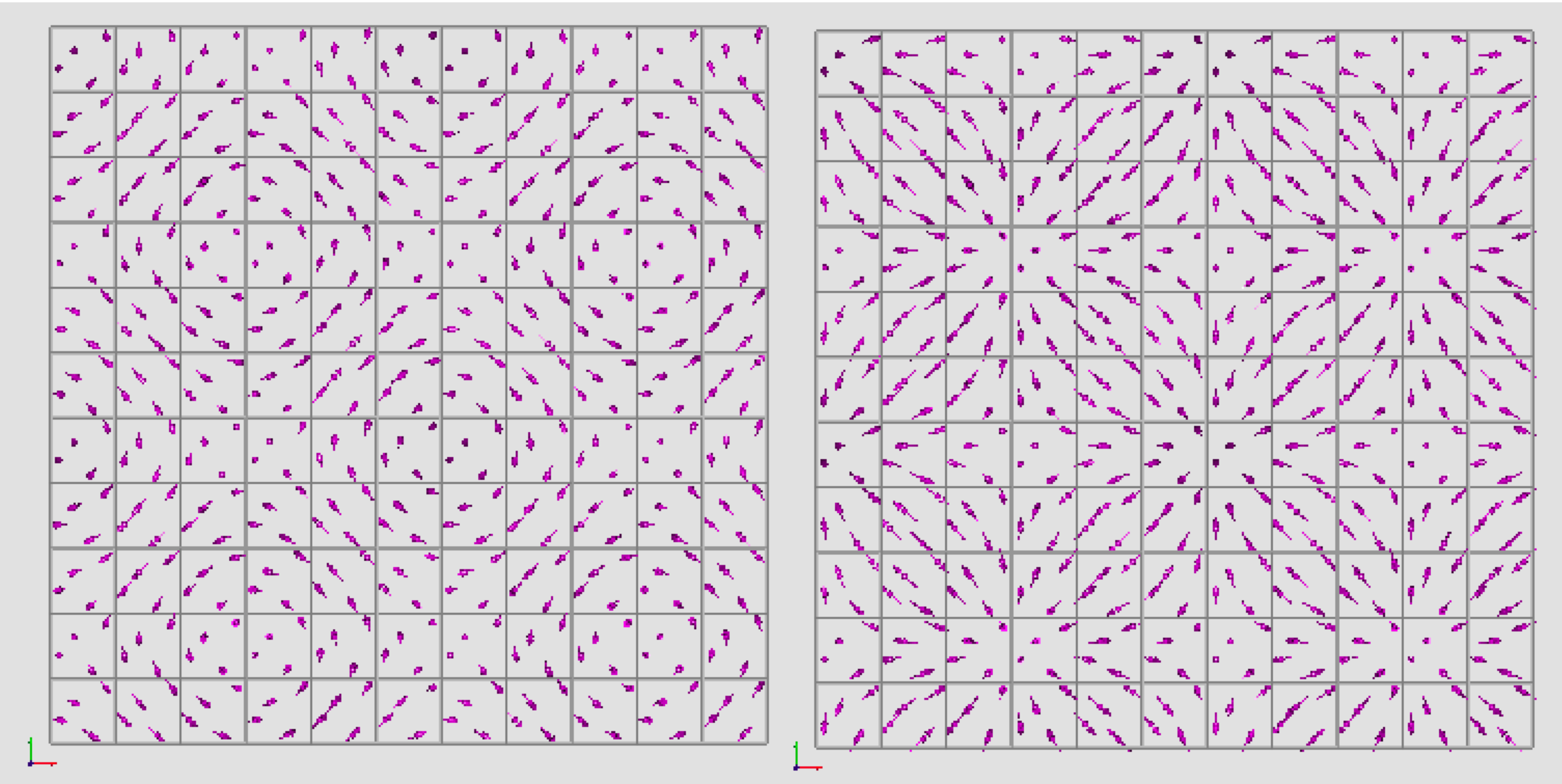

Crystal structure below T_N=170K P2_12_12_1

(222) is not split in both groups

(320) is split in $P2_12_12_1$

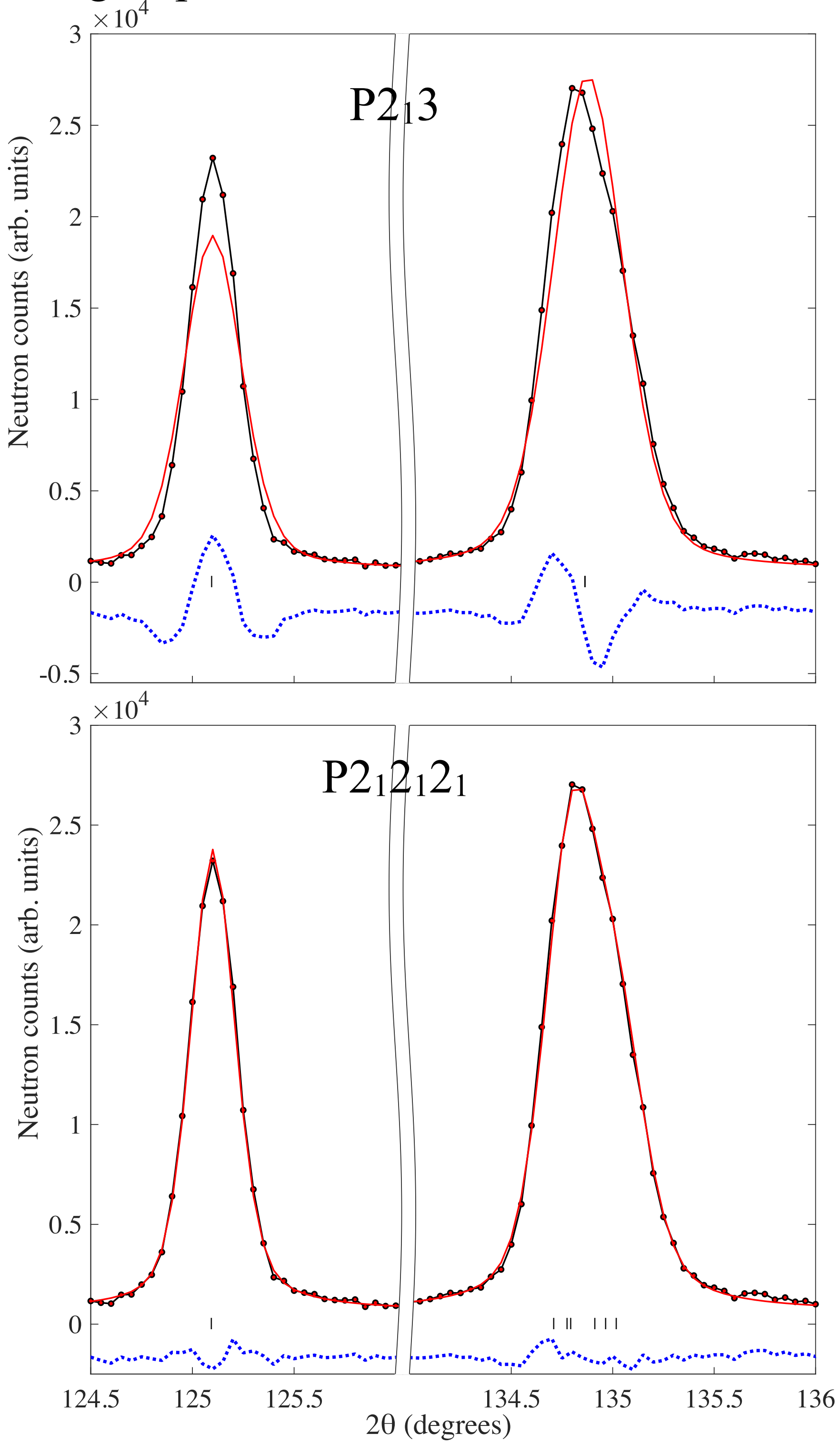

HR mode at HRPT with the wavelength λ = 2.45 Å at T = 1.8 K

Crystal structure below T_N=170K P2_12_12_1

(222) is not split in both groups

(320) is split in $P2_12_12_1$

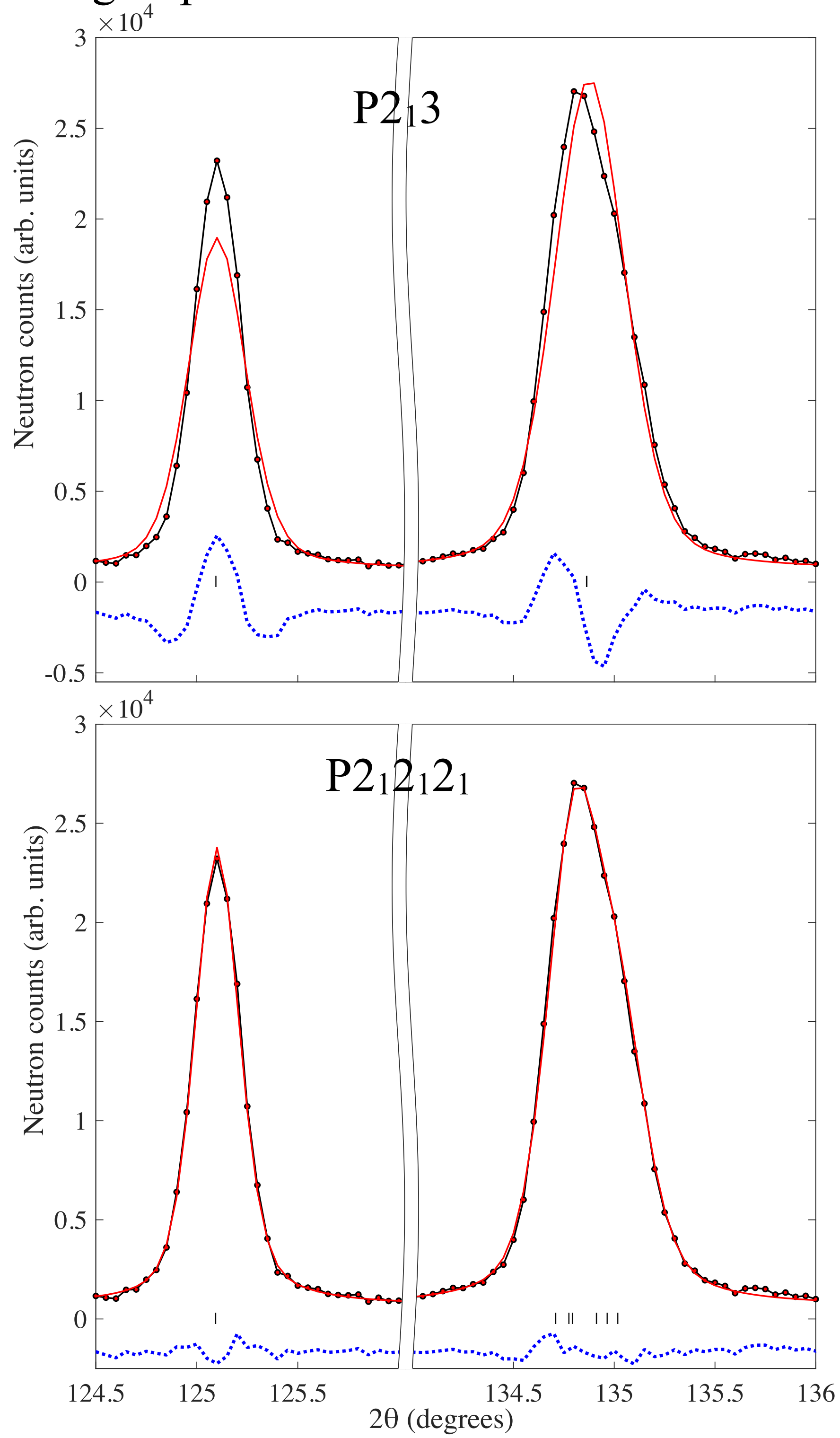

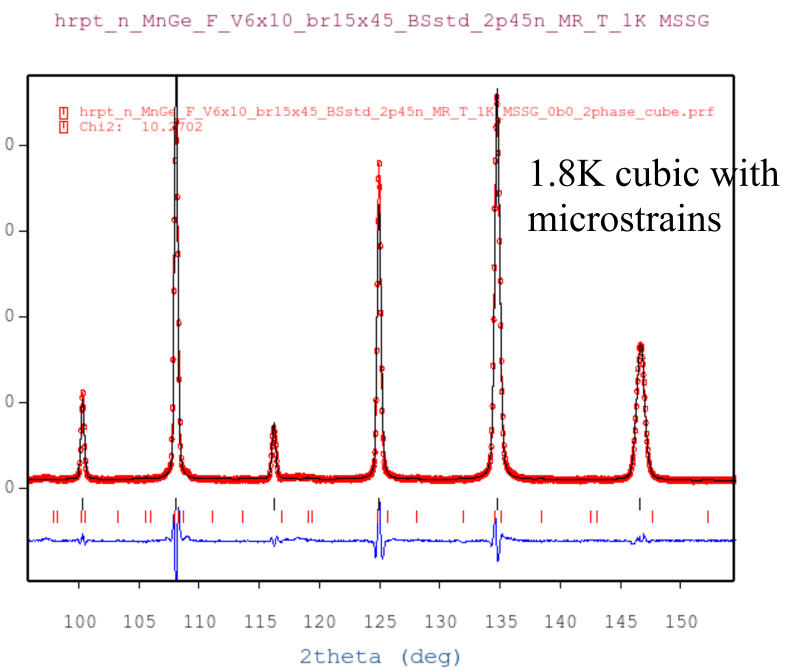

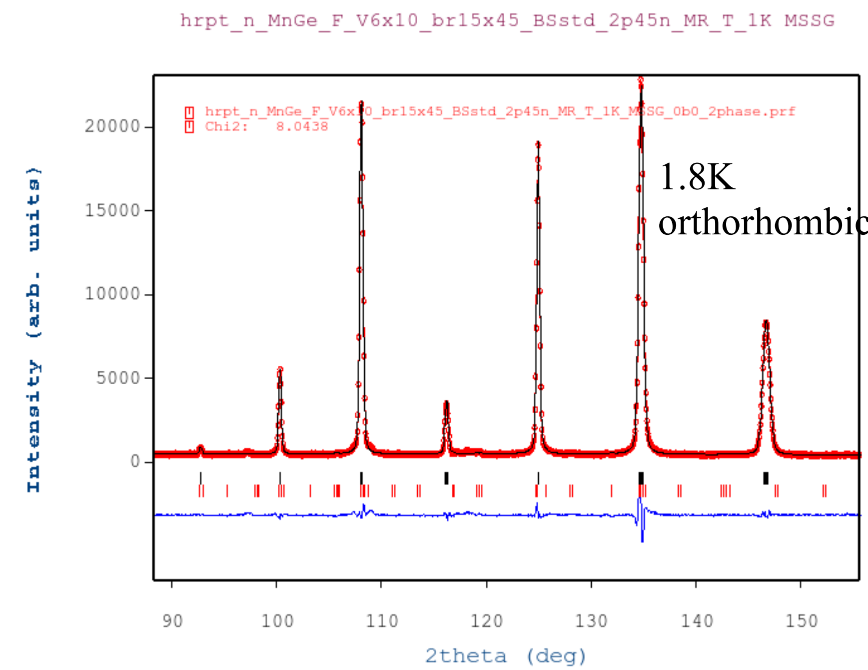

HR mode at HRPT with the wavelength λ = 2.45 Å at T = 1.8 K

The fit of the combined MR and HR data sets using both wavelengths 1.49 Å and 2.45 Å is well converged to $P2_12_12_1$ model.

Orth-metrics: 0.1% and 0.16% along the b and c axes with respect to the a axis

One k-case, standard representation analysis without magnetic group symmetry arguments: Space group $I4_1md$, Ce 4a (0,0,z)

Solution: SM2 irreducible representation

- **Cycloid in ac-plane for k1=[g,0,0]**, in bc=lane for k2=[0,g,0]
- two magnetic domains (twins)

Lowest monoclinic MSSG
8.1.4.2.m33.2 Bm.1'(a,b,0)ss

$k=|\boldsymbol{k}_1|=|\boldsymbol{k}_2|=g$

$$\mathbf{M}_{Ce(i)} = m_{ix}\sin(2\pi kx)\mathbf{e}_{\boldsymbol{x}} + m_{iz}\sin(2\pi kx+\varphi_i)\mathbf{e}_{\boldsymbol{z}}, \quad i=1,2$$

Experimental values (μ_B) :
Ce1: m_{1x}= -0.64(1), m_{1z} =-0.30(6)
Ce2: m_{2x}= -1.50(2), m_{2z} = 0.46(8)

$\varphi_1=\varphi_2\approx 90°$

$\mathrm{Ce1}(0,0,z)$
$\mathrm{Ce2}(0,\frac{1}{2},z+\frac{1}{4})$

Two independent sites. No symmetry relations between Ce1 and Ce2

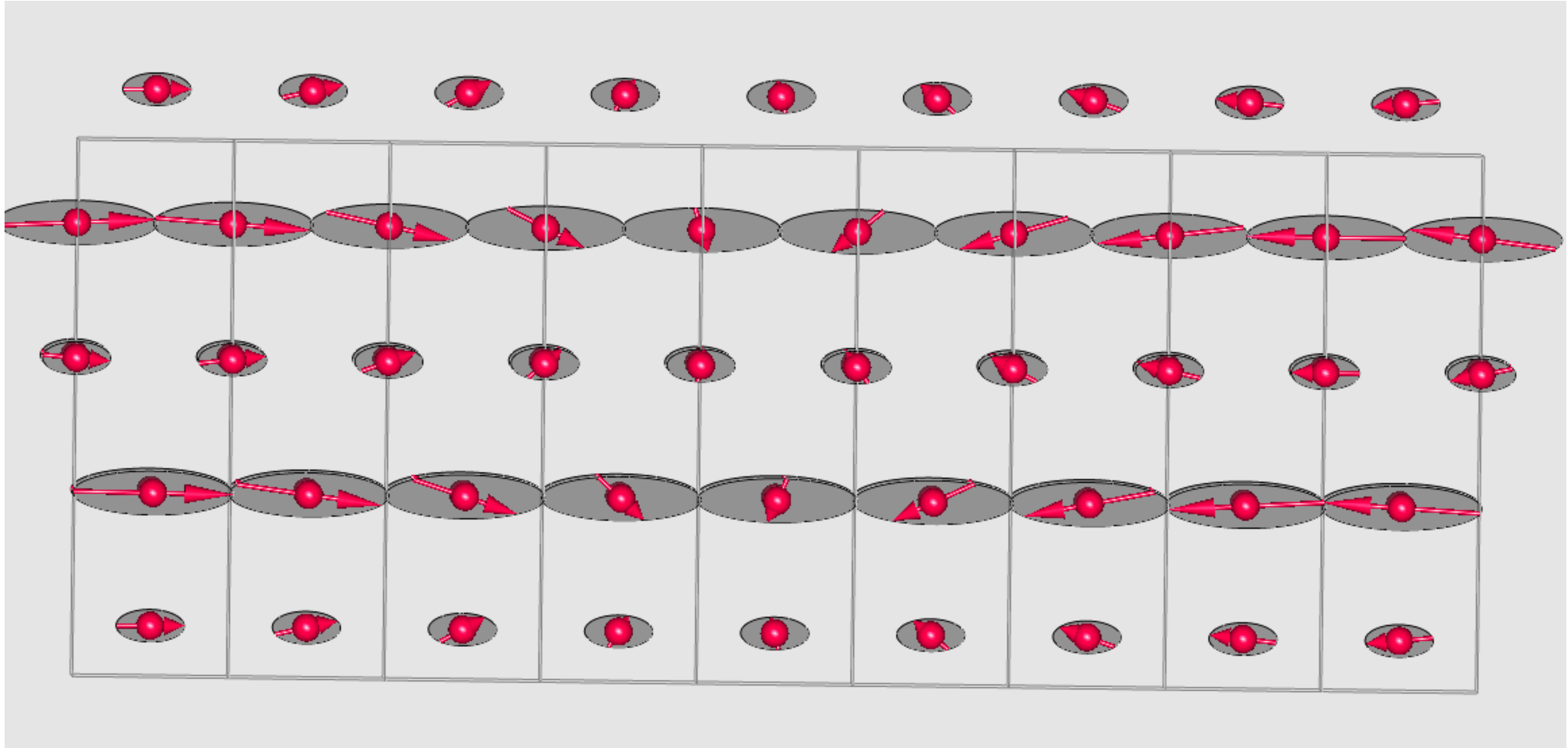

One k-case, standard representation analysis without magnetic group symmetry arguments: Space group $I4_1md$, Ce 4a (0,0,z)

Solution: SM2 irreducible representation

- **Cycloid in ac-plane for k1=[g,0,0]**, in bc=lane for k2=[0,g,0]
- two magnetic domains (twins)

Lowest monoclinic MSSG
8.1.4.2.m33.2 Bm.1'(a,b,0)ss

$k=|\boldsymbol{k}_1|=|\boldsymbol{k}_2|=g$

$$\mathbf{M}_{Ce(i)} = m_{ix}\sin(2\pi kx)\mathbf{e}_{\boldsymbol{x}} + m_{iz}\sin(2\pi kx+\varphi_i)\mathbf{e}_{\boldsymbol{z}}, \quad i=1,2$$

Experimental values (μ_B) :
Ce1: m_{1x}= -0.64(1), m_{1z} =-0.30(6)
Ce2: m_{2x}= -1.50(2), m2z = 0.46(8)

$\varphi_1=\varphi_2\approx 90°$

$Ce1(0,0,z)$
$Ce2(0,\frac{1}{2},z+\frac{1}{4})$

Two independent sites. No symmetry relations between Ce1 and Ce2

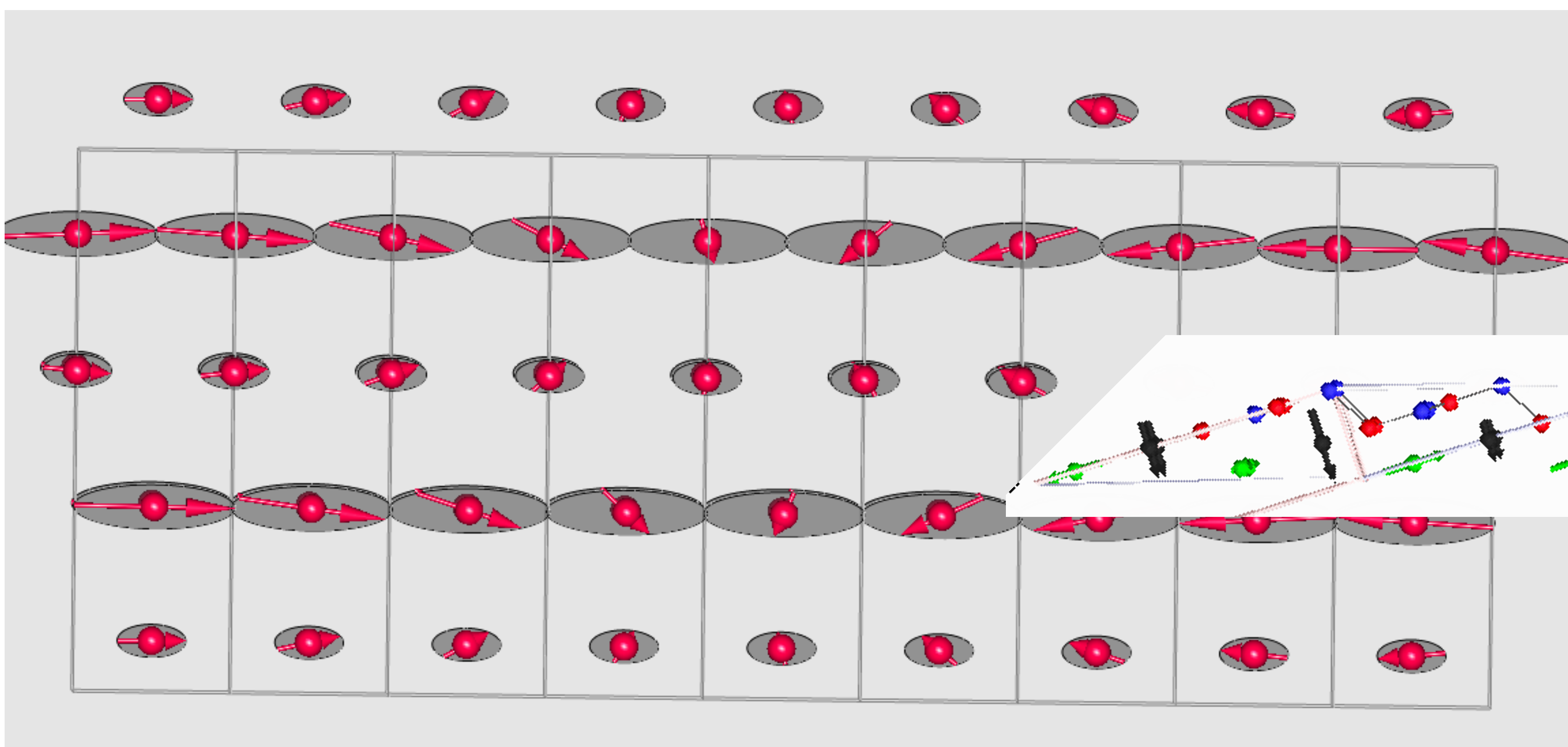

Note: if $\varphi_1=\varphi_2=0 \rightarrow$ amplitude modulation, different symmetry

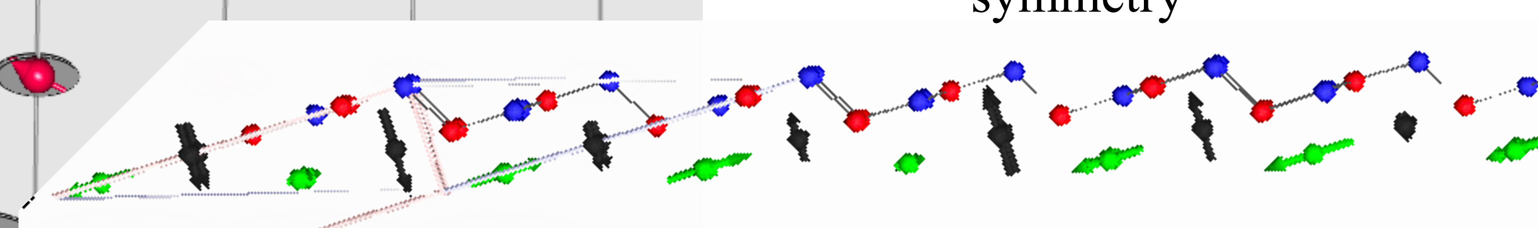

Symmetry of cycloid. 3D+1 superspace group for SM2 irrep

$I4_1md1'$ Advantage of magnetic symmetry when keeping {+**k**,-**k**}

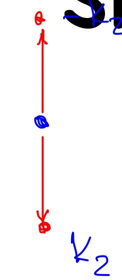

or

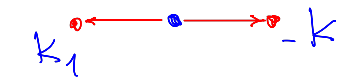

I2mm1'(0,0,g)0s0s

$$\mathbf{M}_{Ce(i)} = m_{ix}\sin(2\pi kx)\mathbf{e_x} + m_{iz}\cos(2\pi kx)\mathbf{e_z}, \quad i = 1, 2$$

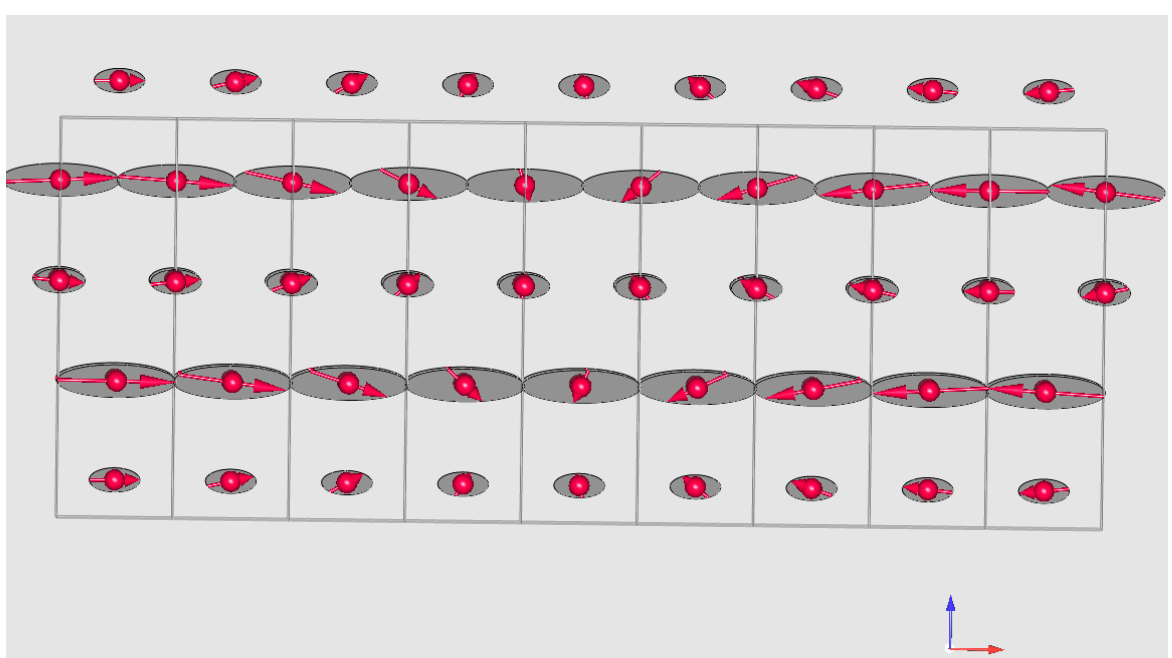

Experimental values:
Ce1: m_{1x}= -0.64(1), m_{1z} =-0.30(6)
Ce2: m_{2x}= -1.50(2), m2z = 0.46(8)

Symmetry of cycloid. 3D+1 superspace group for SM2 irrep

$I4_1md1'$ Advantage of magnetic symmetry when keeping {+**k**,-**k**}

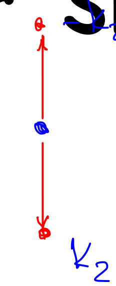

or

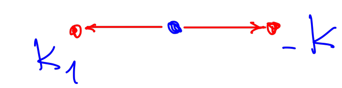

I2mm1'(0,0,g)0s0s

$$\mathbf{M}_{Ce(i)} = m_{ix}\sin(2\pi kx)\mathbf{e}_{\boldsymbol{x}} + m_{iz}\cos(2\pi kx)\mathbf{e}_{\boldsymbol{z}}, \quad i = 1,2$$

phase shift 90 degrees between x and y-components is fixed by symmetry!

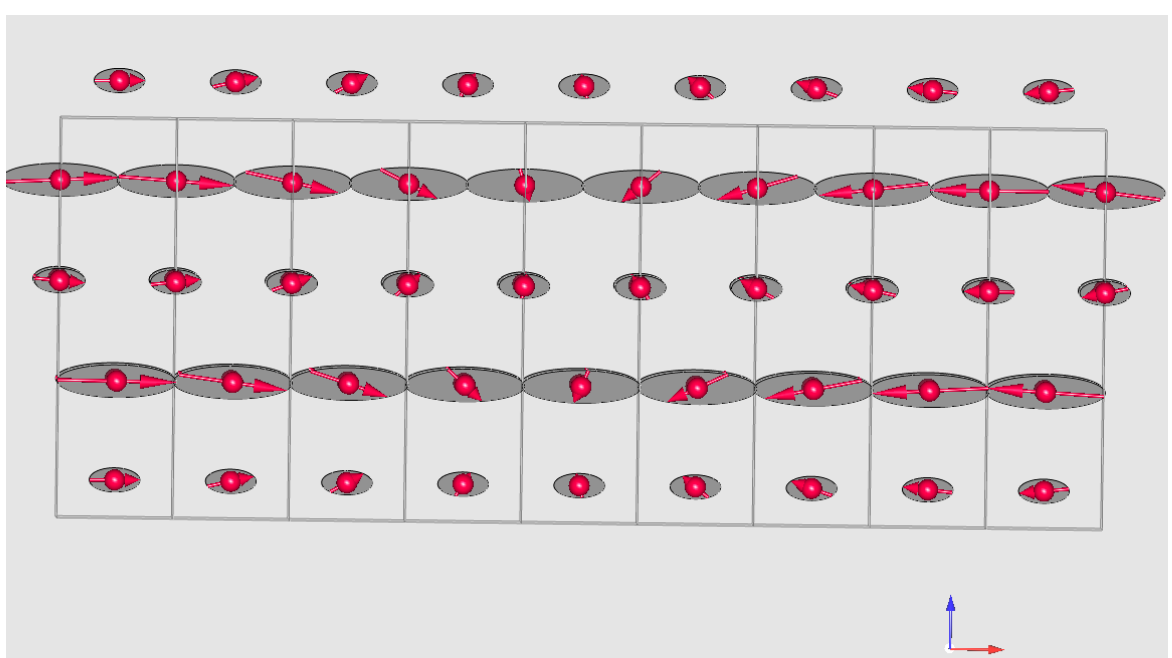

Experimental values:
Ce1: m_{1x}= -0.64(1), m_{1z} =-0.30(6)
Ce2: m_{2x}= -1.50(2), m2z = 0.46(8)

Topological density and charge. H=0

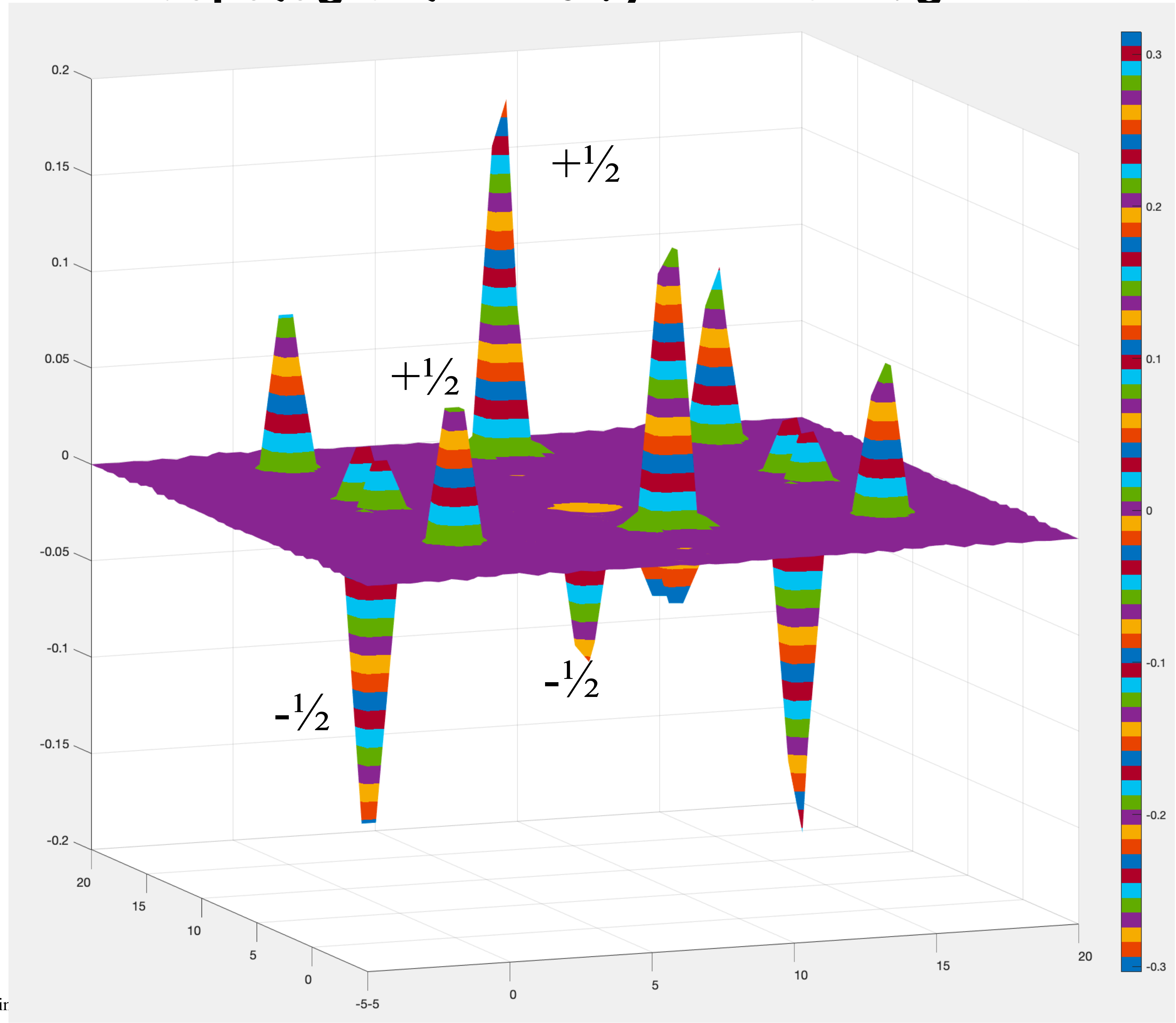

Experimental proof comes from behaviour in external field

Topological Hall Effect THE

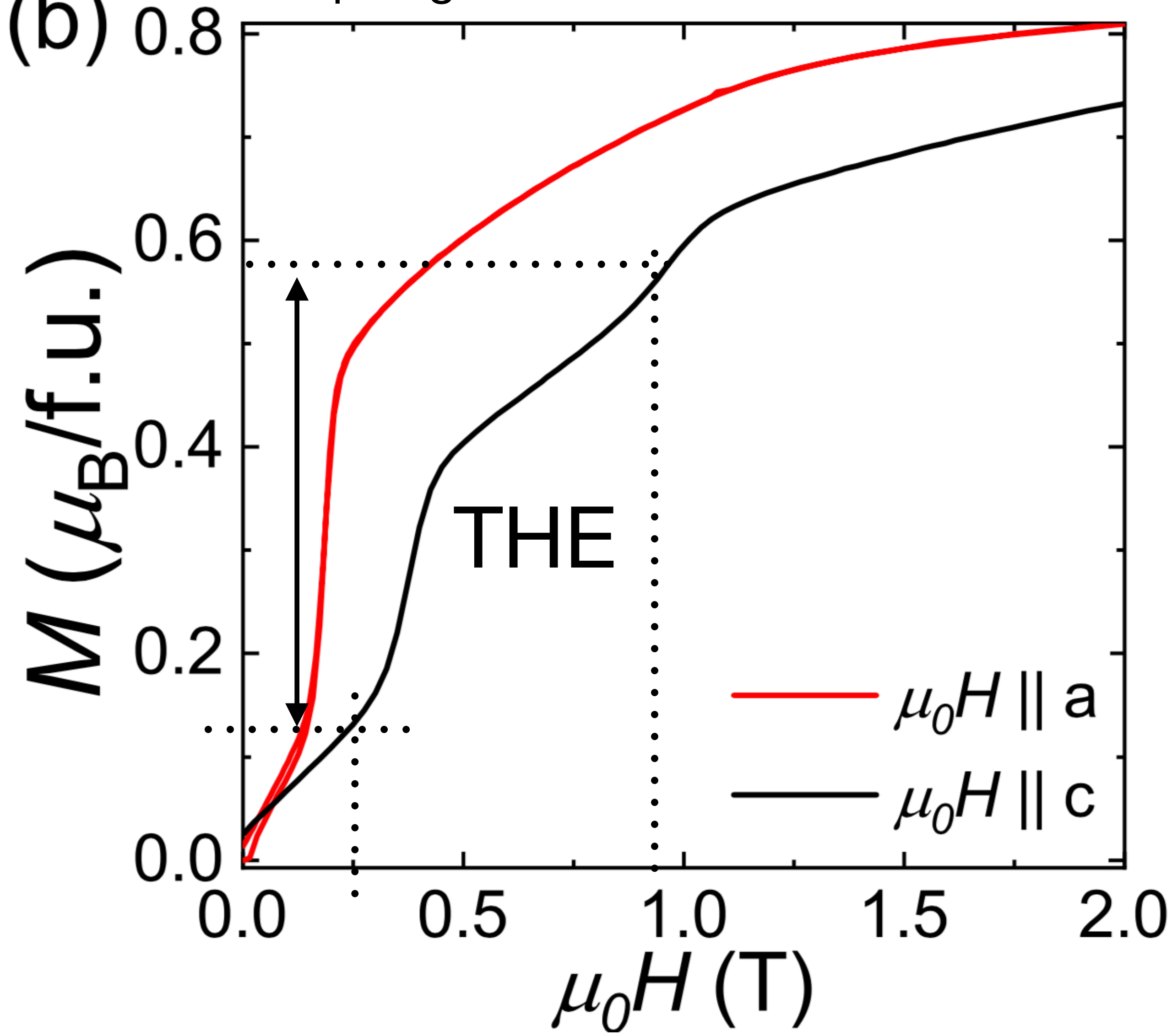

SANS diffraction: k1+k2+0 is 3rd order harmonics in external field

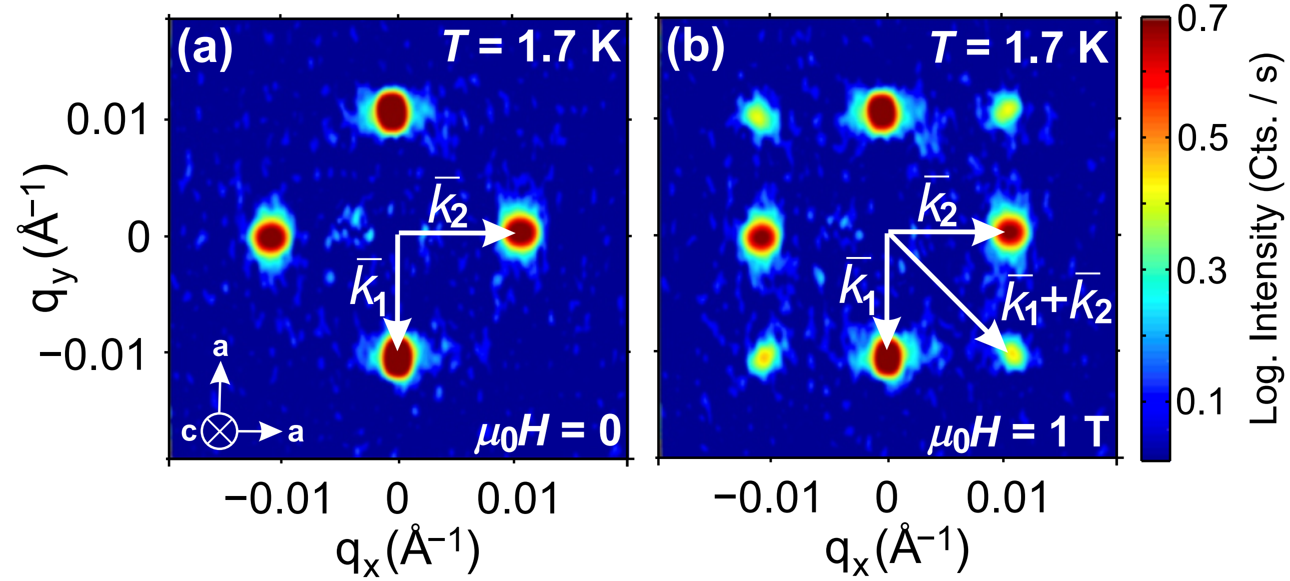

Topological charge per magnetic cell

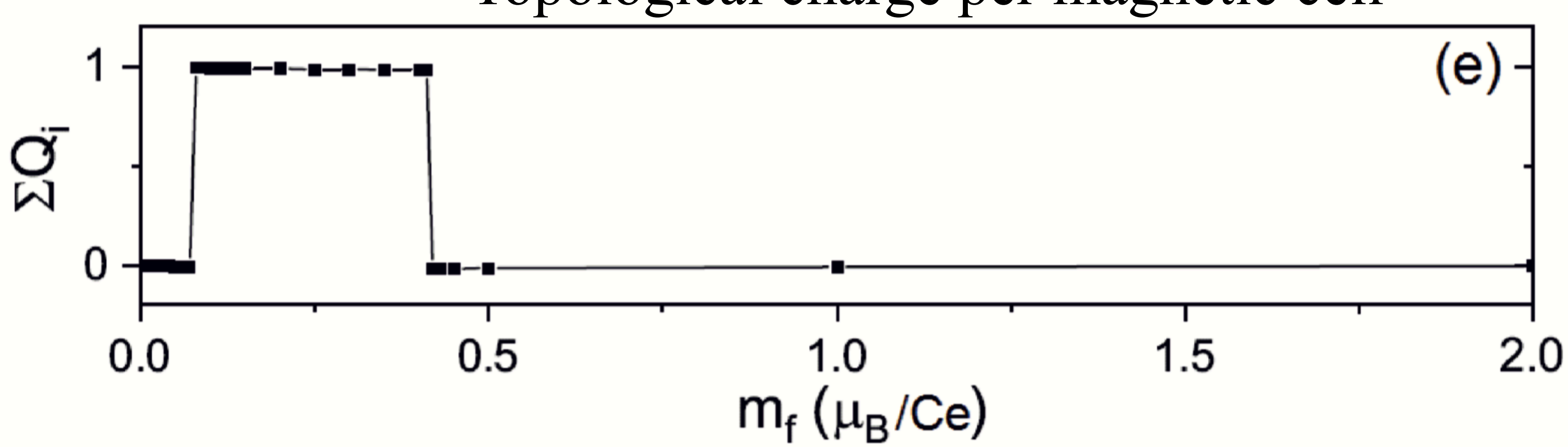

Simulation of external field ~ FM component along z-axis

experiment: (m1,m2,m3,m4) = (0.44(1), 1.02(1), −0.21(5), 0.29(7)) μ_B.

mf = 0 μB mf = 0.3 μB mf = 0.5 μB

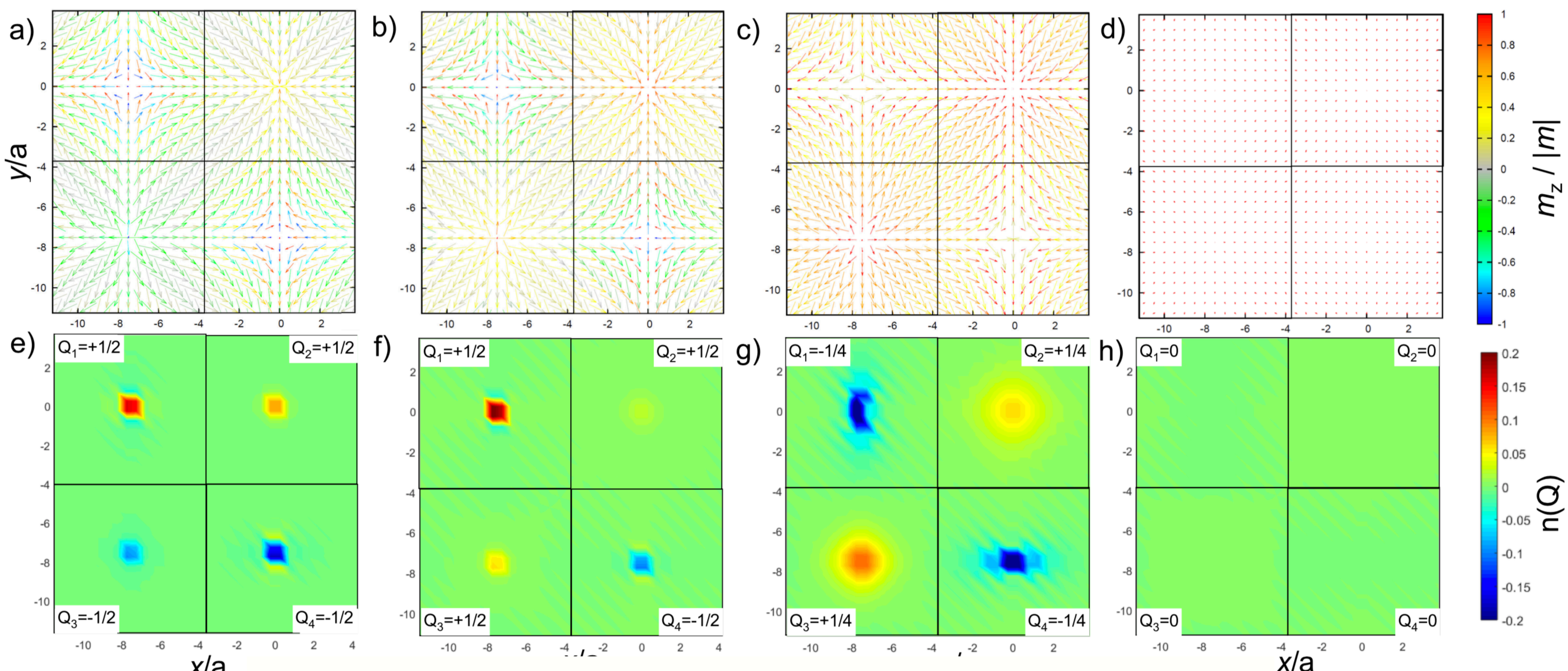

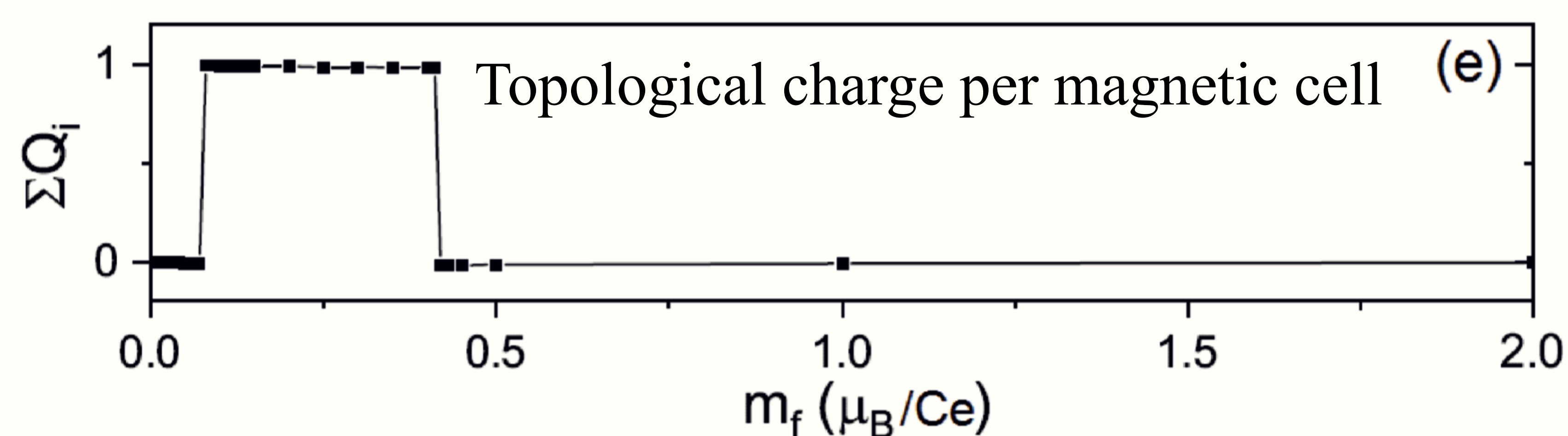

Figure 10. Compari … canting fields along th
z-direction out of th … μ_B. a-d) The first row o
mages shows the vi … $m_f = 0.2\,\mu_B$ (b) are th
same ones shown in … plane lattice parameter a

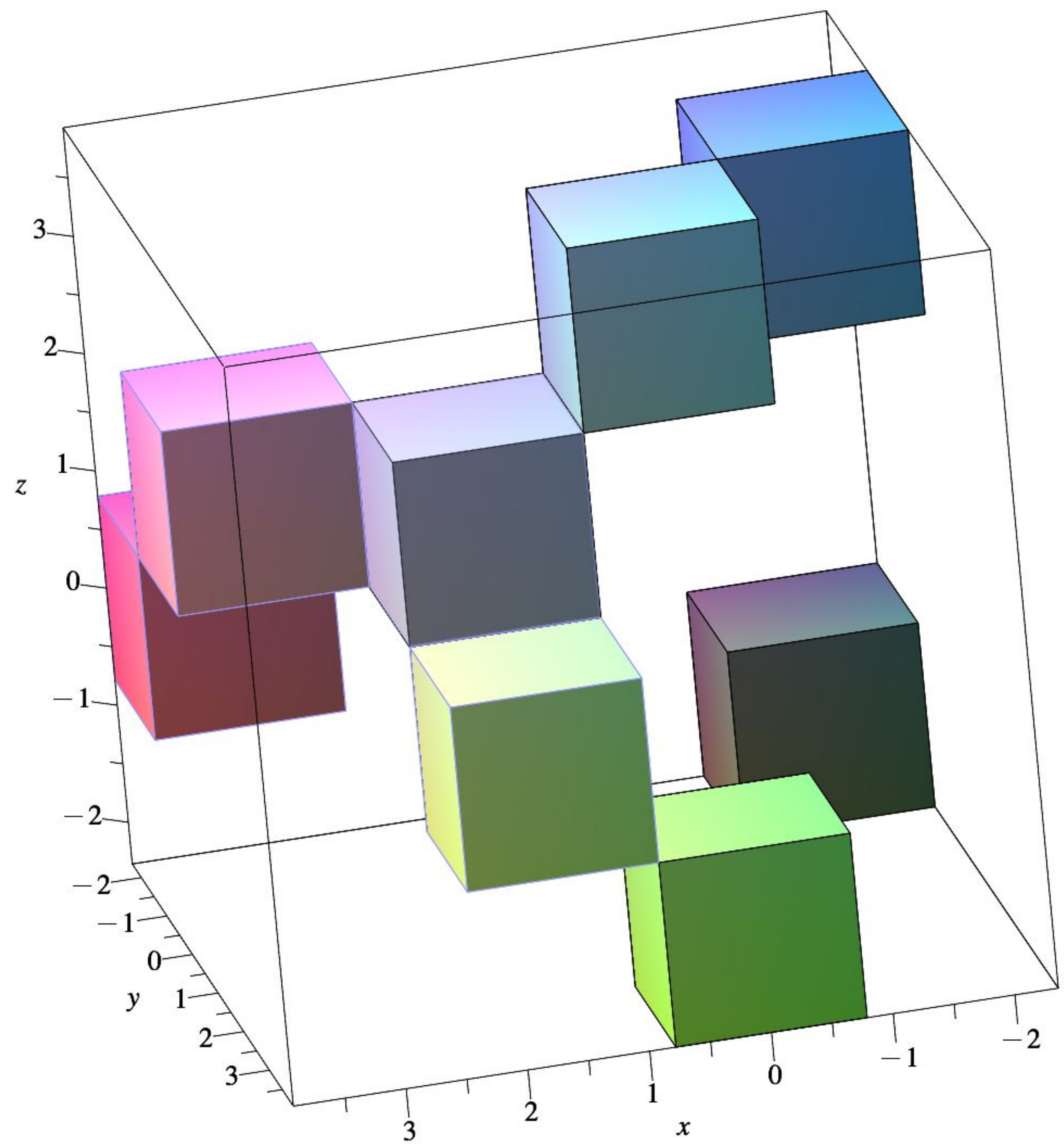

z
3
2
1
0
−1
−2
y
−2
−1
0
1
2
3
x
3
2
1
0
−1
−2

Topological charges in MnGe in external field

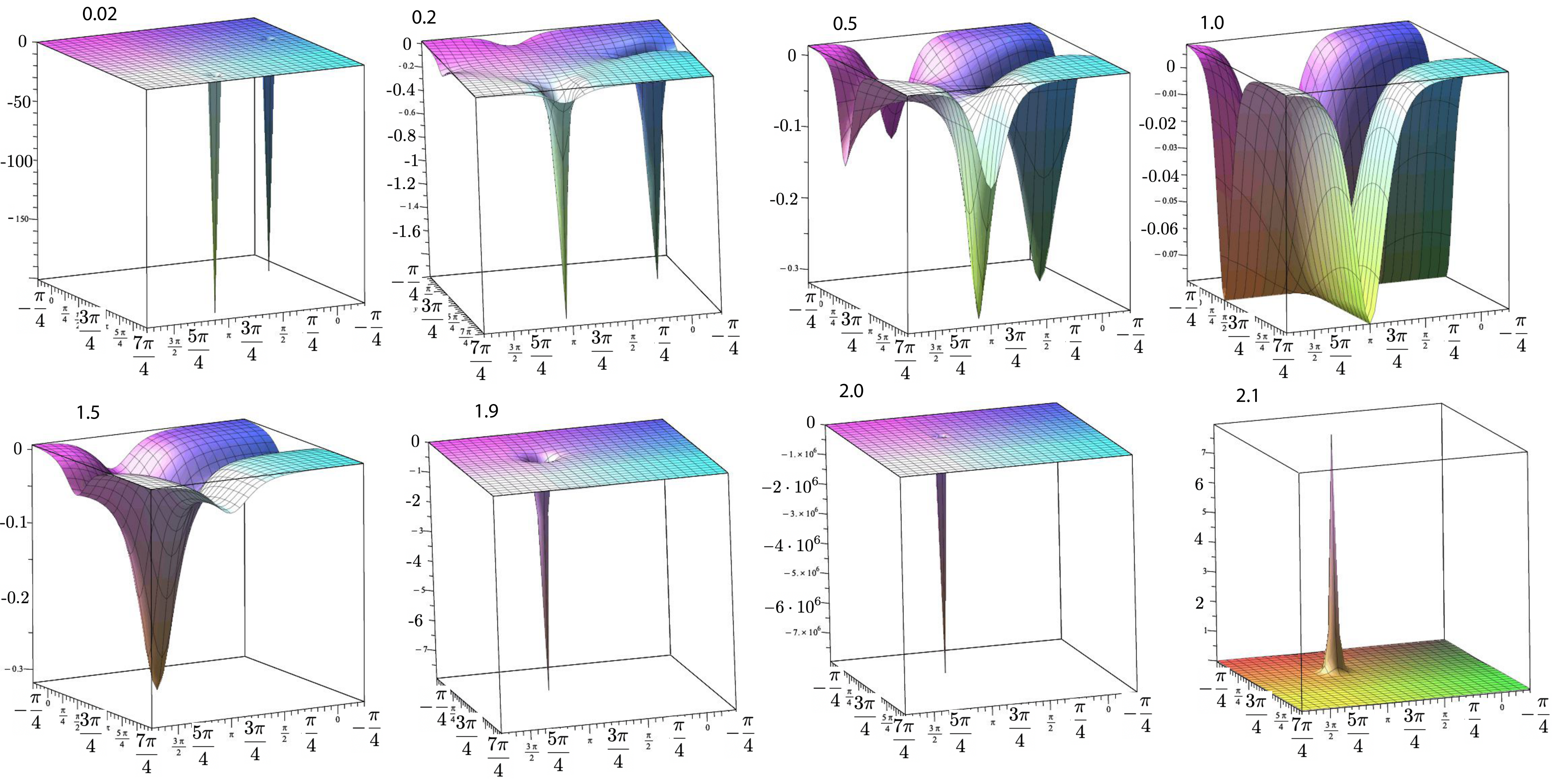

3d3F_AMxz_4x4x4

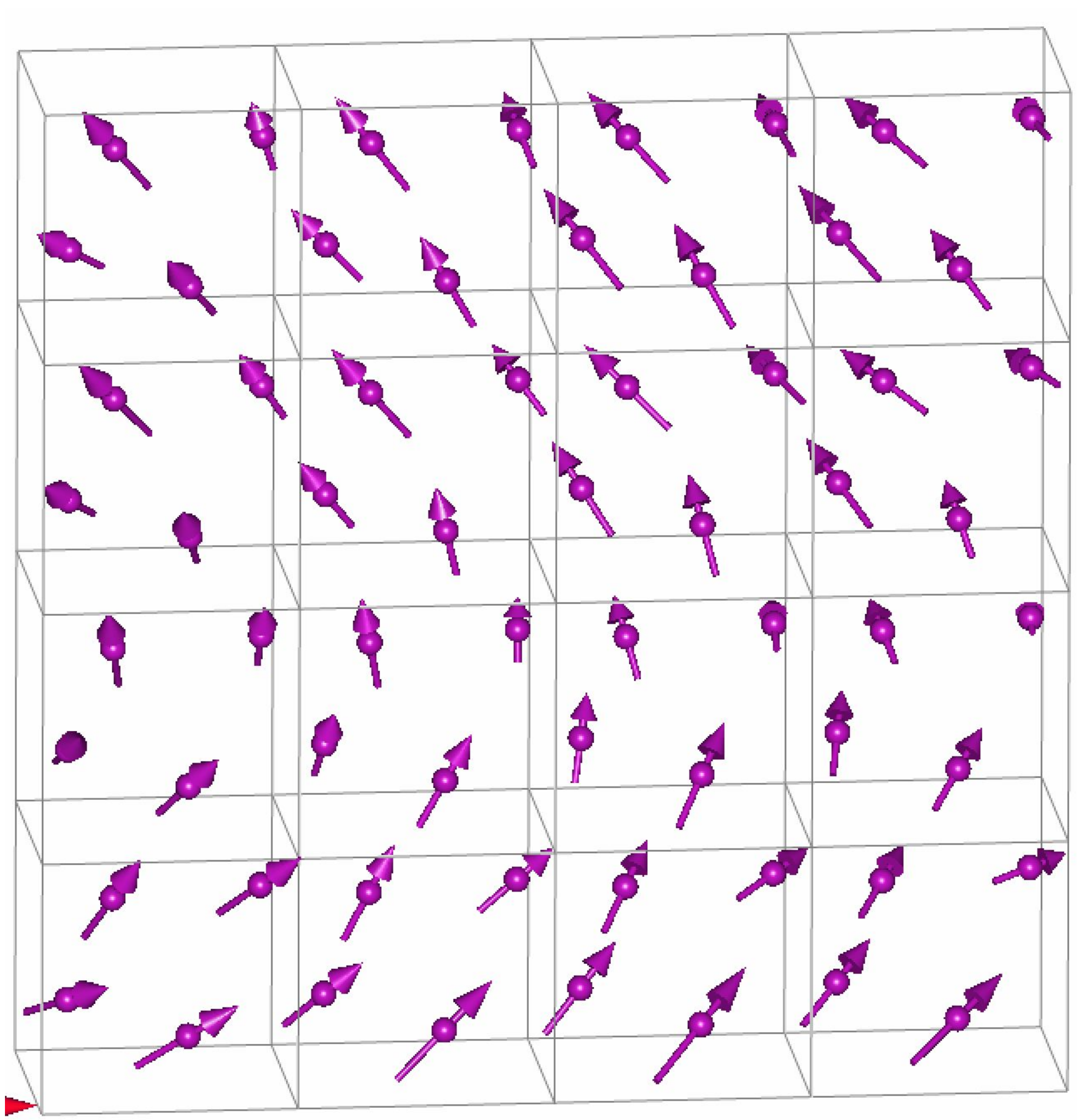

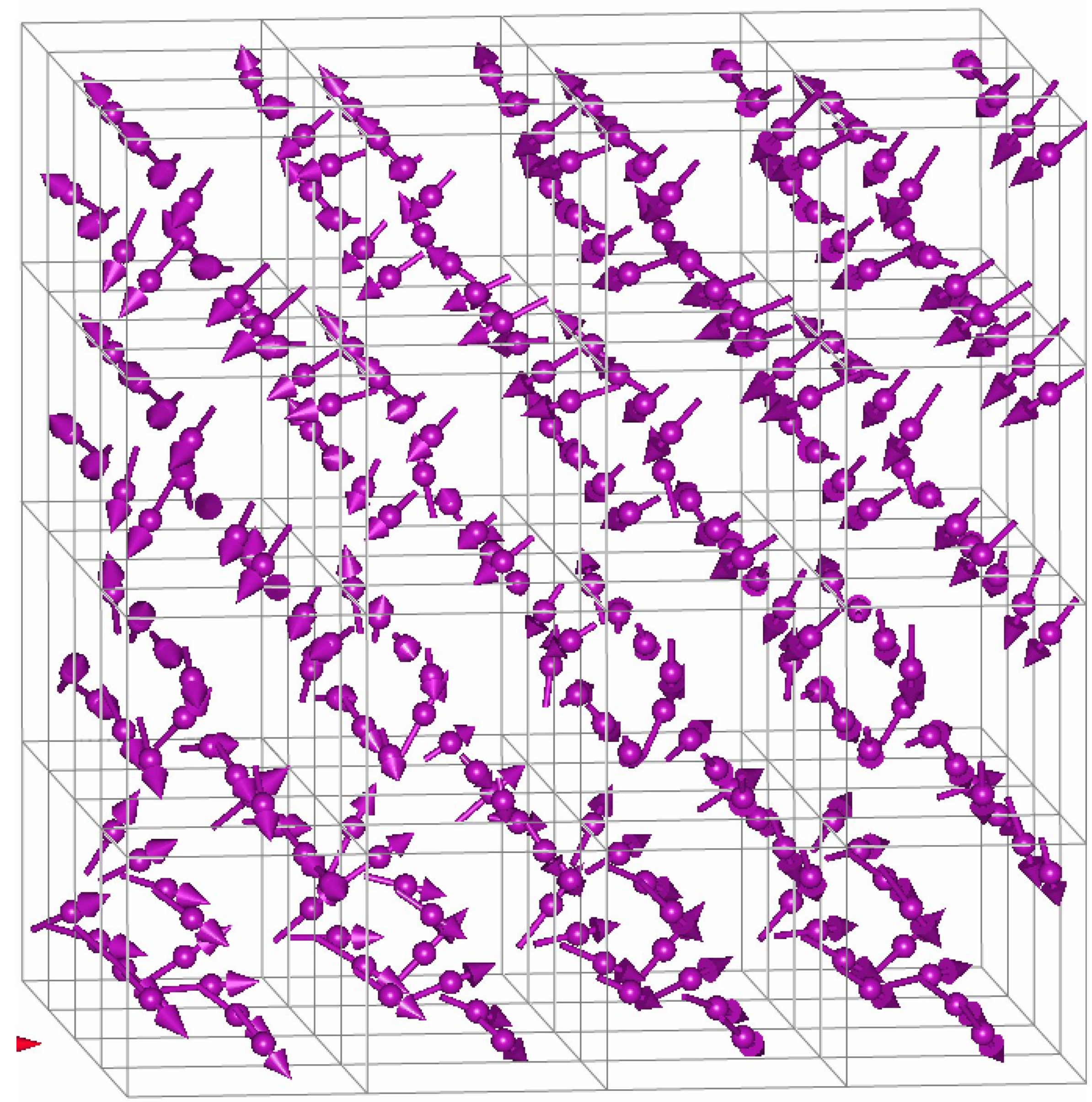

AMxz

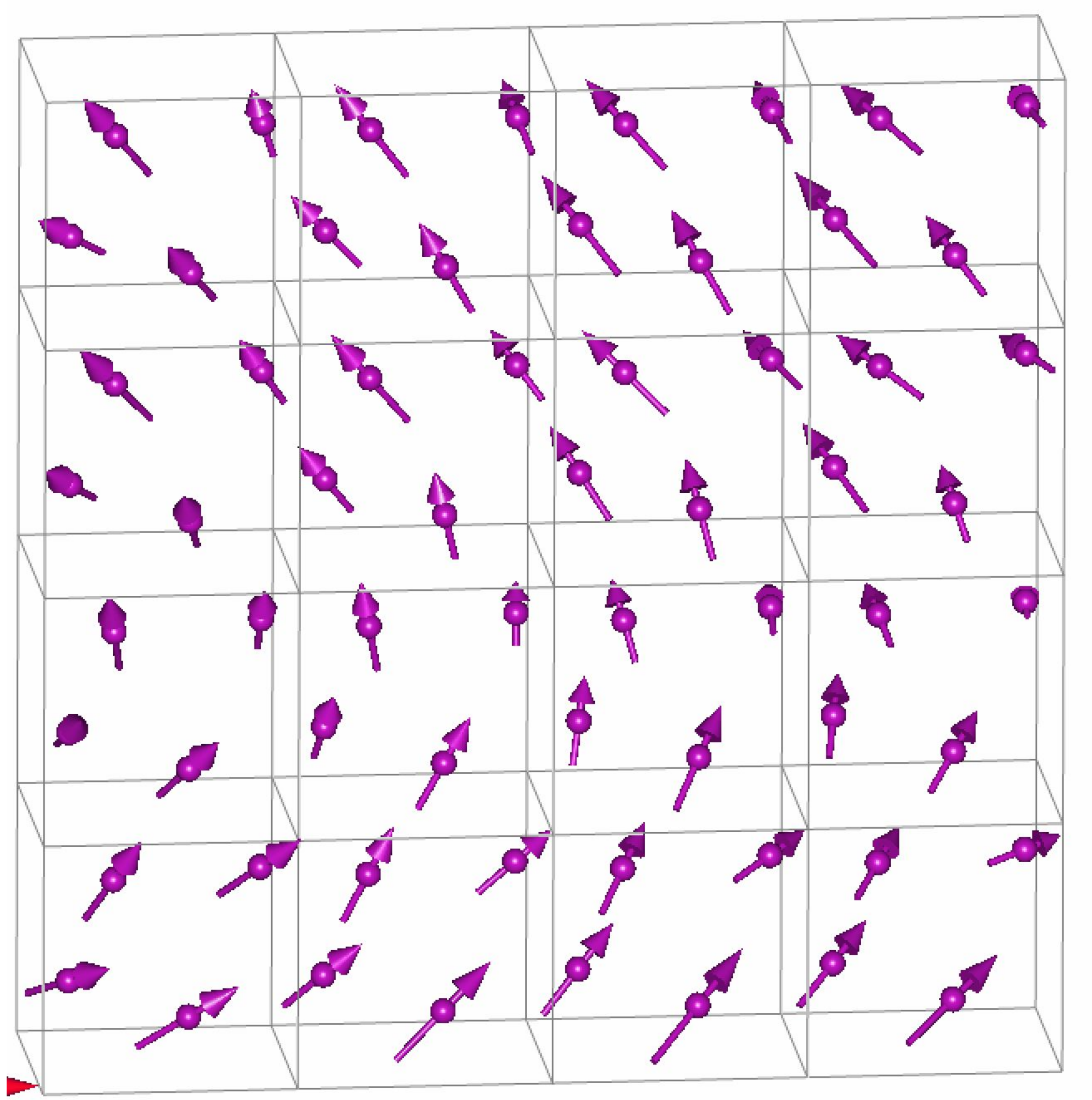

hedgehog

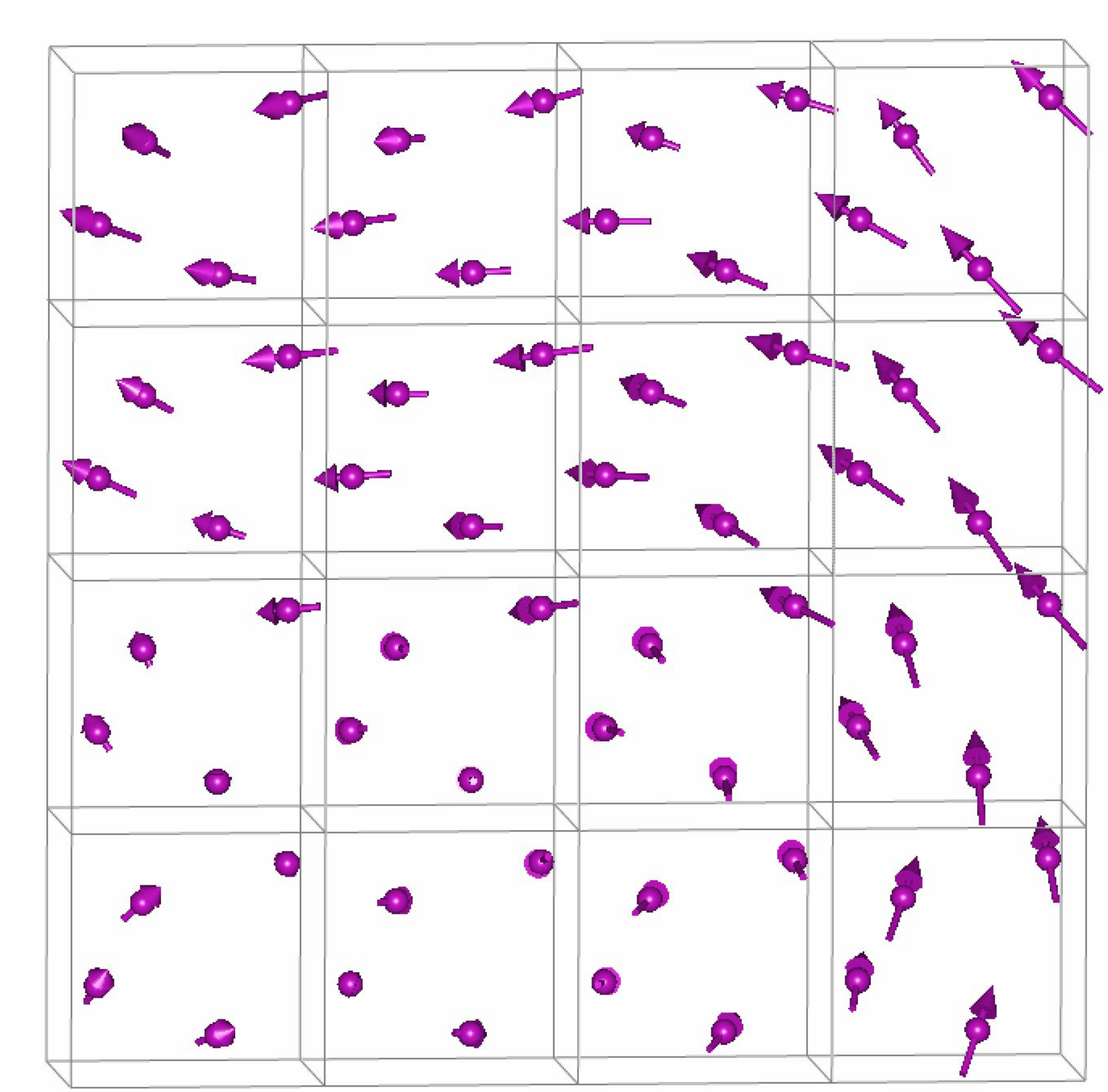

Continuous limit k->0 artificial full star magnetic structure

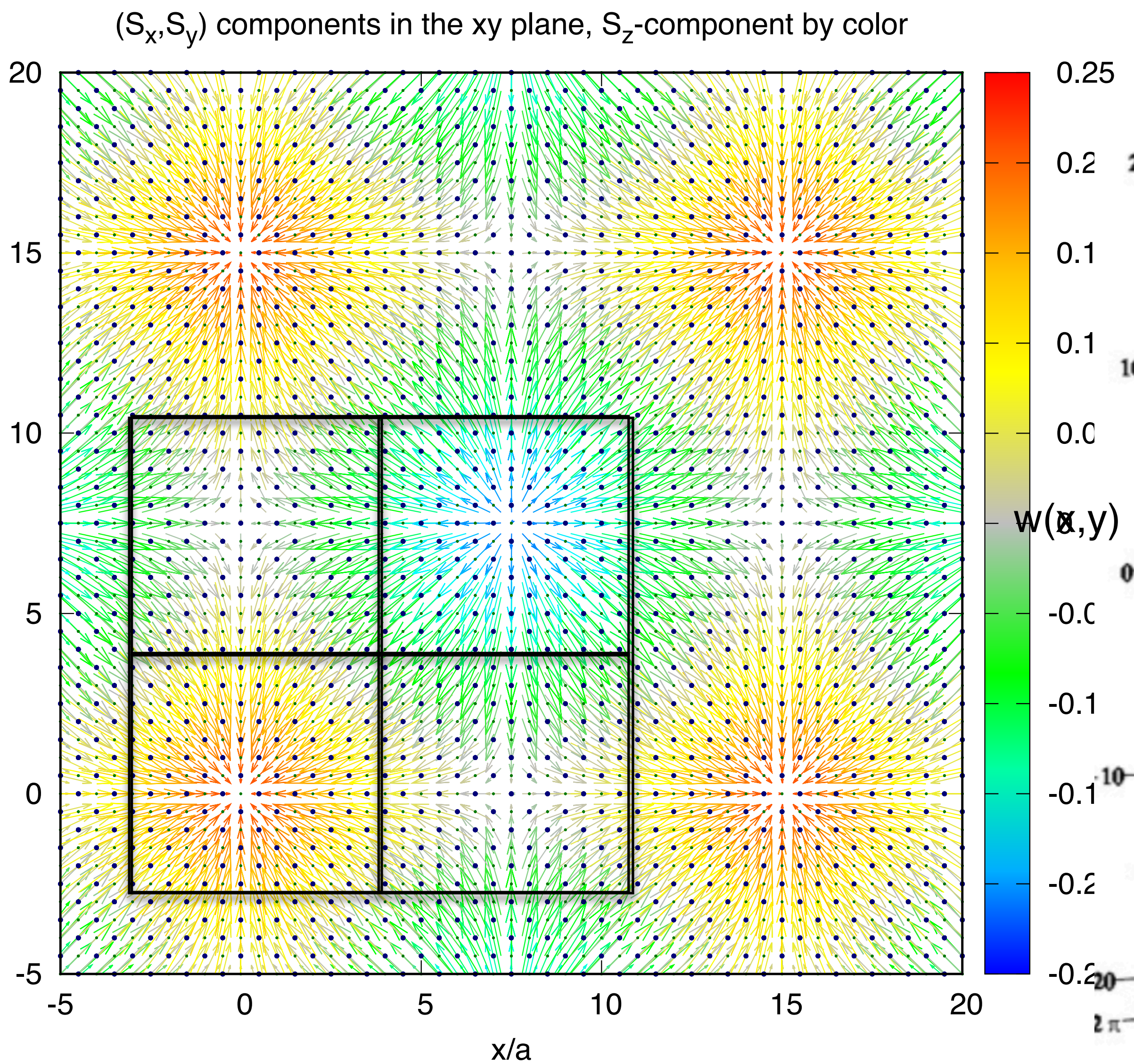

topological density/winding ~ solid angle

$$w(x,y) = \frac{1}{4\pi}(\mathbf{n}\cdot[\frac{\partial \mathbf{n}}{\partial x}\times\frac{\partial \mathbf{n}}{\partial y}]),\ \mathbf{n} = \mathbf{M}/M$$

Topological number/charge

$$Q = \int\int w(x,y)dxdy$$

Q = ±1/2

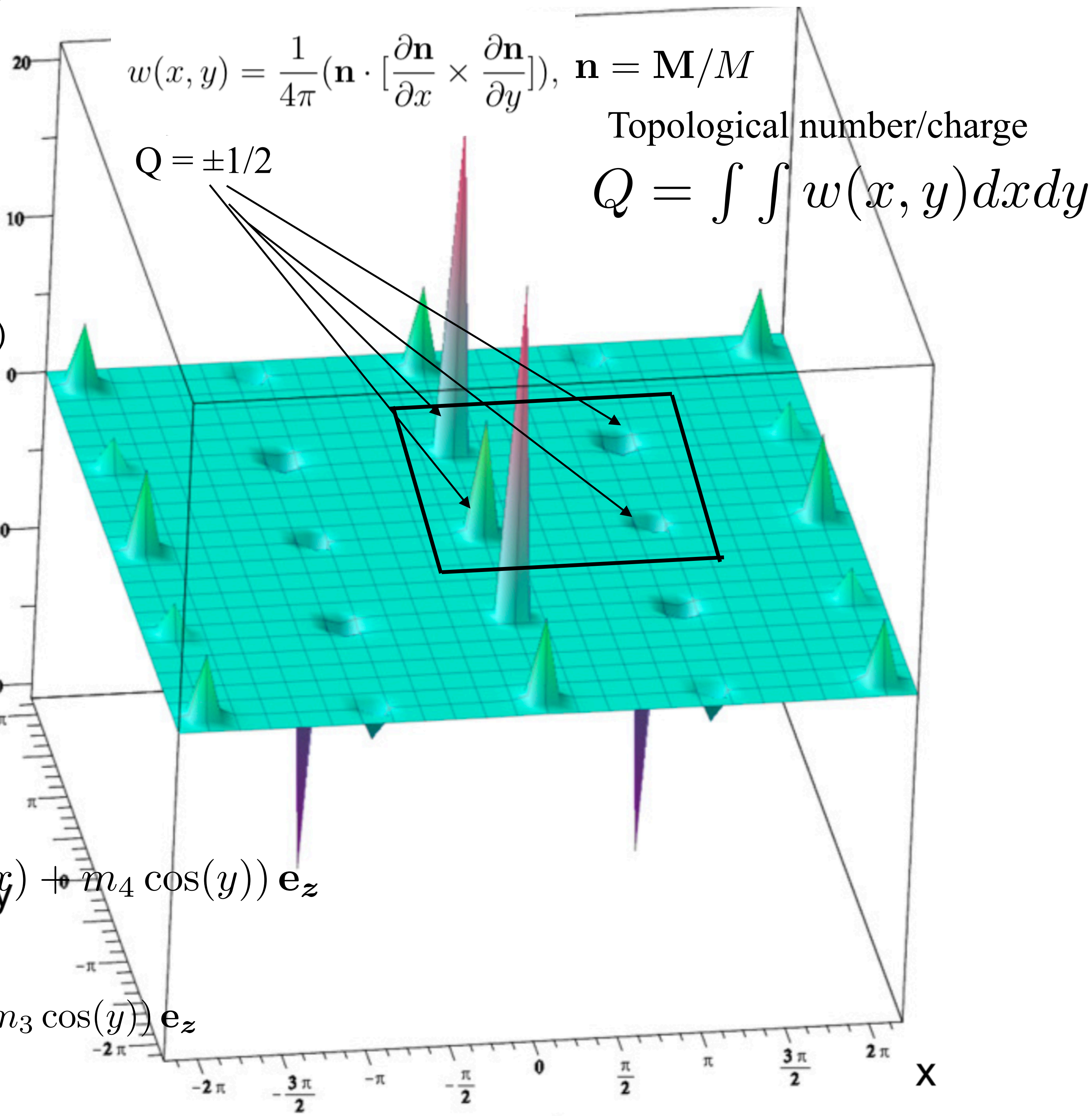

$$\mathbf{M}_{\mathrm{Ce1}} = m_1\sin(x)\mathbf{e}_{\boldsymbol{x}} + m_2\sin(y)\mathbf{e}_{\boldsymbol{y}} + (m_3\cos(x) + m_4\cos(y))\,\mathbf{e}_{\boldsymbol{z}}$$

m1=m2=2 and m3=0.1, m4=0.11

$$\mathbf{M}_{\mathrm{Ce2}} = m_2\sin(x)\mathbf{e}_{\boldsymbol{x}} + m_1\sin(y)\mathbf{e}_{\boldsymbol{y}} + (m_4\cos(x) + m_3\cos(y))\,\mathbf{e}_{\boldsymbol{z}}$$

Extrema can be both in |M|=0 and at max |Mz|

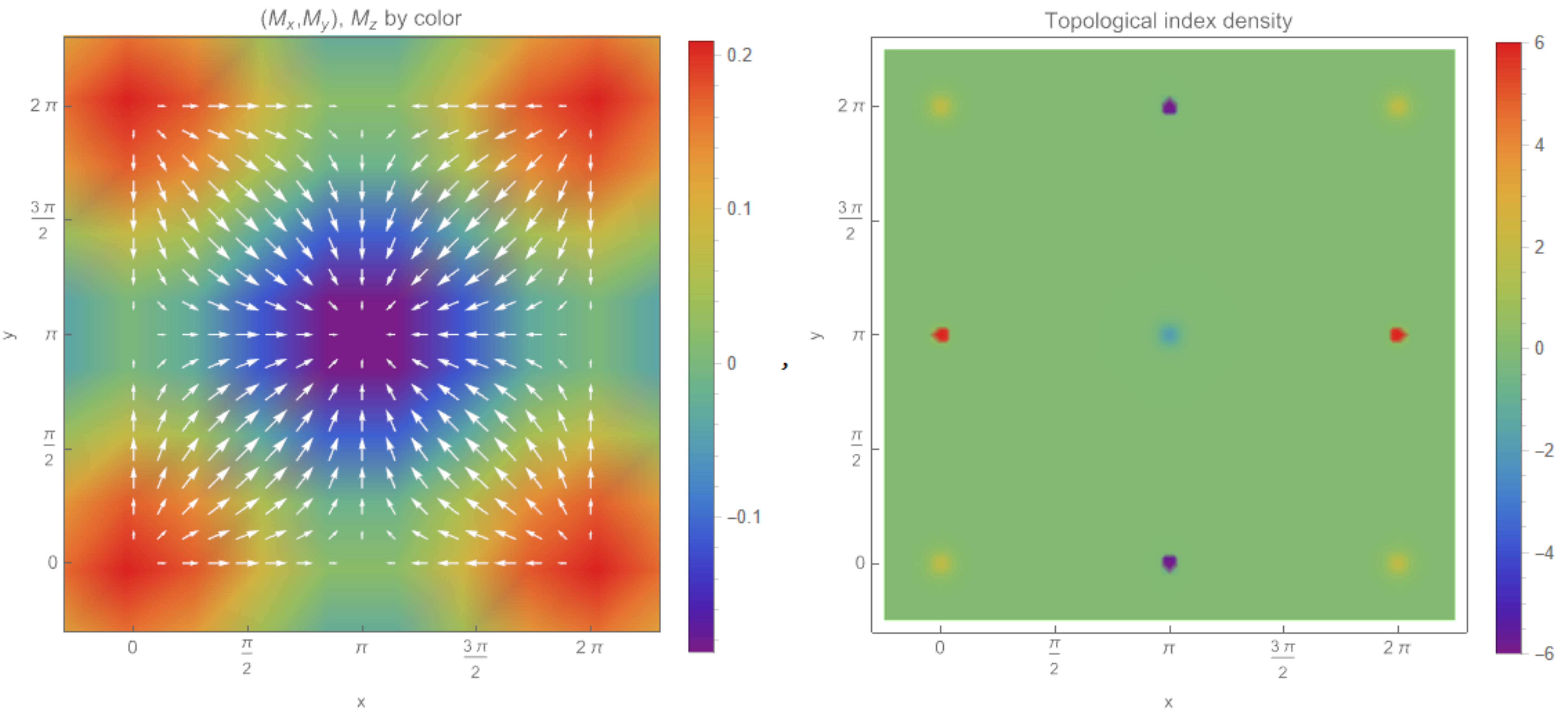

in CeAlGe for Ce1 (mx, my, mz) = [sin y, sin x, 0.5(0.11 cos x +0.11cos y)].

“Bloch” skyrmion (meron) 3D+2 magnetic structure

orthorhombic MSSG 19.2.29.2.m26.3 P2_12_12_1.1′ (0,b1,0)000s(0,0,g2)000s

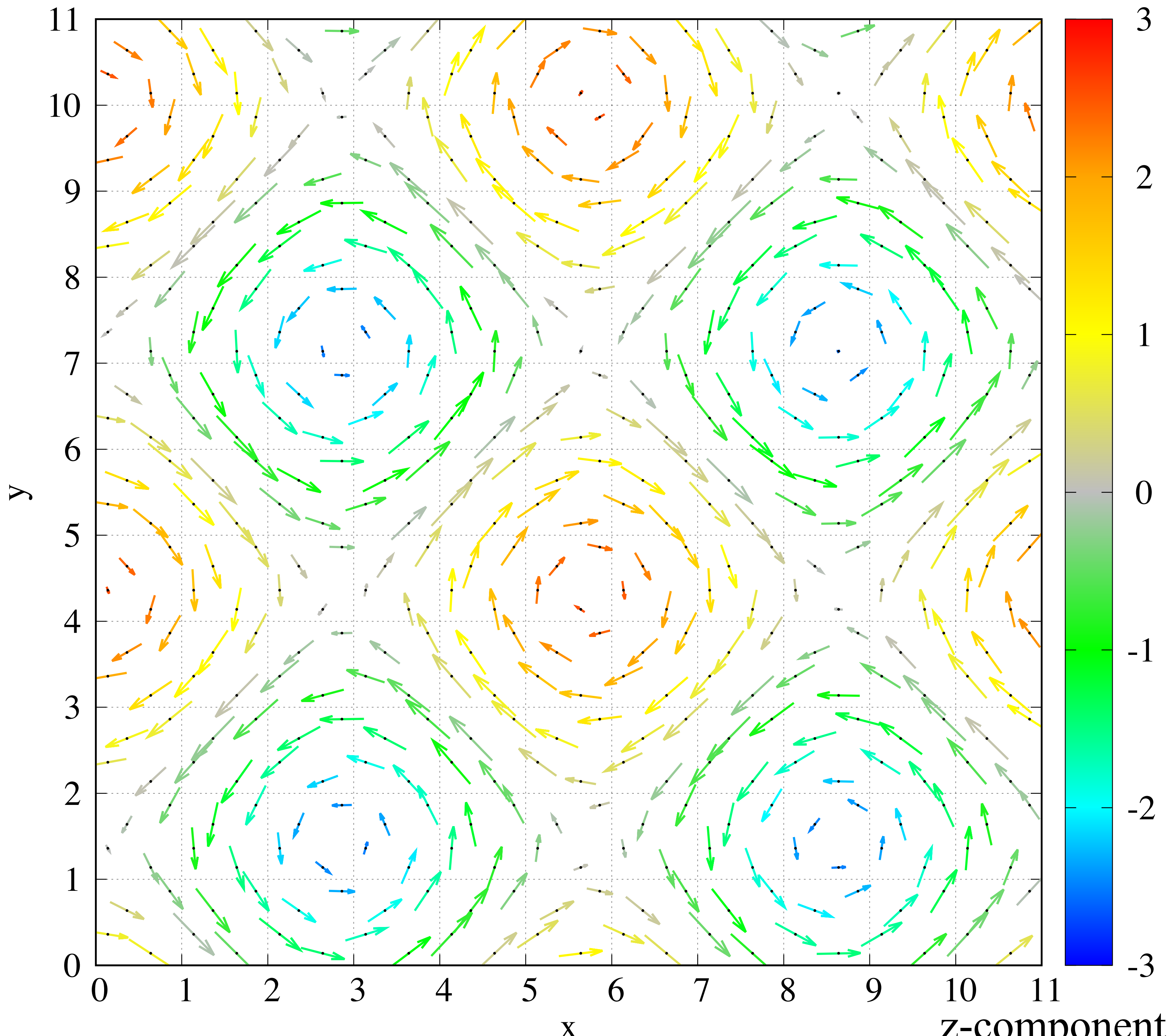

z-component by color

$$w(x, y) = \frac{1}{4\pi}\left(\mathbf{n}\cdot\left[\frac{\partial \mathbf{n}}{\partial x}\times\frac{\partial \mathbf{n}}{\partial y}\right]\right)$$

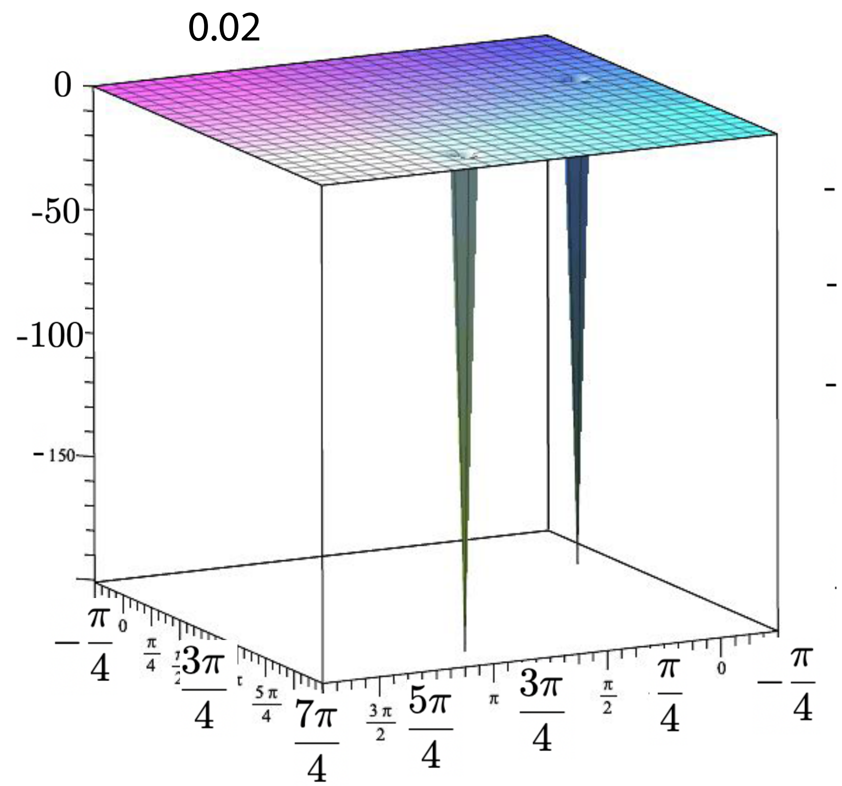

The total topo-charge Q = −1 in infinitesimal field.

singularities and Bloch/Neel

{Mx , My} vs. {x,y}, Mz by color

Extrema can be only in |M|=0

```
9]:= {fig1, fig2} // Row
```

59]=

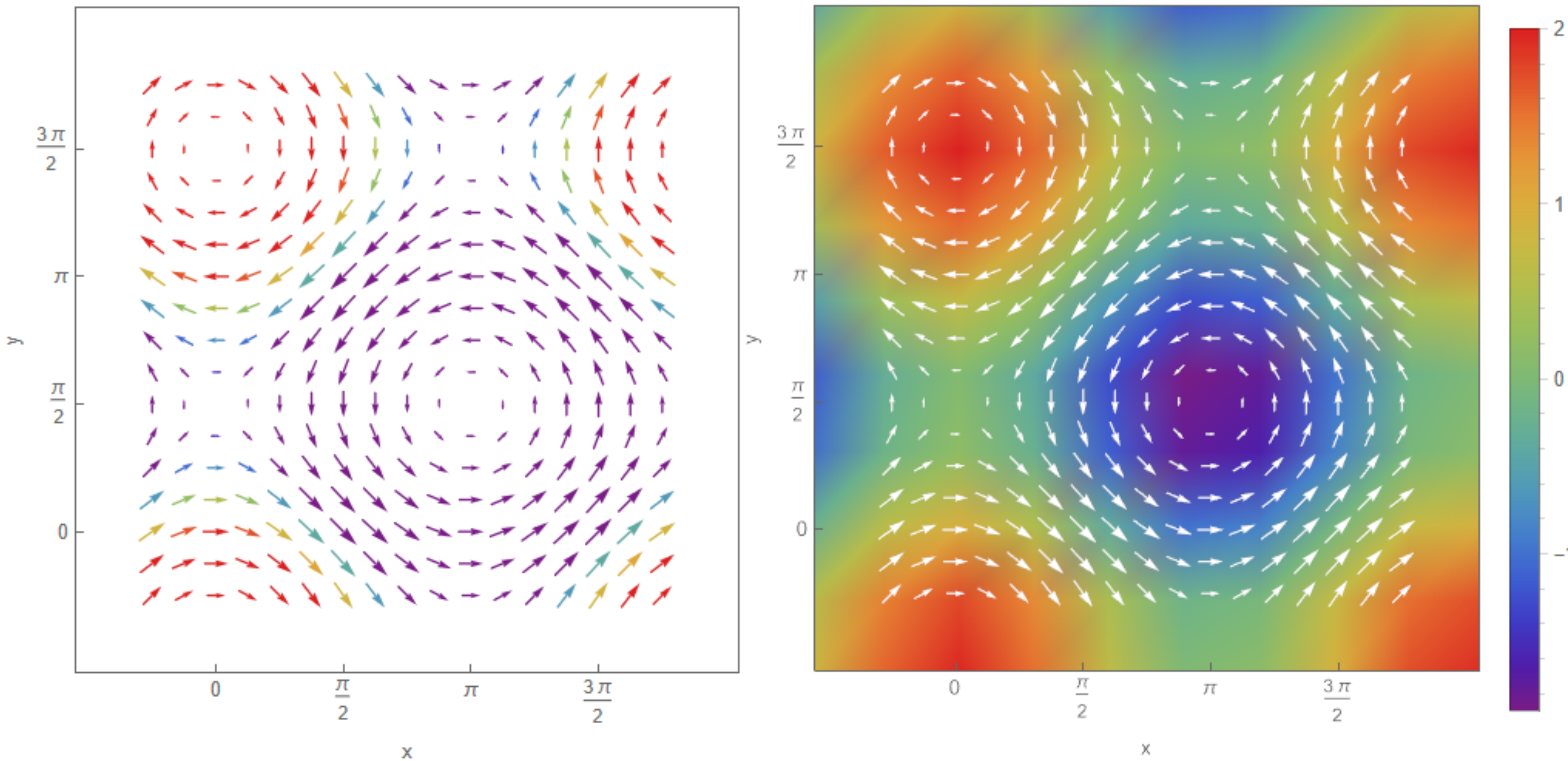

$$(mx, my, mz) = (\cos y, -\sin x, -\sin y + 1.001\cos x).$$

in CeAlGe for Ce1 $(mx, my, mz) = [\sin y,\ \sin x, 0.5(0.11 \cos x + 0.11\cos y)]$.